Stem Cell-Based Strategies to Study, Prevent, and Treat Cartilage Injury and

Osteoarthritis

by

Brian O'Callaghan Diekman

Department of Biomedical Engineering
Duke University

Date:_____
Approved:

_____
Farshid Guilak, Supervisor

_____
Virginia B. Kraus

_____
Kam W. Leong

_____
Steven A. Olson

_____
Lori A. Setton

Dissertation submitted in partial fulfillment of
the requirements for the degree of Doctor of Philosophy in the Department of
Biomedical Engineering in the Graduate School
of Duke University

2012

<u>ABSTRACT</u>

Stem Cell-Based Strategies to Study, Prevent, and Treat Cartilage Injury and

Osteoarthritis

by

Brian O'Callaghan Diekman

Department of Biomedical Engineering
Duke University

Date:_____
Approved:

_____

Farshid Guilak, Supervisor

_____

Virginia B. Kraus

_____

Kam W. Leong

_____

Steven A. Olson

_____

Lori A. Setton

An abstract of a dissertation submitted in partial
fulfillment of the requirements for the degree
of Doctor of Philosophy in the Department of
Biomedical Engineering in the Graduate School
of Duke University

2012

Abstract

Articular cartilage is a smooth connective tissue that covers the ends of bones and protects joints from wear. Cartilage has a poor healing capacity, and the lack of treatment options motivates the development of tissue engineering strategies. The widespread cartilage degeneration associated with osteoarthritis (OA) is dramatically accelerated by joint injury, but the defined initiating event presents a therapeutic window for preventive treatments. In vitro model systems allow investigation of OA risk factors and screening of potential therapeutics. This dissertation develops stem-cell based strategies to 1) treat cartilage injury and OA using tissue-engineered cartilage, 2) prevent the development of OA by delivering stem cells to the joint after injury, and 3) study cartilage by establishing systems to model genetic and environmental contributors to OA.

Adipose-derived stem cells (ASCs) and bone marrow-derived mesenchymal stem cells (MSCs) are promising human adult cell sources for cartilage tissue engineering, but require distinct chondrogenic conditions. As compared to ASCs, MSCs demonstrated enhanced chondrogenesis in both alginate beads and cartilage-derived matrix scaffolds.

We hypothesized that MSC therapy would prevent post-traumatic arthritis (PTA) by altering the balance of inflammation and regeneration. Highly purified MSCs

(CD45$^-$TER119$^-$PDGFRα^+Sca-1$^+$) rapidly expanded under hypoxic conditions. Unexpectedly, MSCs from control C57BL/6 (B6) mice proliferated and differentiated more than MSCs from MRL/MpJ (MRL) "superhealer" mice. We injected B6 or MRL MSCs into mouse knees immediately after fracture, and MSCs of either strain were sufficient to prevent PTA.

Genetically reprogramming adult cells into induced pluripotent stem cells (iPSCs) generates large numbers of patient-matched cells with chondrogenic potential for therapy and cartilage modeling. We produced murine iPSC-derived cartilage constructs with a multi-phase approach involving micromass culture with bone morphogenetic protein-4, flow cytometry cell sorting of chondrocyte-like cells, monolayer expansion, and pellet culture with transforming growth factor-beta 3. Successful differentiation was confirmed by increased chondrogenic gene expression, robust synthesis of glycosaminoglycans and type II collagen, and the repair of an in vitro cartilage defect.

The diverse applications pursued in this research illustrate the power of stem cells to deepen the understanding of cartilage and guide the development of therapies to prevent and treat cartilage injury and OA.

Contents

List of Tables

List of Figures

List of Abbreviations

Note: Abbreviations defined upon first usage in each chapter

ACI   autologous chondrocyte implantation

ACAN1   human aggrecan gene

Acan   mouse aggrecan gene

ANOVA   analysis of variance

ASC   adipose-derived stem cell

BMP   bone morphogenetic protein

BrdU   5-bromo-2'-deoxyuridine

BSA   bovine serum albumin

bFGF   basic fibroblast growth factor

c-Myc   cellular myelocytomatosis oncogene

CDM   cartilage-derived matrix

COL1A1   human type I collagen gene

COL2A1   human type II collagen gene

COL10A1   human type X collagen gene

Col1   mouse type I collagen gene

Col2   mouse type II collagen gene

Col2-GFP   green fluorescent protein controlled by Col2 promoter/enhancer

Col10	mouse type X collagen gene
ConA	concanavalin A
CXCR4	C-X-C chemokine receptor 4
DEX	dexamethasone
DMB	1,9-dimethylmethylene blue dye
dsDNA	double stranded deoxyribonucleic acid
EB	embryoid body
ECM	extra-cellular matrix
EGF	epidermal growth factor
ELISA	enzyme-linked immunosorbent assay
ESC	embryonic stem cell
FBS	fetal bovine serum
GAG	glycosaminoglycan
GFP+	cell sorted as positive for expression of Col2-GFP
HBSS	Hanks buffered saline solution
IBMX	isobutylmethylxanthine
iPSC	induced pluripotent stem cell
IL-1	interleukin-1
IL-1ra	interleukin-1 receptor antagonist
IL-10	interleukin-10

ITS+	insulin transferring selenous acid premix
Klf4	krueppel-like factor 4
LIF	leukaemia inhibitory factor
MEF	mouse embryonic fibroblast
MRL	MRL/MpJ mouse stain
MSC	mesenchymal stem cell
Nanog	homeobox protein nanog
NEAA	non-essential amino acids
OA	osteoarthritis
Oct4	octamer-binding transcription factor 4, also called Pou5f1
PBS	phosphate buffered saline
PDGF	platelet-derived growth factor-BB
PHA	phytohaemagglutanin
P/S	penicillin/streptomycin
P/S/F	penicillin/streptomycin/fungizone
PTA	post-traumatic arthritis
qPCR	quantitative real time reverse-transcription polymerase chain reaction
RT-PCR	reverse-transcription polymerase chain reaction
SEM	standard error of the mean
sFRP2	secreted frizzled related protein-2

Sox9   mouse (sex determining region Y)-box 9 gene

SSEA-1   stage-specific embryonic antigen-1

TGF-β   transforming growth factor-beta

TNF-α tumor necrosis factor-alpha

2-me   beta-mercaptoethanol

Acknowledgements

I am incredibly grateful to all those who have made this dissertation possible and enjoyable. I am especially thankful for the guidance of my adviser, Dr. Farshid Guilak. Farsh is a brilliant scientist and engineer, and my career will be forever shaped by his creative and collaborative approach to research. However, his true gift to me and so many others has been his consistent mentorship and inspiring leadership, which has made the work meaningful and fun. I would also like to thank my committee members for improving this work through their insights and collaboration: Dr. Virginia Kraus, Dr. Kam Leong, Dr. Steven Olson, and Dr. Lori Setton.

The Orthopaedic Bioengineering Lab and Biomedical Engineering Departments have provided a rich environment to be trained as a researcher and I am honored to have worked alongside so many talented and caring people. Dr. Beverley Fermor and Dr. Brad Estes were my first mentors, and I still cannot imagine embarking on a new project without consulting Brad. I have also had the opportunity to work with several ambitious students whose enthusiasm provided constant motivation and valuable contributions to this work: Chris Rowland, Chia-Lung Wu, and Alex Sun. Several of the projects required large teams and I am grateful for all those who contributed their time and expertise. Bridgette Furman, Craig Louer, Steve Johnson, Janet Huebner, Evan Zeitler, and Elisabeth Flannery helped perform the stem cell therapy experiments. Dr.

My sincerest thanks go to my incredibly supportive parents, Mark Diekman and Patti O'Callaghan, for instilling in me the confidence to pursue my passions and for demonstrating how to balance work, family, and community. My brother Casey Diekman has paved the way for me in life and in science, and I could not ask for a better role model. I am also thankful for those who became family during graduate school: Rachel, Blakeley, Steve, Donna, and Tom. The Durham community has made my journey a rich and joyous one, and I am very thankful for our wonderful friends and church community. I thank the Walltown basketball players and Reality Center math students for the hope that they give me; my wish for them is to find something that inspires them in the way this research has inspired me.

To my amazing wife Amanda: thank you, thank you, thank you. The best part of the last six years has been going through life with you. Thanks for supporting me in everything that I do and for spending so much time pretending to be interested in cartilage.

1. Background and Significance

1.1 Composition and function of articular cartilage

Articular cartilage is a thin connective tissue that covers the bony ends of freely

moving joints such as the knee and hip. Cartilage extracellular matrix (ECM) is

composed mainly of type II collagen (~70% of dry weight) and proteoglycans (~20% of

dry weight), which are produced and maintained by chondrocytes. The bulk of the

collagen matrix consists of a cartilage-specific fibrillar network composed of type II with

support from types IX and XI, whereas type VI is concentrated around cells, type X is

present in calcified cartilage, and type I is absent (Eyre, 2002). Most of the proteoglycan

in cartilage exists as large structures known as aggrecan. Aggrecan consists of

proteoglycan subunits containing a central core protein bound to many chondrotin

sulfate and keratin sulfate glycosaminoglycan (GAG) side chains, which then aggregate

through intereactions with hyaluronic acid and link protein (Muir, 1995). Although

variation occurs according to species, age, and location, the high water content of

cartilage (65-85%) results in values of appoximately 50 μg GAG, 150 μg collagen, and

50,000 chondrocytes per mg of wet tissue (Hoemann, 2004).

Human knee and hip joints experience approximately one million loading cycles

each year, with daily activities generating loads of up to ten times body weight (Mow et

al., 1992). Under normal circumstances, the composition of cartilage ECM endows the

tissue with mechanical properties that serve to effectively distribute these loads across joints with little friction and wear. The negatively charged proteoglycans are immobilized witin the collagen matrix, which induces a swelling pressure that resists compression. The frictional force generated as the fluid phase flows throught the solid matrix contributes to the unique response of cartilage to loading (Mow et al., 1980). Cartilage wear is prevented by the low coefficient of friction, which is largely the result of interstitual fluid pressurization limiting the amount of load that is supported by the solid matrix (Ateshian, 2009).

1.2 Treatment of cartilage injury and osteoarthritis

One of the defining features of articular cartilage is the inability for effective repair, due at least in part to the lack of a blood supply. Isolated cartilage defects involving damage to a defined area are common and may progress to the widespread cartilage degeneration seen in osteoarthritis (OA) (Hjelle et al., 2002). Current treatment options for cartilage defects involve accessing cells from the underlying bone marrow through microfracture, transplanting autolgous osteochondral plugs from less weightbearing regions to the defect site, or using expanded autologous chondrocytes for cell-based therapy (Hunziker, 2002). However, these treatment strategies may not be as effective for older patients or patients with large defects, and the limited durability of the repair tissue may lead to long-term failure (Knutsen et al., 2007; Kreuz et al., 2006).

2

OA is the leading cause of disability in the elderly and an estimated 27 million Americans have clinical OA of at least one joint (Lawrence et al., 2008). Although OA is typically recognized as degradation of the cartilage, changes to joint tissues such as bone and synovium are also signficiant features of the disease (Goldring and Otero, 2011). The cause of OA is often multi-factorial and risk factors include particular genetic profiles, obesity, and altered joint loading (Felson et al., 2000). Treatment options to halt or treat OA are generally limited to lifestyle modifications and pain management until the common endpoint of surgical joint replacement (Wieland et al., 2005), with over 750,000 total knee and hip joint replacements in the U.S. each year. The surgical demand from younger and more active patients has risen dramatically despite concerns that total joint replacements are not as well suited to younger patients due to the limited lifetime of the implant (Kurtz et al., 2009). Clearly, novel strategies for the prevention and treatment of OA are needed.

1.3 Cartilage tissue engineering

Regenerative medicine and tissue engineering seek to address a wide range of disease states by using tools such as cells, scaffolds, and bioactive molecules to alter the injury environment and promote functional repair. Specifically, the goal of cartilage tissue engineering is to create a tissue with sufficient biological and mechanical properties that it can aid in restoration of the joint (Guilak et al., 2001).

Autologous chondrocyte implantation (ACI) is approved in the U.S. for use as a cartilage tissue engineering procedure (Brittberg et al., 1994), but most investigators have focused on stem cells to provide a more abundant source of cells without the need for an invasive surgery to harvest autologous cartilage. Embryonic stem cells (ESCs) are derived from the inner cell mass of embryos and can indefinitely self-renew while maintaining the potential to become any cell type in the body (Thomson et al., 1998). Stem cells derived from adult tissues demonstrate a defined number of doublings before senescence and have the potential to differentiate toward multiple but not all cell lineages (Pittenger et al., 1999). Bone marrow-derived mesenchymal stem cells (MSCs) and adipose-derived stem cells (ASCs) are examples of adult stem cells that can be defined by in vitro characteristics such as adherence to plastic, multilineage potential toward bone, cartilage, and fat, and expression of certain cell surface markers (Dominici et al., 2006). Both MSCs and ASCs have been used as cell sources in many different cartilage tissue engineering strategies (Guilak et al., 2010; Noth et al., 2008).

Growth factors help regulate the process of chondrogenesis during cartilage development and have therefore been the main bioactive molecules used to guide the differentiation of adult stem cells in tissue engineering strategies. In particular, transforming growth factor-beta (TGF-β) and bone morphogenetic protein (BMP) molecules act to upregulate the transcription factor Sox9, which then coordinates the

synthesis of type II collagen and aggrecan (Akiyama et al., 2002; Quintana et al., 2009). The expression of the type II collagen gene (Col2) defines a differentiated chondrocyte, a process that can be visualized using the Col2 promoter/enhancer to drive expression of green fluorescent protein (Col2-GFP) (Grant et al., 2000).

Providing a three-dimensional environment is important for establishing an initial structure that can eventually become the engineered cartilage tissue. A second function of scaffolds is to deliver cues to the cells for appropriate differentiation and matrix synthesis. Hydrogels such as agarose and alginate promote a rounded cell shape that is conducive to chondrogenesis (Awad et al., 2004) and have the advantage of filling any containing shape. However, they are generally inert and have poor mechanical properties. Polymer scaffolds can provide more of a mechanical structure, with woven scaffolds achieving mechanical properties on the scale of cartilage even before new matrix production (Moutos et al., 2007). Recently, more attention has been paid toward designing scaffolds that mimic tissue properties in order to instruct cell differentiation and matrix synthesis (Lutolf and Hubbell, 2005). Scaffolds actually derived from native tissue provide one option to provide tissue-specific ECM cues (Badylak et al., 2009). Interestingly, scaffold-free systems in which cells are pelleted or allowed to self-assemble at high density are also very conducive to chondrogenesis because this mimics

the condensation phase of cartilage development (Hu and Athanasiou, 2006; Johnstone et al., 1998).

Despite extensive work on characterizing different stem cell sources, determining growth factor combinations for chondrogenic differentiation, and developing scaffold systems that can provide appropriate mechanical and cell-instructive cues, persistent obstacles to successful cartilage tissue engineering remain. These include the challenges of cell loss, insufficient or inappropriate differentiation, integration of newly formed tissue with the surrounding cartilage and bone, and dealing with the inflammatory environment after implantation (Steinert et al., 2007).

1.4 Adult stem cell therapy

The observation that MSCs can have a beneficial effect without significant engraftment and differentiation has spurred interest in the mechanism of MSC contribution to healing (Caplan and Dennis, 2006; Prockop, 2007). An emerging paradigm suggests that the primary benefit of MSC therapy is immunomodulatory, tilting the balance of the injured environment from inflammation to regeneration. This effect is mediated either through direct secretion of bioactive factors or by "trophic" effects—altering the cytokine and growth factor production of other cells (Caplan and Dennis, 2006; Iyer and Rojas, 2008; Phinney and Prockop, 2007). MSCs do not normally express Major Histocompatibility Complex class II molecules (Le Blanc et al., 2003) and

6

these immune-privileged cells are able to inhibit the proliferation of stimulated T cells in vitro (Aggarwal and Pittenger, 2005) and effectively treat severe graft-versus host disease (Le Blanc et al., 2004).

Investigating the effects of exogenous MSCs on injury in a variety of animal models has supported the notion that enhanced tissue repair is likely due to soluble factors as opposed to engraftment and differentiation. MSCs have been shown to secrete interleukin-1 receptor antagonist (IL-1ra) to protect lung tissue from bleomycin-induced injury (Ortiz et al., 2007), increase interleukin-10 (IL-10) secretion by macrophages to improve survival in a sepsis model (Nemeth et al., 2009), improve outcome after myocardial infarction by secretion of bioactive molecules (Gnecchi et al., 2008; Lee et al., 2009), and facilitate bone healing after fracture by secreting BMP-2 and decreasing interleukin-6 (Granero-Molto et al., 2009).

1.5 Post-traumatic arthritis

Post-traumatic arthritis (PTA) resulting from defined joint trauma such as intra-articular fracture accounts for 12% of all osteoarthritis (OA) patients (Brown et al., 2006), with a large financial burden in terms of lost wages because PTA generally affects a young population. Treatment at the time of trauma such as surgical restoration of articular surface congruity after fracture cannot eliminate the 10-20 fold increased risk for OA after joint injury (Anderson et al., 2011). Inflammation of the synovium and

other tissues in the joint environment after fracture has emerged as an important

contributor to OA pathogenesis (Furman et al., 2006; Guilak et al., 2004). The increase in

cytokines such as interleukin-1 (IL-1) and tumor necrosis factor α (TNF-α) after injury

(Pickvance et al., 1993) can lead to inflammatory cascades and subsequent cartilage

degradation (Fernandes et al., 2002; Guerne et al., 1989). Support for the importance of

inflammation comes from a closed-joint intra-articular fracture model in the mouse,

which allows for investigation of the natural progression of PTA (Furman, 2009; Furman

et al., 2007).

There is a lack of data on the contribution of endogenous MSCs to intra-articular

fracture healing or the subsequent development of PTA. Multipotent stem cells are

present in the joint space after fracture, as demonstrated by the derivation of a cell

population with MSC properties from hemarthrosis in joints after fracture (Lee et al.,

2008). Additionally, treatment of chondral defects with microfracture or other marrow

stimulating techniques rely on accessing the subchondral bone marrow to allow

infiltration of progenitor cells (Frisbie et al., 2003; Kramer et al., 2006). In addition to the

bone marrow, other tissues in the joint may contribute progenitor cells as multipotent

stem cells have also been isolated from the infrapatellar fat pad (Wickham et al., 2003),

muscle (Usas and Huard, 2007), synovium (De Bari et al., 2001), cartilage (Alsalameh et

al., 2004; Dowthwaite et al., 2004), and trabecular bone (Noth et al., 2002). Most studies

8

investigating stem cell therapy for orthopaedic applications have focused on

osteochondral defects (Wakitani et al., 1994; Zscharnack et al.) or long-bone fracture

(Bruder et al., 1998; Granero-Molto et al., 2009). However, one series of studies

investigated the delivery of BMP-2 overexpressing stem cells after osteotomy of the knee

joint in mice and rats (Zachos et al., 2007a; Zachos et al., 2007b). The delivered stem cells

were effective in fracture healing and contributed to cartilage repair, but the specific

endpoint of post-traumatic arthritis was not investigated.

1.6 Regeneration in MRL/MpJ "superhealer" mice

The MRL/MpJ (MRL) "superhealer" inbred mouse strain has unusual

regenerative capabilities that were first observed by the rapid closure of surgical ear

holes (Clark et al., 1998). This trait is genetically determined by many loci across

multiple chromosomes (Yu et al., 2005), but reduced expression of the cell cycle inhibitor

p21 after injury recently emerged as a likely mediator of the regenerative capacity

(Bedelbaeva et al., 2010). MRL mice with a mutation encoding Fas, known as MRL/lpr,

have been commonly used as a model for lupus, but MRL mice without the mutation

develop weak autoimmunity only later in life (Nagata and Suda, 1995).

MRL mice have shown enhanced regeneration as compared to control strains in

several injury models in addition to surgical ear holes. MRL mice showed rapid

reepithelization after a burn injury to the cornea (Ueno et al., 2005), regrowth of

histologically normal heart tissue after cryoablation (Leferovich et al., 2001), faster

replacement of digit tips after amputation (Chadwick et al., 2007), and the regeneration

of articular cartilage after osteochondral injury (Fitzgerald et al., 2008). Other injury

models such as ischemia-reperfusion of the heart (Abdullah et al., 2005) and spinal cord

injury (Kostyk et al., 2008) showed a lack of improved outcome in MRL mice. When

MRL and B6 mice were subjected to intra-articular fracture, B6 mice progressed to PTA

while MRL mice were protected (Ward et al., 2008).

1.7 Inflammation in MRL/MpJ "superhealer" mice

Several lines of evidence from the ear hole model indicate a difference in the

inflammatory response of MRL mice as compared to the non-healing control strain B6.

During wound healing, MRL mice upregulate more genes involved in tissue repair

while B6 mice upregulate more genes associated with inflammation (Li et al., 2001).

Inflammatory cells arrive at the wound site in both strains, but the provisional matrix

formed at the injury site in MRL is more quickly degraded by matrix metalloproteinases

MMP-2 and MMP-9 which allows for true regeneration as opposed to scarring

(Gourevitch et al., 2003). Typically, only fetal mammalian wounds heal without scarring

due to an altered inflammatory environment that allows for the formation of normal

tissue (Harty et al., 2003).

Additional research using the intra-articular fracture model found that the protection from PTA in MRL mice correlated with lower systemic levels of pro-inflammatory IL-1α and higher levels of anti-inflammatory IL-4 and IL-10 (Ward et al., 2008). MRL mice also have a reduced number of activated macrophages present in the synovium and these macrophages are eliminated from the joint environment more quickly than in B6 mice (Lewis, 2010). Macrophages are a key cell type involved in both the inflammatory and resolution phases of wound healing (Porcheray et al., 2005; Serhan and Savill, 2005) and have also been implicated in the development of OA through the production of MMPs as well as inflammatory cytokines (Blom et al., 2007; Bondeson et al., 2010).

1.8 The isolation of murine mesenchymal stem cells

The isolation and characterization of MSCs from mice has been complicated by slow growth and the persistence of contaminating cell populations during in vitro culture (Peister et al., 2004; Phinney et al., 1999; Tropel et al., 2004). A widely used protocol uses low cell densities to allow the MSC colonies to emerge over time (Peister et al., 2004). Other studies used frequent washing of the dish after isolation or immunodepletion of unwanted cell types in order to start with a cell population enriched with MSCs for culture (Baddoo et al., 2003; Phinney, 2008; Soleimani and Nadri, 2009). Various growth factors (Phinney et al., 1999; Tropel et al., 2004) or the

11

application of low oxygen tension (Boregowda et al., 2012; Short et al., 2009) have been

used to stimulate proliferation. Different sources of the MSCs have also been

investigated, as bone digested with collagenase was shown to be an enriched source of

MSCs as compared to bone marrow (Short et al., 2009; Zhu et al., 2010).

Morikawa et al established a purified MSC population from collagenase-digested

bone by flow cytometry cell sorting for cells that co-expressed platelet derived growth

factor receptor alpha (PDGFRα) and stem cell antigen-1 (Sca-1) (Morikawa et al., 2009).

These rare cells were confirmed to be self-renewing MSCs in that secondary MSCs

isolated 16 weeks after initial isolation and transplantation to a recipient mouse were

clonally multipotent in vitro (Morikawa et al., 2009). The MSCs were found to be

located in the arterial perivascular space near the inner surface of the cortical bone and

provide components of the HSC niche, consistent with known properties of MSCs

(Sacchetti et al., 2007).

1.9 Induced pluripotent stem cells for therapy and modeling

Induced pluripotent stem cells (iPSCs) are "reprogrammed" adult cells that

demonstrate pluripotent properties similar to ESCs. This was first accomplished using

mouse fibroblasts by the introduction of four transcription factors: Oct4, Sox2, Klf4, c-

Myc (Takahashi and Yamanaka, 2006) and was later accomplished using human

fibroblasts (Takahashi et al., 2007; Yu et al., 2007). These transcription factors can be

delivered with a single vector containing all four of the necessary reprogramming genes to limit the number of insertion sites (Carey et al., 2009).

There are two main goals of research with iPSCs. The first is the large-scale production of patient-matched progenitor cells that could be used in cell therapy and tissue engineering strategies without the risk of donor site morbidity or immune rejection (Sun et al., 2010). The self-renewal of iPSCs in culture allows for a nearly limitless supply of cells, with extended passaging associated with a lengthening of telomeres and gene expression similar to that of ESCs (Chin et al., 2009; Marion et al., 2009). The second goal is to generate "disease in a dish" models by reprogramming cells from afflicted patients in order to screen possible therapeutics (Park et al., 2008). Generating iPSC models of disease allows for the in vitro study of exceptional human or mouse phenotypes in ways that are not possible using adult cells, such as studying processes of early development or differentiating iPSCs into specific cell types for high throughput drug screens. There are numerous challenges for the creation of such in vitro models, including selection of the appropriate somatic cell to reprogram, differentiation of iPSCs to faithfully reproduce the disease state, and dealing with the loss of epigenetic signatures of the disease during the reprogramming process (Saha and Jaenisch, 2009).

1.10 Chondrogenesis of pluripotent stem cells

Work with mouse and human ESCs established methods for the chondrogenic differentiation of pluripotent cells. As with adult stem cells, growth factors associated with cartilage development have been employed to induce chondrogenesis, including TGF-β1 (Hwang et al., 2006a), TGF-β3 (Fecek et al., 2008; Yeung et al., 2009), BMP-2 (Kramer et al., 2000; Toh et al., 2007), BMP-4 (Kramer et al., 2000; Nakayama et al., 2003), BMP-6 (Seda Tigli et al., 2009), and platelet derived growth factor (PDGF) (Nakayama et al., 2003) Monolayer culture with the right growth factor regimen can induce chondrogenesis in ESCs (Oldershaw et al., 2010; Waese and Stanford, 2011), but without a 3D structure it is challenging to assess the formation of tissue-engineered cartilage. The formation of embryoid bodies (EBs) results in aggregates that encourage the simultaneous differentiation of multiple cell lineages. In attempts to limit the heterogeneity resulting from EBs, several investigators have skipped this step and proceeded directly to systems such as micromass (Gong et al., 2010; Yamashita et al., 2010) or pellet culture (Nakagawa et al., 2009). Another strategy has been to alter the cell microenvironment to induce chondrogenic differentiation, including the use of Arg-Gly-Asp (RGD) modified hydrogels (Hwang et al., 2006b) or collagen microspheres (Yeung et al., 2009).

Chondrogenic differentiation has also been achieved from both mouse (Teramura et al., 2010) and human iPSCs (Kim et al., 2011; Medvedev et al., 2011; Wei et al., 2012). Each of these studies employed EB culture and then used the outgrowth cells without selection in 3D systems. While staining for cartilaginous matrix was seen in each case, starting with an undefined population of cells from EB culture may limit the effectiveness of tissue-engineered cartilage for either therapy or modeling. Importantly, two studies demonstrate chondrogenesis from the synovial cells or chondrocytes of OA patients (Kim et al., 2011; Wei et al., 2012), suggesting that patients most in need of regenerative approaches have a potential supply of therapeutic cells using iPSC technology.

1.10 Research goals and significance

The overall goals of this research are to develop fundamental techniques and provide a rationale for stem cell-based strategies that seek to:

1) treat cartilage injury and osteoarthritis by creating tissue-engineered cartilage from human adult stem cells,

2) prevent the development of post-traumatic arthritis by delivering stem cells to the joint after injury, and

3) study cartilage by establishing a system for producing tissue-engineered cartilage constructs from induced pluripotent stem cells of patients or mouse strains with specific properties.

There are limited treatment options to treat small cartilage lesions or widespread joint degeneration. The first research goal seeks to directly address this need by investigating the most effective ways to produce tissue-engineered cartilage for use in treating focal cartilage defects or resurfacing the joint surface with a biological replacement.

Another major clinical problem is the accelerated development of OA after joint injury, although the defined initiating event allows for the possibility of preventive treatments before degradation of cartilage has occurred. The second research goal seeks to deliver stem cells directly to the knee joint of a mouse after fracture in order to assess this treatment option and provide information on other avenues for preventing post-traumatic arthritis.

Finally, the many complex factors that lead to the development of OA make it challenging to perform mechanistic studies on how cartilage responds to specific environmental or genetic contributors to OA. Mouse models have shown incredible insight into the etiology of OA, but in vitro studies allow for much tighter control over variables and the ability for scale-up. The third research goal seeks to establish a system

for generating cartilage tissue-engineered constructs from iPSCs so that mouse strains and patients with known phenotypes related to cartilage and OA can be studied for the response to specific catabolic stimuli such as mechanical injury or inflammatory cytokines.

1.11 Hypotheses and aims

The research goals were addressed through five hypotheses and specific aims. Aim 1 utilized human adult stem cells and a scaffold derived from native porcine cartilage to investigate the contributions of cell type, growth factors, and cell microenvironment to cartilage tissue engineering. Aims 2 and 3 were accomplished by developing a novel method for the isolation and expansion of murine MSCs. Cells isolated from two strains of mice were delivered to the joints of mice after intra-articular fracture in order to prevent the subsequent development of OA. Aims 4 and 5 involved the establishment of a robust method to promote chondrogenesis in murine iPSCs and then sort successfully differentiated cells using flow cytometry. These cells were then expanded in monolayer and used to create cartilage constructs or contribute to the repair of in vitro cartilage defects.

Hypothesis 1: Human adult stem cells derived from adipose tissue and bone marrow will display distinct responses to chondroinductive growth factors and cell microenvironments.

Specific Aim 1: Assess the chondrogenic differentiation of ASCs and MSCs induced by combinations of TGF-β3 and BMP-6 in either alginate hydrogels or in cartilage-derived matrix scaffolds.

Hypothesis 2: MSCs from "superhealer" MRL mice will have altered in vitro properties as compared to MSCs from control B6 mice.

Specific Aim 2: Isolate a defined population of multipotent MSCs from the bones of B6 and MRL mice and perform in vitro characterization to assess their yield, colony forming unit potential, proliferation, differentiation, chemotaxis, and immunomodulatory capabilities.

Hypothesis 3: MSC therapy will prevent the development of PTA after intra-articular fracture by altering the inflammatory environment of the joint. MRL MSCs will be more effective than B6 MSCs at preventing PTA.

Specific Aim 3: Deliver culture-expanded MSCs from MRL and B6 mice directly to the joint space of B6 mouse knees after intra-articular fracture and assess the gene expression of inflammatory cytokines, the presence of inflammatory mediators in synovial fluid and serum, and the degeneration of cartilage.

Hypothesis 4: Culture systems promoting aggregation of cells and the presence of growth factors will induce chondrogenesis in a subset of murine iPSCs, which can be

18

identified by Col2 gene expression and production of cartilaginous matrix in pellet culture.

Specific Aim 4: Utilize a variety of three-dimensional culture systems and growth factor delivery strategies to maximize chondrogenic differentiation of iPSCs as assessed by gene expression and a Col2-GFP reporter.

Hypothesis 5: Successfully pre-differentiated iPSCs will generate tissue-engineered constructs with enhanced deposition of cartilaginous matrix and stronger cartilage defect repair as compared to cells that did not respond to pre-differentiation.

Specific Aim 5: Perform flow cytometry cell sorting based on Col2 expression in response to micromass culture with BMP-4. After expanding the sorted cells, culture either as pellets for analyzing the production of collagen and GAGs or deliver cells in agarose to fill in vitro cartilage defects.

2. Chondrogenesis of adult stem cells from adipose tissue and bone marrow: Induction by growth factors and cartilage-derived matrix

A version of this chapter was published as the following:

2.1 Introduction

Cartilage tissue engineering seeks to combine cells, biomaterial scaffolds, and bioactive signals to create functional tissue replacements to treat cartilage injuries or osteoarthritis (Guilak et al., 2001; Song et al., 2004). Primary chondrocytes expanded in vitro are one cell source that has been used for autologous chondrocyte implantation (ACI) (Brittberg et al., 1994), but there has been growing interest in alternative cell sources for cartilage tissue engineering. Adult stem cells derived from adipose tissue (adipose-derived adult stem cells, ASCs) (Gimble and Guilak, 2003; Zuk et al., 2001) and bone-marrow (bone marrow-derived mesenchymal stem cells, MSCs) (Caplan, 1991; Pittenger et al., 1999) have shown significant chondrogenic potential for such a tissue engineering approach (Erickson et al., 2002; Guilak et al., 2004; Mackay et al., 1998; Yoo et al., 1998). ASCs have attracted interest due to ease of isolation procedure and relative abundance of cells available as compared to MSCs (Aust et al., 2004; Varma et al., 2007), but remain less well characterized.

While many studies tend to refer to these cell types using similar terminology, i.e., adipose-derived mesenchymal stem cells (Im et al., 2005; Kern et al., 2006; Rider et al., 2008; Sakaguchi et al., 2005), a growing number of studies have shown human ASCs and MSCs to be very similar but not identical cell types in monolayer culture with regard to morphology, proliferation, gene expression, and cell surface markers (Afizah et al., 2007; De Ugarte et al., 2003a; De Ugarte et al., 2003b; Hennig et al., 2007; Huang et al., 2005; Im et al., 2005; Izadpanah et al., 2006; Kern et al., 2006; Kim and Im, 2008; Kim et al., 2008; Lee et al., 2004; Liu et al., 2007; Mehlhorn et al., 2006; Noel et al., 2008; Rebelatto et al., 2008; Rider et al., 2008; Sakaguchi et al., 2005; Segawa et al., 2008; Wagner et al., 2005; Winter et al., 2003). Some differences include ASCs being smaller (Izadpanah et al., 2006), ASCs achieving higher passage numbers before senescence (Izadpanah et al., 2006; Kern et al., 2006; Lee et al., 2004), differential expression of genes related to proliferation (Lee et al., 2004; Wagner et al., 2005), and ASCs having reduced or absent transforming growth factor beta (TGF-β) receptor ALK-5 (Hennig et al., 2007) and cell surface marker vascular cell adhesion molecule 1 (CD106) (De Ugarte et al., 2003a; Kern et al., 2006; Noel et al., 2008; Rider et al., 2008). In addition to these biological characterizations, many studies have compared the chondrogenic potential of the two cell types. With the exception of a few studies (De Ugarte et al., 2003b; Izadpanah et al., 2006; Kern et al., 2006; Lee et al., 2004), it has been observed that under standard chondrogenic differentiation conditions, MSCs have an enhanced potential for

21

chondrogenesis as compared to ASCs by measures such as glycosaminoglycans (GAG) production, type II collagen gene expression and deposition, pellet size, and consistency among donors for differentiation (Afizah et al., 2007; Huang et al., 2005; Im et al., 2005; Liu et al., 2007; Mehlhorn et al., 2006; Noel et al., 2008; Rebelatto et al., 2008; Rider et al., 2008; Sakaguchi et al., 2005; Segawa et al., 2008; Winter et al., 2003).

However, it is important to note that these studies have used identical culture conditions for ASCs and MSCs, typically utilizing TGF-β and dexamethasone (DEX) to induce chondrogenesis, with some studies adding additional growth factors (Im et al., 2005; Izadpanah et al., 2006; Sakaguchi et al., 2005; Segawa et al., 2008). The tacit assumption in such studies is that culture conditions "optimized" for MSCs will also be "optimal" for ASCs. However, emerging evidence suggests that any comparison study between ASCs and MSCs will be affected by the specific culture conditions used. ASCs have been shown to be more efficiently induced toward a chondrogenic lineage by a high dose of bone morphogenetic protein-6 (BMP-6) than by TGF-β or other cocktails (Estes et al., 2006). Hennig et al demonstrated that the addition of BMP-6 to a TGF-β culture medium resulted in robust chondrogenesis of ASCs similar to MSCs with TGF-β (Hennig et al., 2007). Kim and Im demonstrated that a larger concentration of growth factors was able to overcome initial differences in chondrogenic differentiation between ASCs and MSCs (Kim and Im, 2008). The response of adult stem cells to soluble factors that induce differentiation is therefore one method of identifying differences amongst

22

tissue sources. A study design that incorporates multiple chondrogenic media

conditions may be able to better assess these divergent responses to growth factors than

previous single condition studies. Our first hypothesis was that ASCs and MSCs are

distinct cell types with unique responses to growth factors or other chondroinductive

culture conditions.

In addition to the growth factor conditions, the extracellular environment can

also influence cellular growth and differentiation. Pellet culture has been used

extensively as a model system to compare chondrogenesis in MSCs and ASCs because it

recapitulates the condensation that occurs during cartilage development and maintains

the potential for cell-cell interaction (Johnstone et al., 1998). Alginate bead culture is a

model system that encourages a rounded cell phenotype to induce stem cells toward a

chondrocyte-like lineage (Awad et al., 2004). Recent studies have shown that scaffolds

consisting of reconstituted native cartilage-derived matrix (CDM) can induce the

chondrogenesis of ASCs (Cheng et al., 2009) or MSCs (Yang et al., 2008), potentially

through the establishment of interactions between cell surface receptors and

extracellular matrix ligands present on the native tissue proteins. Such cell-matrix

interactions are important in cartilage development (Shakibaei, 1998) and homeostasis

(Svoboda, 1998), as well as collagen remodeling by mesenchymal stem cells (Chang et

al., 2007). Studies using tissues such as heart (Ott et al., 2008), bladder (Chun et al.,

2007), tendon (Basile et al., 2008), and recently the clinical transplantation of a donor

airway (Macchiarini et al., 2008) have also shown the value in using native tissue architecture to provide instructive cues for tissue engineering (Badylak et al., 2009). Using the cell environment to induce chondrogenesis in place of or in addition to growth factors allows for further understanding of the role of the extracellular matrix in regulating chondrogenesis. Thus, our second hypothesis was that chondrogenesis in ASCs and MSCs will be affected by the cell microenvironment (alginate or CDM).

2.2 Materials and Methods

2.2.1 Monolayer cell expansion

Human ASCs were obtained from subcutaneous abdominal adipose tissue (Zen-Bio). ASCs from 7 female donors (average age 41) were combined after initial expansion to make a "superlot". Cells were cultured at 8000 cells/cm^2 through four passages in DMEM/F12 (BioWhittaker) containing 0.25 ng/ml TGF-β1 (R&D Systems), 5 ng/ml epidermal growth factor (EGF) (Roche Diagnostics), and 1 ng/ml basic fibroblast growth factor (bFGF) (Roche) as well as 10% fetal bovine serum (FBS, Atlas Biologicals) as described previously (Estes et al., 2006). Human MSCs were obtained from the posterior superior iliac crest of donors as approved by an Institutional Review Board as described previously (Lennon and Caplan, 2006a). MSCs from 3 female donors (average age 27) were combined in a "superlot" after initial expansion. Cells were cultured at 5000 cells/cm^2 through four passages in DMEM-low glucose (Gibco) containing 1 ng/ml bFGF and 10% FBS (Sigma-Aldrich,).

2.2.2 Chondrogenic differentiation

ASCs and MSCs were either resuspended in 1.2% alginate ($5x10^6$ cells/ml) and

dropped in 102 mM calcium chloride solution with a 1 ml pipette to form beads, or

seeded onto 6 mm diameter cartilage-derived matrix (CDM) scaffolds (500,000 cells in 30

μl media added for 1 hour before culture medium added). CDM was prepared by

homogenizing porcine articular cartilage at a concentration of 0.1 g wet weight/ml

distilled water and then lyophilizing for 24 h as described previously (Cheng et al.,

2009).

Alginate and CDM constructs were cultured for 14 or 28 days. Low attachment

24 well plates (Corning Life Sciences) were used with 1 ml of culture medium, changed

every other day. Culture media contained DMEM-high glucose (Gibco), 1% penicillin-

streptomycin (Gibco), 37.5 μg/ml L-ascorbic acid 2-phosphate (Sigma-Aldrich), 40 μg/ml

L-proline (Sigma-Aldrich), and 1% ITS+ Premix (Collaborative Biomedical) plus

combinations of the following chondroinductive agents (see figures 1 and 3): 100 nM

dexamethasone (DEX) (Sigma-Aldrich), 10 ng/ml TGF-β3 (R&D Systems), 10 or 500

ng/ml BMP-6 (R&D Systems). A subset of the alginate bead conditions were used for

CDM constructs. Day 14 constructs were evaluated with quantitative real time RT-PCR

(qPCR) and day 28 constructs were either digested for biochemical analysis or prepared

for immunohistochemistry as described below.

2.2.3 RNA isolation and real-time quantitative RT-PCR (qPCR)

Fourteen day qPCR samples were prepared for RNA isolation (n=3 independent samples per group). CDM constructs were snap frozen in liquid nitrogen and pulverized using a mortar and pestle, while alginate beads were treated with 150 mM NaCl and 55 mM Na Citrate to release the cells. RNA was isolated using TRIzol reagent (Invitrogen) and quantified with spectrophotometry (Nanodrop ND-1000). The RNA was reverse transcribed with SuperScript VILO (Invitrogen) and analyzed for gene expression using EXPRESS qPCR SuperMix Universal (Invitrogen) on an iCycler (Bio-Rad). Primer probes (Applied Biosystems) were used to determine transcript levels in triplicate for a housekeeping gene and 4 different genes of interest: 18S ribosomal RNA (endogenous control; assay ID Hs99999901_s1), aggrecan (ACAN1; assay ID Hs00153936_m1), type I collagen (COL1A1; assay ID Hs00164004_m1), type II collagen (COL2A1; custom assay: FWD Primer 5-GAGACAGCATGACGCCGAG-3; REV primer 5-GCGGATGCTCTCAATCTGGT-3; Probe 5-FAM-TGGATGCCACACTCAAGTCCCTCAAC-TAMRA-3) (Mehlhorn et al., 2006), and type X collagen (COL10A1; assay ID Hs00166657_m1). The standard curve method was used to determine starting transcript quantity (copy number) for each gene using plasmids containing the gene of interest. Data were analyzed by calculating the fold difference compared to day 0 cells of the same type, with each sample first normalized to its own 18s value.

2.2.4 Biochemical analysis

Day 28 biochemical samples (n=3 independent samples per group) were

analyzed for double stranded DNA (dsDNA) and sulfated GAG. Both alginate and

CDM constructs were digested for 16 hours with 1 ml of 125 µg/ml papain. The

PicoGreen fluorescent dsDNA assay (Molecular Probes) with λ DNA standard curve

was used to calculate µg of dsDNA as a surrogate for cell number (Estes et al., 2006).

The 1,9-dimethylmethylene blue (DMB) assay (Enobakhare et al., 1996) with pH

adjusted to 1.5 was used to quantify total sulfated GAG against a chondroitin-4-sulfate

standard curve (Awad et al., 2003).

2.2.5 Immunohistochemistry and histology

Day 28 immunohistochemistry samples were fixed overnight at 4 °C in a pH 7.4

solution containing 4% paraformaldehyde, 100 mM sodium cacodylate, and 50 mM

BaCl$_2$. Both alginate and CDM constructs were taken through a series of increasing

ethanol solutions and xylene steps to clear the constructs. Samples were then embedded

in paraffin and cut into 5 µm sections. Monoclonal antibodies to type I collagen (ab6308,

Abcam), type II collagen (II-II6B3; Developmental Studies Hybridoma Bank, University

of Iowa), type X collagen (C7974, Sigma-Aldrich), and chondroitin 4-sulfate (2B6

antibody, gift from Dr. Virginia Kraus) were used. Sections for collagen staining were

treated with Pepsin (Digest-All, Zymed) and sections for chondroitin 4-sulfate were

treated with trypsin, soybean trypsin inhibitor, and chondroitinase ABC (all Sigma-

Aldrich) to expose the epitopes. The anti-mouse IgG secondary antibody (Sigma-Aldrich, Product No. B7151) was linked to horseradish peroxidase and reacted with aminoethyl carbazole using the Histostain-Plus ES Kit (Zymed). General histological staining using 0.1% aqueous Safranin-O, 0.02% fast-green, and hematoxylin was also performed on xylene cleared sections. Human osteochondral plugs were prepared in the same manner as samples and were used as positive controls for each antibody. Negative controls without primary antibody were also prepared for each slide.

2.2.6 Statistical analysis

Two factor ANOVA and Fisher's PLSD post-hoc test (α=0.05) was used to determine significance for cell type and culture condition. Outliers were removed according to Chauvenet's Criterion (Taylor, 1982).

2.3 Results

2.3.1 The effect of growth factors on gene expression

Gene expression is presented as the fold difference in copy number from day 0 values for each cell type (Figure 2-1). For the alginate beads, the main effects of cell type and culture condition, as well as the interaction term, were statistically significant by ANOVA for all genes studied (p<0.001) (Figure 2-1A). ACAN1 expression was enhanced in control conditions for MSCs (17 fold increase over day 0 cells) but not ASCs. The presence of only DEX caused a decrease in MSC ACAN1 expression as compared to control (p<0.001) but had no effect on ASCs. Both ASCs and MSCs

responded robustly to growth factor induction, with all three growth factor groups significantly increased relative to control ($p<0.001$). ASCs had the highest upregulation of ACAN1 with 500 ng/ml BMP-6 (857 fold increase) and MSCs had the highest upregulation with 10 ng/ml TGF-β3 and DEX (573 fold increase). With both BMP-6 and TGF-β present in the culture medium, no differences were observed between the cell types in terms of ACAN1 upregulation ($p>0.05$).

COL2A1 expression in ASCs was only significantly upregulated as compared to control when both TGF-β3 and BMP-6 were administered ($p<0.001$), while COL2A1 expression in MSCs was significantly upregulated in all growth factor groups ($p<0.001$). The highest expression was seen in the TGF-β3 plus DEX group, with a 130,450 fold increase from day 0 values.

COL10A1 expression was significantly higher in MSCs as compared to ASCs for each culture condition tested ($p<0.001$). For ASCs, COL10A1 expression remained below day 0 values in every group except those containing TGF-β3. For MSCs, COL10A1 expression was downregulated compared to control in both the DEX and 500 ng/ml BMP-6 groups ($p<0.001$) and was strongly upregulated in conditions containing TGF-β3 (1720 and 2319 fold increases over day 0 cells for TGF-β3 and dual cocktail of TGF-β3 and BMP-6, respectively).

COL1A1 expression was significantly increased in all three growth factor groups as compared to control in both cell types (p<0.01). In each culture condition, MSCs had a higher fold increase over day 0 values than ASCs (p<0.001).
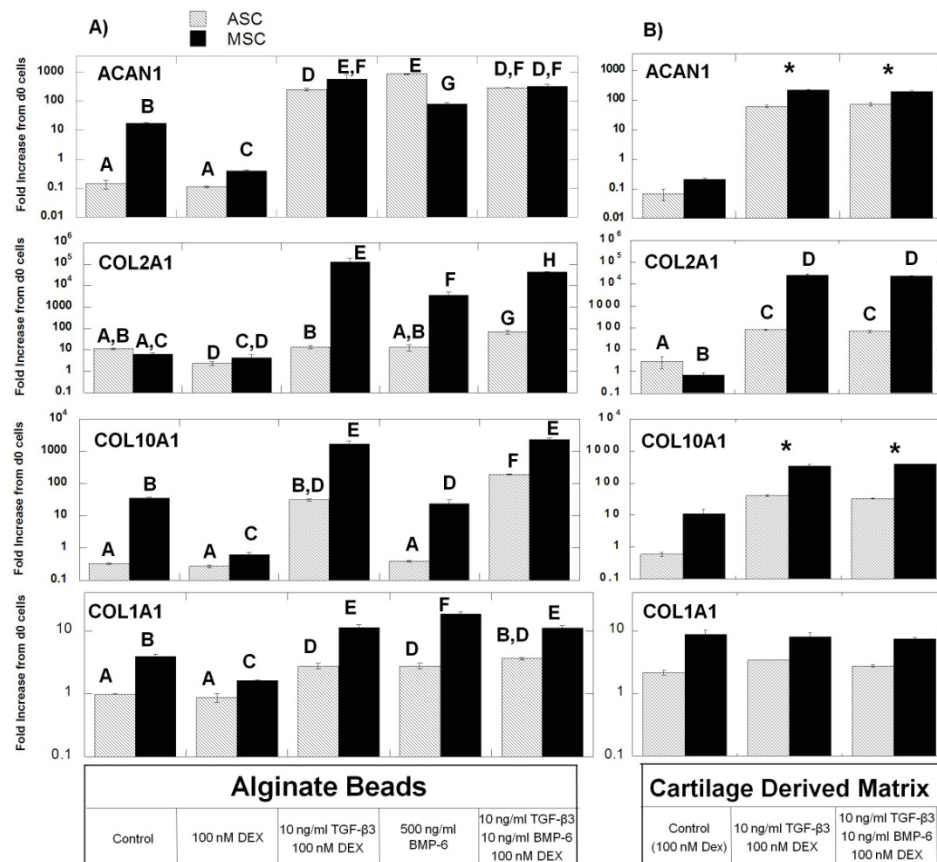
Figure 2-1: Effects of growth factors and cell microenvironment on gene expression. Day 14 qPCR for (A) alginate bead and (B) CDM constructs seeded with ASCs or MSCs (as labeled). Data presented as fold difference from day 0 cells for ACAN1, COL2A1, COL10A1, and COL1A1. Groups not sharing a letter are statistically different by Fisher PLSD post-hoc. Asterisk indicates media condition is significantly different from control by Fisher PLSD post-hoc.

2.3.2 The effect of extracellular environment on gene expression

For the CDM constructs, the main effects of cell type and culture condition were statistically significant by ANOVA (p<0.001) for each gene studied with the exception of

the effect of culture condition on COL1A1 expression (Figure 2-1B). The interaction

term of cell type and culture condition was only significant for COL2A1. The two

growth factor groups investigated were a subset of those studied in the alginate bead

system and both included 10 ng/ml TGF-β3 plus 100 nM DEX, with one group also

containing 10 ng/ml BMP-6.

In CDM constructs, ACAN1 upregulation was higher in MSCs than ASCs

($p<0.05$) and was significantly higher in the growth factor conditions as compared to

control ($p<0.001$), with no difference between the two groups. The highest ACAN1

upregulation over day 0 cells was the MSCs TGF-β3 only group with a 217 fold increase.

COL2A1 expression was enhanced in the growth factor groups over control conditions

for both cell types ($p<0.001$), but to a much greater degree in MSCs with an average

increase of 23,927 fold over day 0 cells for MSCs and 74 fold for ASCs.

For COL10A1 expression, MSCs had significantly higher upregulation than ASCs

in CDM constructs ($p<0.001$) and the growth factors induced higher COL10A1

expression as compared to the control conditions ($p<0.001$). Finally, COL1A1 expression

was higher in MSCs as compared to ASCs ($p<0.001$) but there was no difference among

the media conditions ($p>0.05$).

2.3.3 Biochemical composition of CDM scaffolds and alginate beads

Figure 2-2 depicts the gross appearance of the CDM scaffolds after 28 days of

culture. The texture of the scaffolds in the growth factor groups is altered and is

smoother than the seeded constructs cultured in control conditions or the unseeded

construct. There was contraction of the CDM scaffolds as compared to the 6 mm

diameter starting scaffold, with the most contraction occurring in growth factor treated

groups.
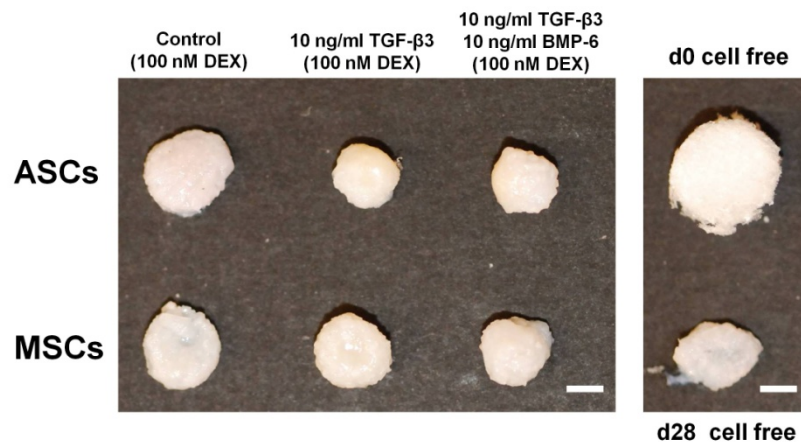
Figure 2-2: Morphology of CDM constructs. Gross appearance of CDM scaffolds seeded with ASCs or MSCs under control, TGF-β, and TGF-β plus BMP-6 conditions (as labeled) at day 28. An unseeded CDM construct at day 0 and an unseeded construct cultured for 28 days are also shown. Scale bar is 2 mm.

The viability and cell proliferation was measured by using dsDNA as a surrogate

and is expressed as the percentage of each cell type's starting dsDNA (Figure 2-3). The

amount of sulfated GAG was measured using the DMB assay and is presented both in

terms of total GAG and GAG per DNA (Figure 2-3). In both the alginate bead and CDM

systems, MSCs had significantly higher DNA values as compared to ASCs under each

culture condition ($p < 0.05$). The highest values in alginate beads were seen in the TGF-β3

and BMP-6 group, with 126% of day 0 DNA in MSCs and 46% in ASCs, and the highest

values in the CDM were seen in the TGF-β3 only group, with 277% in MSCs and 98% in

ASCs. Total GAG production in the alginate beads was higher in the MSCs as compared

to ASCs for both conditions containing TGF-β3 (p<0.001) but was higher in the ASCs for

the 500 ng/ml BMP-6 group (p<0.001). Total GAG production in the CDM was higher in

the MSCs under all conditions (p<0.05), and was highest in the TGF-β3 only group (316

μg for MSCs and 134 μg for ASCs). The trends were slightly altered in the alginate

beads when GAG production was normalized to DNA content, as GAG per DNA was

higher in ASCs as compared to MSCs for the TGF-β3 only group in addition to the BMP-

6 group (p<0.001).
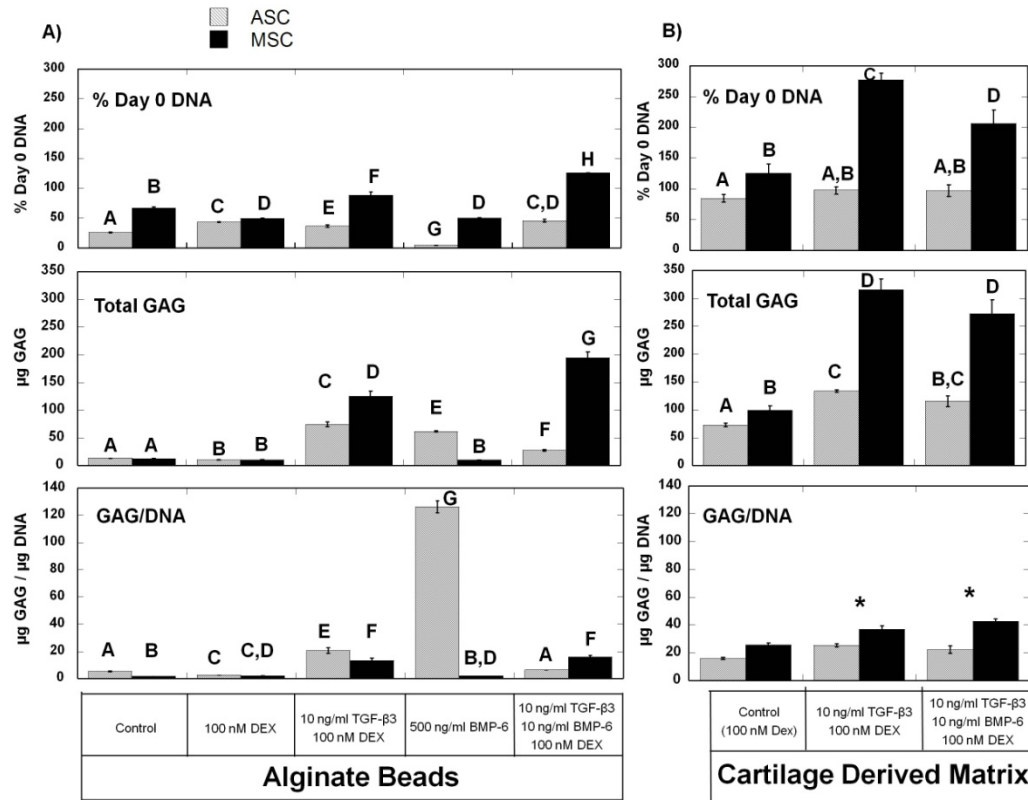
Figure 2-3: Biochemical analysis at day 28. Percentage of day 0 DNA, total GAG content (μg), and GAG content per DNA (μg/μg) for (A) alginate bead and (B) cartilage-derived matrix constructs seeded with ASCs or MSCs (as labeled). Groups not sharing a letter are statistically different by Fisher PLSD post-hoc for cell type and culture condition. Asterisk indicates media condition is significantly different from control by Fisher PLSD post-hoc.

2.3.4 Immunohistochemistry for matrix proteins

The immunohistochemical staining of day 28 CDM scaffolds for type I, II, and X collagen, as well as chondroitin-4-sulfate, is shown in Figure 2-4. All scaffolds demonstrate staining for type II collagen and chondroitin-4-sulfate with minimal staining for types I and X collagen. The native porcine matrix is still present at 28 days and partially contributes to the positive staining for the extracellular matrix proteins of

cartilage. Cell seeded scaffolds demonstrated enhanced retention of native matrix as

compared to the unseeded CDM scaffold. Neotissue was synthesized by both ASCs and

MSCs in response to growth factor conditions and was clearly distinguished from native

matrix by intensity of staining as well as texture. The neotissue was more abundant in

MSC seeded scaffolds as compared to ASCs, with matrix staining positive for type II

collagen and chondroitin-4-sulfate completely filling in the CDM in response to TGF-β3.

The two growth factor groups, TGF-β3 and TGF-β3 plus BMP-6, elicited generally

similar matrix deposition from both cell types, with the exception that MSC synthesis of

chondroitin-4-sulfate appeared to be stronger in the TGF-β3 only group. Type I collagen

staining was detected in the neotissue at similar levels for each scaffold but was not

nearly as abundant as type II collagen. No significant staining for type X collagen was

observed.
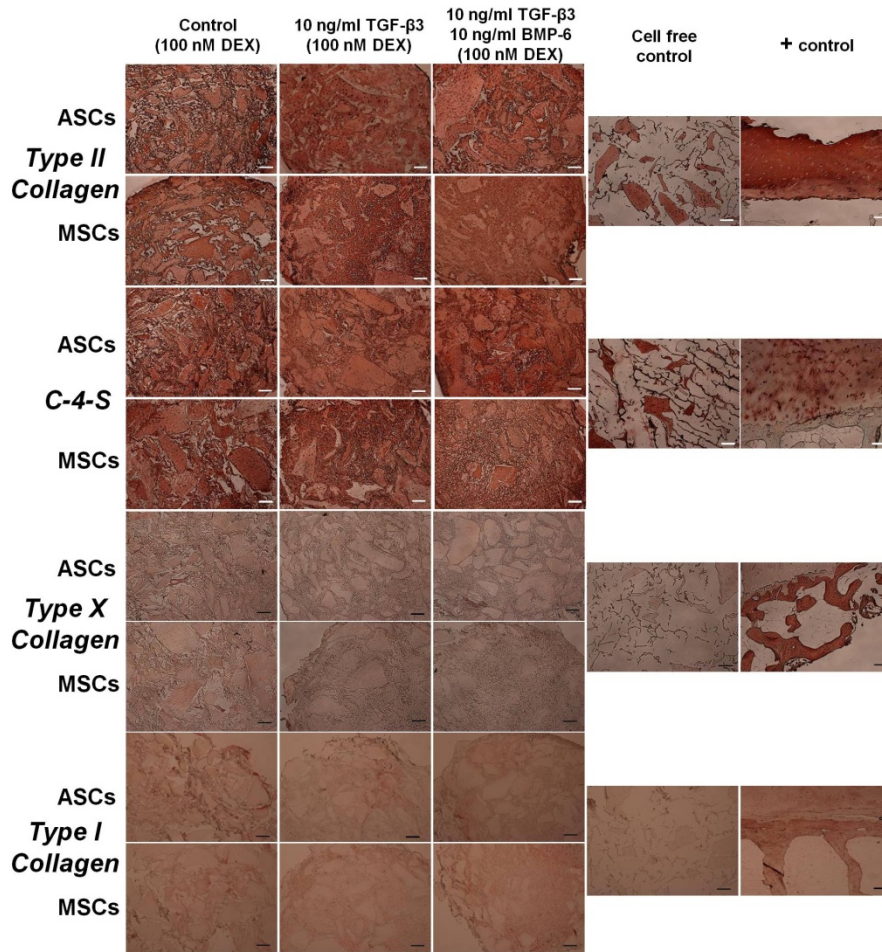
Figure 2-4: Immunohistochemistry of CDM scaffolds. Immunohistochemistry for type II collagen, chondroitin-4-sulfate, type X collagen, and type I collagen. Cartilage-derived matrix seeded with ASCs or MSCs under control, TGF-β, and TGF-β plus BMP-6 conditions (as labeled) at day 28. A human osteochondral plug is the positive control and an unseeded CDM construct cultured for 28 days is provided as an additional control. Pictures 4x magnification with 200 μm scale bar.

2.3.5 Cell shape of ASCs and MSCs in CDM scaffolds

High magnification images of Safranin-O/Fast Green stained sections indicated

that the cell morphology of MSCs had become rounded in response to growth factors

while the ASCs appeared to remain spindle-shaped (Figure 2-5).
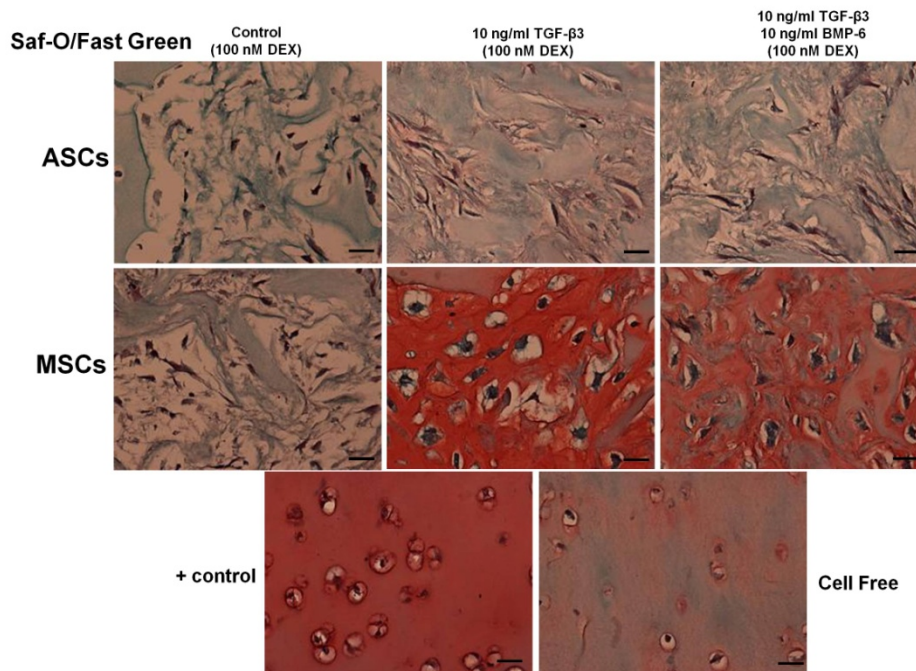
Figure 2-5: Cell shape of ASCs and MSCs in CDM scaffolds. Safranin-O/Fast Green staining with hematoxylin counterstain. Cartilage-derived matrix seeded with ASCs or MSCs under control, TGF-β, and TGF-β plus BMP-6 conditions (as labeled) at day 28. A human osteochondral plug is the positive control and an unseeded CDM construct cultured for 28 days is provided as an additional control. Pictures 40x magnification with 20 μm scale bar.

2.3.6 The effect of serum on stem cell chondrogenesis

Experiments were performed to evaluate the effect of serum on ASCs and MSCs

during differentiation (Figure 2-6). In the CDM system, the extent of new matrix

production was not significantly altered by serum (Figure 2-6B), but gross appearance

suggested that 10% serum did affect the culture system by enhancing cell mediated

contraction (Figure 2-6A). In the alginate bead system, ASCs produced more type II

collagen in response to TGF-β when 10% serum was included (Figure 2-6C). MSCs

produced less type II collagen in response to TGF-β when serum was present.
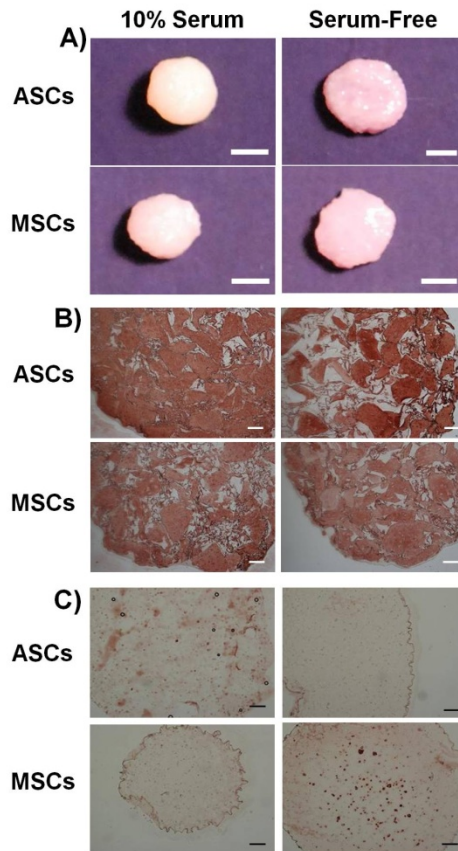
Figure 2-6: Effect of serum on chondrogenesis. CDM and alginate constructs cultured in the presence of 10% fetal bovine serum or in serum-free conditions (as labeled) for 28 days. (A) Gross appearance of ASC or MSC seeded CDM constructs in control conditions containing 100 nM DEX. (B) Type II collagen immunohistochemistry of ASC or MSC seeded CDM constructs in control conditions containing 100 nM DEX. (C) Type II collagen immunohistochemistry of ASC or MSC seeded alginate bead constructs cultured with 10 ng/ml TGF-β3 and 100 nM DEX. Scale bars are 2 mm for (A) and 200 μm for (B) and (C).

2.4 Discussion

Adult stem cells from adipose tissue and bone marrow underwent chondrogenic induction by growth factors in both alginate bead culture and cartilage-derived matrix scaffolds, demonstrating upregulation of cartilage-specific genes and the synthesis of

cartilaginous proteins. Under the conditions used in this study, MSCs demonstrated an overall greater chondrogenic response than ASCs as indicated by higher COL2A1 upregulation and more extensive matrix synthesis across all media conditions in both alginate beads and CDM. However, the level of induction of chondrogenic genes was highly dependent on the exact culture conditions used in each experiment. Thus, the conclusion that MSCs are inherently more chondrogenic than ASCs is not warranted from this work or similar comparison studies due to the strong dependence of results on the monolayer expansion (Estes et al., 2008), three-dimensional culture conditions (Hennig et al., 2007; Kim and Im, 2008), and time point of analysis (Afizah et al., 2007; Mehlhorn et al., 2006; Winter et al., 2003). "Optimal" conditions for both cell types remain to be discovered over time, but this study was not designed with that goal in mind. Instead, we sought to demonstrate the unique nature of MSCs and ASCs through divergent responses to chondrogenic growth factors and extracellular matrices. Our findings also show that CDM may provide a novel culture system for the study of stem cell chondrogenesis, alone or in combination with exogenous growth factors.

While ASCs and MSCs exhibited many of the same trends in response to chondrogenic induction, some distinct responses to the specific growth factors used in alginate bead culture were observed. ASCs had significantly higher ACAN1 upregulation in response to BMP-6 than to TGF-β, while the opposite was true for MSCs. This trend was supported by GAG content when normalized for DNA content but not

when total GAG content was used due to the low cell viability in the ASCs BMP-6 group. The large response of ASCs to high dose BMP-6 supports previous work (Estes et al., 2006).

MSCs showed a stronger propensity than ASCs toward a "hypertrophic" chondrocyte phenotype, as observed by the upregulation of COL1A1 and COL10A1 without the addition of growth factors. However, both cell types showed similar upregulation of these genes in response to growth factor supplementation as compared to control conditions. Enhanced COL10A1 in MSCs as compared to ASCs has been seen by others (Huang et al., 2005; Liu et al., 2007; Mehlhorn et al., 2006). Interestingly, higher COL10A1 upregulation in MSCs appears to be in response to 3D conditions and not monolayer expansion, as we saw a 3 fold higher COL10A1 copy number in ASCs than MSCs at day 0 (data not shown). A high dose of BMP-6 in addition to TGF-β has been shown to cause upregulation of COL10A1 in MSCs (Sekiya et al., 2001), while BMP-6 alone caused a downregulation of COL10A1 in ASCs (Estes et al., 2006). Our data in alginate beads illustrate that 500 ng/ml BMP-6 without TGF-β resulted in COL10A1 expression similar to control values in ASCs and slightly downregulated compared to control for MSCs, but that TGF-β induced significant COL10A1 upregulation in both ASCs and MSCs.

An important finding of this study was the comparison of the chondrogenic potential of ASCs and MSCs in a scaffold derived from native cartilage.

41

Immunohistochemistry for type II collagen and chondroitin-4-sulfate indicated that

MSCs seeded in CDM synthesized abundant new cartilaginous matrix that filled in any

open areas of the native porcine cartilage scaffold. New matrix was also seen in ASC

constructs but had not fully filled in the CDM scaffold by the 28 day time point. Part of

the enhanced matrix synthesis may be explained by the increased proliferation of MSCs

as compared to ASCs, although GAG/DNA measures indicate significantly higher GAG

synthesis when controlled for cell number as well as total GAG content. MSCs in

growth factor conditions adopted a spherical morphology amongst the neotissue, while

ASCs retained the elongated phenotype characteristic of monolayer culture. The cell

type differences in immunohistochemical results correlated to growth factor induced

gene expression data at day 14, as significantly greater upregulation in COL2A1 and

ACAN1 was seen in MSCs as compared to ASCs.

In general, similar results were seen in terms of gene expression and biochemical

assays between the alginate bead system and CDM, although viability/cell proliferation

was enhanced in the CDM. MSCs had a different response to growth factors in the two

model systems. In the alginate beads, both percentage of day 0 DNA and total GAG

content were significantly higher in the dual cocktail of TGF-β and BMP-6 as compared

to TGF-β alone, while TGF-β alone had higher viability and higher (although not

statistically significant) GAG as compared to the dual cocktail in CDM. The CDM also

limited MSC upregulation of COL10A1 in response to conditions containing TGF-β

(33.36 average fold increase over control in CDM vs. 57.76 in alginate beads) without

decreasing the upregulation of COL2A1 (35,187 average fold increase over control in

CDM vs. 14,031 in alginate beads). This was supported by the lack of extensive staining

for type X collagen in the CDM scaffolds at day 28. The observation that cell-matrix

interactions may limit the hypertrophic phenotype during MSC chondrogenesis could

be important for future work. The hypertrophic chondrocyte phenotype during

chondrogenic differentiation has been well documented for MSCs (Mueller and Tuan,

2008; Pelttari et al., 2006) and ongoing work is attempting to address it (Kim et al., 2008).

A recent study demonstrated that adult stem cells from bone-marrow, adipose tissue,

and synovium all demonstrated some degree of calcification in vivo after in vitro growth

factor based chondrogenesis (Dickhut et al., 2009).

For both ASCs and MSCs, the CDM without exogenously added growth factors

induced minimal new matrix synthesis and no upregulation in chondrogenic gene

expression, illustrating the importance of growth factor supplementation. Previous

work using CDM indicated that significant chondrogenic induction of ASCs can be

achieved without the use of growth factors (Cheng et al., 2009). One difference between

the studies is that the current study was serum-free during differentiation while the

previous work included 10% FBS throughout the culture period. Thus, the presence of a

variety of growth factors and cytokines in serum may significantly influence, and

potentially interact with, the effects of the CDM on chondrogenesis. While this study

43

saw effects of serum on contraction but not matrix production, serum has been shown to be inhibitory to cartilage production in synovial fibroblast (Bilgen et al., 2007; Kurth et al., 2007) and chondrocyte culture (Ballock and Reddi, 1994). Serum-free chondrogenic conditions have been standard for MSC culture ever since early observations in rabbit MSCs that pellets did not form in the presence of 10% serum (Johnstone et al., 1998). ASCs have been successfully differentiated down a chondrogenic lineage in 10% serum in alginate beads (Awad et al., 2003; Estes et al., 2006) and in 1% serum in micromass culture (Zuk et al., 2001). The current study demonstrated that in alginate beads treated with TGF-β, ASCs produced more type II collagen in the presence of serum while MSCs produced more type II collagen without serum. Similarly, ASCs show enhanced ACAN1 expression in control conditions if 10% FBS is present (data not shown). While further study is needed to confirm the observation that ASCs differentiate at least as well in the presence of serum, the present findings taken together with previous literature suggest responsiveness to serum may be another possible difference between the two cell types. A second difference between this study and Cheng et al (Cheng et al., 2009) is the greater degree of contraction seen during culture in the present study, even though serum-free conditions were used. The mechanical properties of the specific CDM scaffolds could affect chondrogenic differentiation as mechanical cues such as substrate stiffness (Engler et al., 2006) and cell shape (McBeath et al., 2004) have been shown to affect stem cell differentiation toward other lineages.

The guiding hypothesis that ASCs and MSCs are unique cell types that respond to different culture conditions led us to choose to expand each cell type in monolayer conditions that have been shown to be effective at priming that particular cell type for chondrogenesis instead of using identical culture conditions (Estes et al., 2008; Solchaga et al., 2005). For example, lot-selected FBS specific to each cell type was used, with the MSC serum chosen by a rigorous selection process described elsewhere (Lennon and Caplan, 2006a). Since bFGF has been demonstrated to have substantial effects on downstream chondrogenesis in both MSCs and ASCs (Chiou et al., 2006; Solchaga et al., 2005), both cell types were expanded in the presence of 1 ng/ml bFGF.

2.5 Summary

Extracellular environment and growth factors are both important for guiding the chondrogenic differentiation of adult stem cells. This work establishes the potential for cartilage-derived matrix scaffolds as a valuable model for comparing stem cell chondrogenesis across different tissue sources. MSCs demonstrated more robust chondrogenesis as compared to ASCs and also showed a greater tendency to display the hypertrophic chondrocyte phenotype in the specific conditions studied, although these results do not speak to the intrinsic chondrogenic potential that is ultimately possible for the two cell types. This study supports previous work illustrating the distinct nature of ASCs and MSCs by their responses to different growth factors and culture conditions.

3. Characterization of a prospectively isolated mesenchymal stem cell population from C57BL/6 and MRL/MpJ "superhealer" mice

3.1 Introduction

The MRL/MpJ (MRL) "superhealer" inbred mouse strain is one of the few models of mammalian regeneration. Since the original observation of rapid closure of ear wounds (Clark et al., 1998), MRL mice have shown enhanced regeneration as compared to the control C57BL/6 (B6) strain in injury models of cornea, heart, digit tips, articular cartilage, and intra-articular fracture (Chadwick et al., 2007; Fitzgerald et al., 2008; Leferovich et al., 2001; Ueno et al., 2005; Ward et al., 2008). Several lines of evidence suggest that adult stem cells may be responsible for the healing phenotype of MRL mice.

Mesenchymal stem cells (MSCs), alternately referred to as multipotent mesenchymal stromal cells (Horwitz et al., 2005), have been defined by in vitro characteristics (Dominici et al., 2006) and most of the work with MSCs has focused on the differentiation into specific cell types (Caplan, 2007; Pittenger et al., 1999; Prockop, 1997). However, an emerging paradigm indicates that MSCs function primarily to alter the inflammatory environment by either direct secretion of bioactive factors or the "trophic" effects of altering cytokine and growth factor production of other cells (Caplan and Dennis, 2006; Iyer and Rojas, 2008; Phinney and Prockop, 2007; Prockop, 2007). The role of MSCs in tilting the balance of the injured environment from inflammation to

regeneration is consistent with what is observed in the MRL mouse after injury. As

compared to B6 mice during closure of ear wounds, MRL mice upregulated more tissue

repair genes instead of inflammatory genes (Li et al., 2001) and remodeled the

provisional matrix to allow for regeneration instead of scarring (Gourevitch et al., 2003).

In a model of intra-articular fracture, protection from osteoarthritis in MRL mice

correlated with lower local and systemic levels of inflammatory cytokines such as

interleukin-1 (IL-1), as well as a reduced number of activated macrophages present in

the synovium (Furman, 2009; Lewis, 2010; Ward et al., 2008).

Several studies have investigated the specific cell types and cellular features

responsible for healing in MRL mice. Bone-marrow transfer between B6 and MRL mice

after irradiation indicated some effect of donor marrow but that the recipient mouse is

primarily responsible for the ear healing phenotype, implicating non-bone marrow cell

types or radiation resistant cells of the marrow (Bedelbaeva et al., 2004; Heber-Katz,

1999; Kench et al., 1999). Endogenous MSCs are very resistant to irradiation due to their

slow cycling (Morikawa et al., 2009). In a cell therapy experiment, Alfaro et al found

that bone-marrow derived MSCs from MRL mice showed enhanced engraftment,

deposition of granulation tissue, and functional improvement in a model of myocardial

injury (Alfaro et al., 2008). This was attributed to higher expression levels of the Wnt

inhibitor secreted frizzled related protein 2 (sFRP2). Differences between the strains

may also be related to the cell cycle and expression of the p21 cell cycle checkpoint

47

protein in cells at the site of injury, as lack of p21 expression after DNA damage was shown to be essential to the healing phenotype of MRL mice (Bedelbaeva et al., 2010).

The isolation and characterization of MSCs from mice is complicated by slow growth and the persistence of contaminating cell populations during in vitro culture (Phinney et al., 1999). Strategies to overcome these limitations have included extended culture periods at particular densities (Meirelles Lda and Nardi, 2003; Peister et al., 2004; Sun et al., 2003), modified plating techniques (Soleimani and Nadri, 2009; Taipaleenmaki et al., 2008) or immunodepletion to remove undesirable cell types (Anjos-Afonso and Bonnet, 2008; Baddoo et al., 2003; Phinney, 2008; Tropel et al., 2004), utilizing compact bone as an enriched source as compared to bone marrow (Guo et al., 2006; Short et al., 2009; Sung et al., 2008; Zhu et al., 2010), and the application of growth factors (Baddoo et al., 2003; Tropel et al., 2004) or low oxygen tension during expansion (Short et al., 2009). Morikawa et al were able to prospectively isolate a very pure population of MSCs utilizing collagenase digested bone and flow cytometry cell sorting for cells co-expressing platelet derived growth factor receptor α (PDGFRα, also known as CD140a) and stem cell antigen-1 (Sca-1) (Morikawa et al., 2009).

In this study, we found that culturing prospectively isolated MSCs at a low oxygen tension resulted in very fast expansion rates, thus providing a pure and extensive source of murine MSCs. As a first step to understanding the contribution of MSCs to the healing phenotype of MRL mice, we investigated whether MSCs isolated

48

from B6 and MRL mice would display distinct in vitro properties with regard to frequency, proliferation, multilineage differentiation, chemotaxis, or immunomodulation.

3.2 Materials and Methods

3.2.1 MSC isolation

Male MRL/MpJ (The Jackson Laboratory) or C57BL/6 (Charles River Laboratories) were sacrificed at 8-10 weeks of age with CO_2 in accordance with a protocol approved by the Duke University Institutional Animal Care and Use Committee. Femurs and tibias were cleaned of excess tissue and kept on ice in HBSS media (Sigma-Aldrich) containing 2% fetal bovine serum (FBS; Sigma-Aldrich), 1 mM Hepes (Invitrogen), and 1% penicillin/streptomycin/fungizone (P/S/F; Invitrogen). Bones were crushed in a mortar and pestle and exposed bone marrow was gently removed by washing. Bone fragments were digested for 60 minutes on a shaker at 37 °C with 0.2% collagenase type I (Worthington Biochemical) in DMEM-LG (Invitrogen) containing 1 M Hepes and 1% P/S/F and then filtered through a 70 μm strainer (BD biosciences). Cells were centrifuged and resuspended in ACK buffer containing 0.15 M NH_4Cl, 10 mM $KHCO_3$, and 0.1 mM Na_2EDTA in dH_2O to lyse erythrocytes. Cells resuspended in PBS (Invitrogen) with 1% FBS were treated with Fc block and labeled with antibodies to mouse CD45 (FITC), TER-119 (FITC), Sca-1 (Alexa 647), and PDGFRα (PE) or isotype controls for 30 minutes at 4 °C (all from Biolegend). A Cytomation

49

MoFlo® sorter (Beckman Coulter) with 100 µm nozzle was used to capture cells

negative for CD45/TER-119 and positive for both Sca-1 and PDGFRα (Morikawa et al.,

2009).

3.2.2 MSC expansion

After sorting, MSCs were cultured at 100 cells/cm^2 in expansion medium

consisting of αMEM (Invitrogen), 20% FBS, and 1% P/S/F in a hypoxic incubator (37 °C,

2% O_2, 5% CO_2, remaining gas N_2). After 8 days with media changes every 3 days, cells

were trypsinized using 0.05% trypsin-EDTA (Sigma-Aldrich) and plated at 3000

cells/cm^2. Subsequent passages were carried out every 3-4 days upon 90% confluence.

3.2.3 Colony-forming unit (CFU-F) assay

Freshly sorted MSCs were plated at 250 cells per well of a 6 well plate (9.5 cm^2) in

expansion medium. After 7 days with no medium changes, wells were stained with 3%

crystal violet, washed repeatedly with PBS, and then analyzed for defined colonies of

greater than 10 cells using standard microscopy.

3.2.4 Tail fibroblast isolation and expansion

Fibroblasts isolated from the tails of both mouse strains served as a non-

progenitor control cell type. The overlying skin was removed and tails were minced

into approximately 1 cm pieces before overnight digestion with 0.2% collagenase type I

in DMEM-LG with 5% FBS and 1% P/S/F. Digested tissue was then filtered through a 70

µm strainer and cells were plated at 50,000 cells/cm^2 in DMEM-LG with 15% FBS and 1%

P/S/F in normoxic conditions (20% O_2, 5% CO_2). At confluence, cells were passaged and plated at 5000 cells/cm^2, with media changed every 3 days.

For the cell expansion experiment, some tail fibroblasts were plated at 2% O_2 to investigate the effects of hypoxia. An additional method of tail fibroblast isolation based on cell outgrowth was also used for the cell expansion experiment. Pieces of minced tail were plated directly onto 0.1% gelatin coated flasks and fibroblasts were allowed to migrate out of the tissue and attach to the plate. After 5-7 days, tissue pieces were removed and the cells were passaged as with the collagenase method.

3.2.5 Flow cytometry

Passage 3 cells were divided into aliquots of 100,000 cells, treated with Fc block for 10 minutes at 4 °C, then incubated for 30 minutes at 4 °C with antibodies to following cell surface markers and appropriate isotype controls (all from Biolegend): mouse CD45 (FITC), CD49d (FITC), TER-119 (FITC), CD44 (PE-Cy5), CD29 (PE-Cy5), C-X-C chemokine receptor 4 (CXCR4) (Alexa 647), CD11b (APC), PDGFRα (PE), Sca-1 (Alexa 647). A C6 benchtop flow cytometer (Accuri Cytometers) was used for analysis and percentages obtained by subtracting the value of isotype controls.

3.2.6 Adipogenic differentiation

Passage 2-3 cells were plated at 10,000 cells per well of 48 well plates (0.95 cm^2) for 2 days in expansion medium at normoxic conditions. Media was then switched to control medium consisting of DMEM/F12 (Lonza) with 3% FBS and 1% P/S/F or

adipogenic differentiation medium (Guilak et al., 2006) consisting of control medium

plus (all from Sigma-Aldrich) 33 μM biotin, 17 μM pantothenate, 1 μM bovine insulin, 1

μM dexamethasone, and for the first three days only 250 μM isobutylmethylxanthine

(IBMX) and 2 μM rosiglitazone (Avandia™). Cells were cultured for 14 days, with 90%

of the media changed every 3 days. After 14 days, cells were imaged and then fixed

with 4% paraformaldehyde for 20 minutes at room temperature followed by a PBS

wash. Oil Red O stain (EMD Chemicals) at 0.5% in isopropanol was diluted 3:2 in

distilled water, filtered, and then 200 μl used to stain the monolayers for 15 minutes at

room temperature. Cells were washed with 60% isopropanol and photographed. Stain

was released with 250 μl of 100% isopropanol for 5 minutes and then quantified by

absorbance at 535 nm using a dilution curve of the highest stained well to show

linearity.

3.2.7 Osteogenic differentiation

Passage 2-3 cells were plated at 10,000 cells per well of 48 well plates (0.95 cm^2)

for 2 days in expansion medium at normoxic conditions. Media was then switched to

control medium consisting of DMEM-HG with 10% FBS and 1% P/S/F or osteogenic

differentiation medium (Wan et al., 2006) consisting of control medium plus 10 mM β-

glycerophosphate (Sigma-Aldrich), 250 μM ascorbate (Sigma-Aldrich), 2.5 μM retinoic

acid (Sigma-Aldrich), and 50 ng/ml hBMP-2 (R&D systems). Cells were cultured for 21

days, with 90% of the media changed every 3 days. After differentiation, cells were

fixed with 4% paraformaldehyde for 20 minutes at room temperature followed by two

washes with dH_2O. Alizarin Red S (Electron Microscopy Sciences) at 2% in dH_2O with

pH 4.1-4.3 using ammonium hydroxide was added for 20 minutes at room temperature

with gentle shaking. After two washes with dH_2O, wells were photographed and then

Alizarin stain was released for quantification (Gregory et al., 2004). After 200 µl acetic

acid (10% v/v) was added for 30 minutes at room temperature with shaking, cells were

scraped and transferred to an Eppendorf for vortexing. Heated extraction was

performed at 85 °C for 10 minutes followed by 5 minutes on ice. After centrifugation of

20,000 xg for 15 minutes, 125 µl of the supernatant was transferred to a 96 well plate.

Fifty µl of ammonium hydroxide (10% v/v) was added to neutralize the acid and

absorbance was measured at 405 nm using a dilution curve of the highest stained well to

show linearity.

3.2.8 Chondrogenic differentiation

Rounded pellets containing 250,000 passage 2-3 cells were formed in 15 ml

polypropylene tubes by centrifugation at 300 xg for 5 minutes. After 2 days, media was

switched from expansion medium to serum-free control medium consisting of DMEM-

HG (Invitrogen), 1% ITS+ (BD), 50 µg/ml ascorbate (Sigma-Aldrich), 40 µg/ml proline

(Sigma-Aldrich), and 1% P/S/F (Sigma-Aldrich) or chondrogenic differentiation medium

(Blom et al., 2007) consisting of control medium plus 10 ng/ml transforming growth

factor-beta 3 (hTGF-β3) (R&D) and 500 ng/ml bone morphogenetic protein-6 (hBMP-6)

(R&D). Pellets were cultured for 28 days, with 90% of the media changed every 3 days.

After 28 days, pellets were processed for histology and immunohistochemistry by

Safranin-O/Fast-Green and type II collagen or biochemical analysis by DNA for cell

number and 1,9-dimethylmethylene blue (DMB) for glycosaminoglycan (GAG) content

as described previously (Estes et al., 2010).

3.2.9 Chemotaxis assay

Passage 3 cells were serum starved overnight by changing the media to 1% FBS

expansion media. Cells were then trypsinized, washed, and resuspended in control

medium consisting of αMEM with 0.1% BSA. The bottom wells of 10 μm ChemoTx

plates (Neuro Probe) were filled with 31 μl control medium or medium containing 1, 3,

5, 10% serum or 1, 10, 50 ng/ml platelet derived growth factor (rPDGF-BB) (R&D

Systems) as chemoattractants. Cell suspension containing 30,000 cells in 55 μl was

placed on top of the filter and given 4 hours at 37 °C for migration. After 4 hours, cells

that migrated through were transferred to a separate 96 well plate while cells that

remained on the top of the filter were wiped away. This was aided by the use of 40 μl of

HBSS with 2 mM EDTA to help remove attached cells from the filter and centrifugation

to ensure all migrated cells were collected. Cells were quantified using the Cyquant

assay as directed (Invitrogen) with 1 hour incubation at 37 °C, implementing a standard

curve using known quantities of cells and calculating a chemotactic index by

normalizing to the serum-free control for that cell type.

3.2.10 Inhibition of splenocyte proliferation assay

MSCs and tail fibroblasts at passage 3 were treated with 25 µg/ml mitomycin C

(Sigma-Aldrich) for 30 minutes at 37 °C to inhibit proliferation and were plated at 20,000

cells in 100 µl of expansion medium per well of a 96 well plate for 2 days. Spleens were

freshly isolated from sacrificed mice and disaggregated into a Petri dish containing

RPMI media with 10% heat inactivated serum. After repeated passes through a 20.5 ga

needle and a 70 µm strainer, splenocytes were centrifuged and resuspended in ACK

buffer to lyse red blood cells. Appropriate wells received 200,000 splenocytes for the

assay. The base medium of RPMI (Invitrogen), 10% serum, 1% P/S/F, and 50 µm β-

mercaptoethanol (Sigma-Aldrich) was supplemented in some wells with 5 µg/ml

concanavalin A (ConA, Sigma-Aldrich) and 5 µg/ml phytohaemagglutanin (PHA,

Sigma-Aldrich) to stimulate splenocyte proliferation. After 2 days, 5-bromo-2'-

deoxyuridine (BrdU, Roche Applied Science) was added to the medium for the final 18

hours of culture and proliferation was quantified using an antibody to BrdU and

absorbance as directed (Roche).

3.2.11 Statistical analysis

Statistical analysis was carried out using a T-test for comparison of two groups

and analysis of variance (ANOVA) with Fisher's LSD post-hoc analysis for comparison

of multiple groups, using α=0.05. Standard error of the mean is displayed in figures.

3.3 Results

3.3.1 Expansion of B6 and MRL MSCs

MSCs were isolated from collagenase digested bones of B6 and MRL mice based on the expression of cell surface markers. A representative isolation of cells from MRL mice shows 0.70% of all cells were negative for the hematopoietic markers CD45 and TER-119, and 5.09% of these cells were positive for both PDGFRα and Sca-1 (Figure 3-1A). B6 and MRL mice contained a similar frequency of MSCs, with yields of approximately 300-600 MSCs per mouse. Within the sorted MSC population, MRL mice demonstrated a higher frequency of colony forming cells as assessed by the CFU-F assay (19 ± 1.15 vs. 10 ± 0.58 colonies per 250 starting cells, p<0.05).

MSCs from both strains established colonies that quickly grew to confluence and maintained a spindle-shaped morphology through 3 passages (Figure 3-1B). MSCs expanded at high rates in αMEM media containing 20% lot-selected FBS in a 2% O_2 environment, with B6 MSCs expanding greater than 100,000 fold in three weeks (Figure 3-1C). MSCs from B6 mice demonstrated a consistent trend of greater expansion as compared to MRL MSCs, resulting in a 13 fold higher cumulative fold increase at the end of 3 passages (154,141 ± 113,095 vs. 11,728 ± 5069 cells per starting cell).
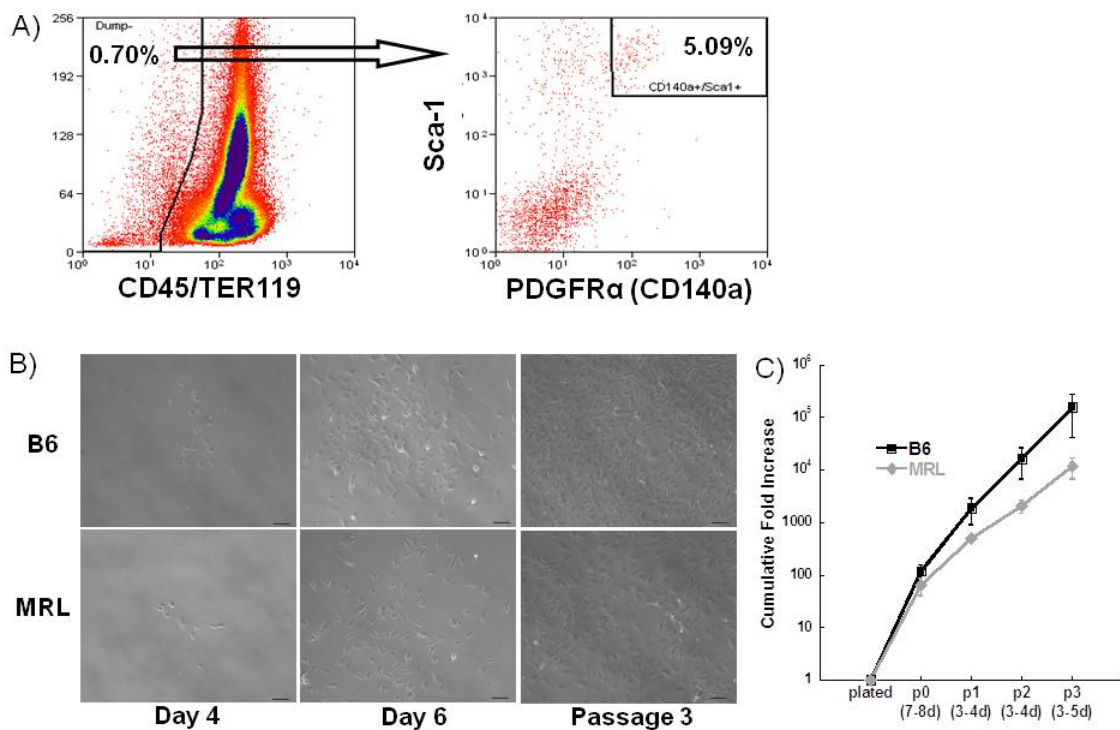
Figure 3-1: Cell sorting and expansion. A) Sorting strategy for representative MRL MSC isolation. B) MSCs plated down after sorting, expanded rapidly, and retained morphology in culture. Scale bars = 100 μm. C) Cumulative fold increase at 2% O$_2$; results averaged from 3 isolations with SEM displayed.

3.3.2 Cell surface marker expression by flow cytometry

To confirm in vitro cultured MSCs maintained their phenotypes, flow cytometry was used to assay surface marker expression on passage 3 cells. The MSCs from both strains displayed the expected phenotypes after 3 passages, being uniformly positive for CD44 and Sca-1 and uniformly negative for CD11b and CD45 (Table 3-1). Most MSCs also retained the presence of PDGFRα, used for initial sorting (91.4% of B6 and 81.9% of MRL). The cultured MSCs from both strains were negative for cell surface markers related to homing such as CD49d and CXCR4, and low cell yields prevented the

57

possibility of analyzing freshly isolated cells. Fibroblasts isolated from the tails of both

strains of mice served as a non-progenitor control cell type. Tail fibroblasts exhibited

many of the same markers as MSCs (Table 3-1).

Table 3-1: Cell surface phenotype of passage 3 MSCs and tail fibroblasts

Cell Surface Marker	B6 MSC	MRL MSC	B6 Tail Fib	MRL Tail Fib
CD44	≥ 95%	≥ 95%	≥95%	≥95%
Sca-1	≥ 99%	98.8%	≥99%	97.7%
PDGFRα/CD140a	91.4%	81.9%	35.1%	75.0%
CD11b	≤ 1%	≤ 1%	≤1%	≤1%
CD45	≤ 0.1%	≤ 0.1%	0.6%	≤0.1%
TER119	≤ 0.1%	≤ 0.1%	≤0.1%	≤0.1%
CD49d	≤ 0.1%	≤ 0.1%	≤0.1%	0.3%
CD29	≥ 95%	≥ 95%	≥95%	≥95%
CXCR4	≤ 0.1%	≤ 0.1%	0.6%	≤0.1%

3.3.3 Multilineage differentiation of B6 and MRL MSCs

After 14 days in adipogenic media, more lipid droplets formed in B6 MSC

cultures and quantification by release of lipid staining demonstrated a significant

increase in adipogenesis as compared to MRL MSCs ($0.11 \pm .005$ vs. $.092 \pm .005$

absorbance units, $p<0.05$, Figure 3-2C). B6 MSCs also demonstrated increased

osteogenesis as compared to MRL MSCs when quantified by heated extraction of

mineralization staining (0.73 ± 0.26 vs. 0.22 ± 0.064 adjusted absorbance units, $p<0.05$,

Figure 3-2F). Chondrogenesis was assessed by GAG production GAGs and staining for

GAGs and type II collagen after 28 days of pellet culture. B6 MSC pellets contained

more GAGs than MRL MSCs (68.65 ± 1.23 vs. 20.25 ± 0.077 µg per pellet, p<0.05, Figure

2-3I). Tail fibroblasts from MRL mice demonstrated the capacity for osteogenic

differentiation and tail fibroblasts from both strains showed chondrogenic capacity

above the levels of non-induced controls, but only MSCs showed differentiation to the

adipogenic lineage.
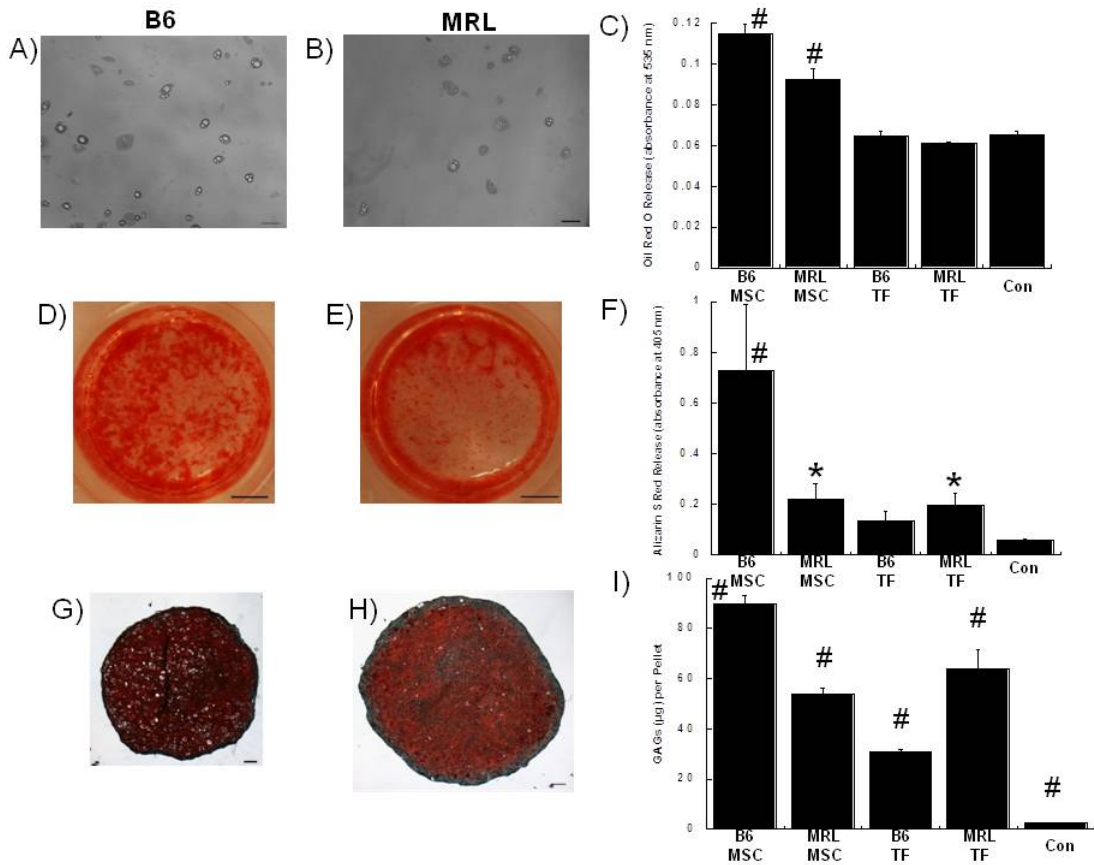
Figure 3-2: Multi-lineage differentiation. A,B) Adipogenic lipid accumulation; D,E) Osteogenic Alizarin Red S staining; G,H) Chondrogenic Safranin-O/Fast Green staining. C,F,I) Quantification, results from ≥3 samples per group of one representative isolation with SEM displayed. Asterisk indicates significance to control and pound symbol indicates significance to all groups. Scale bar = 100 μm (A,B,G,H) or 25 mm (D,E).

3.3.4 Chemotaxis

For all cell types, the chemotactic index increased with increasing levels of serum as expected (Figure 3-3A). There was a trend toward greater chemotaxis in both MRL cell types. For PDGF-BB, maximum chemotaxis occurred at 10 ng/ml in all cell types with the exception of B6 MSCs (Figure 3-3B). MRL tail fibroblasts showed significantly greater chemotaxis as compared to both B6 cell types at 10 ng/ml PDGF-BB (p<0.05).

60
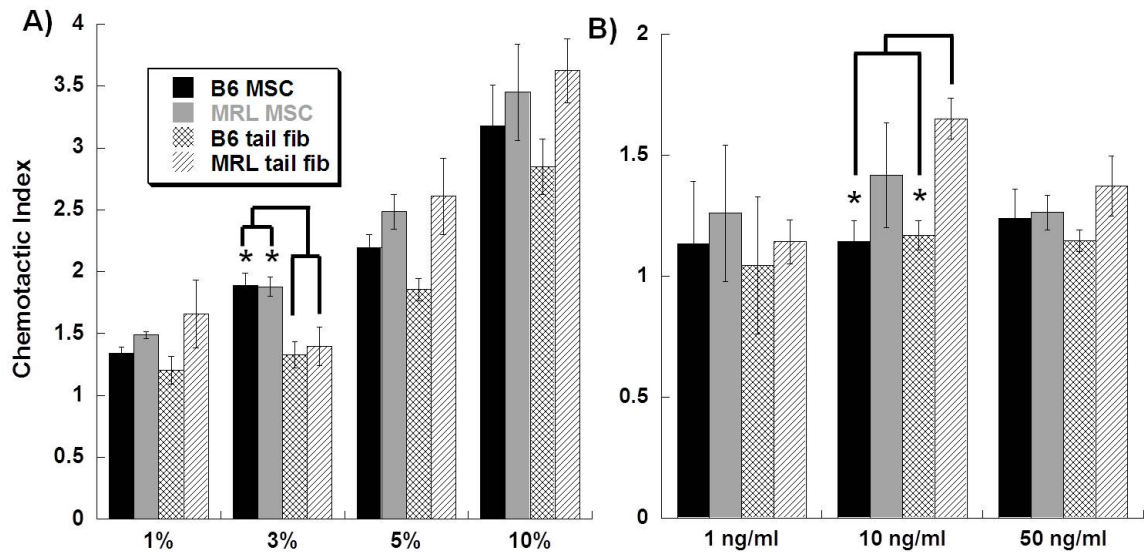
Figure 3-3: Chemotaxis toward serum and PDGF-BB. Chemotactic index representing the fold increase in chemotaxis compared to own cell type serum-free control for A) serum dose response and B) PDGF-BB dose response. Results from ≥3 wells of a representative experiment. Asterisk indicates significance.

3.3.5 Inhibition of splenocyte proliferation

MSCs and tail fibroblasts from both strains were able to inhibit the proliferation of splenocytes stimulated by the T cell mitogens ConA and PHA (Figure 3-4). All groups were significantly different than stimulated splenocytes ($p<0.05$). There was no significant effect of MSC strain ($p>0.05$) even though there was a trend toward more robust suppression of splenocyte proliferation in B6 MSCs compared to MRL MSCs as assessed by the percentage of stimulated splenocyte proliferation (4.53 ± .077 vs. 8.80 ± 1.30).
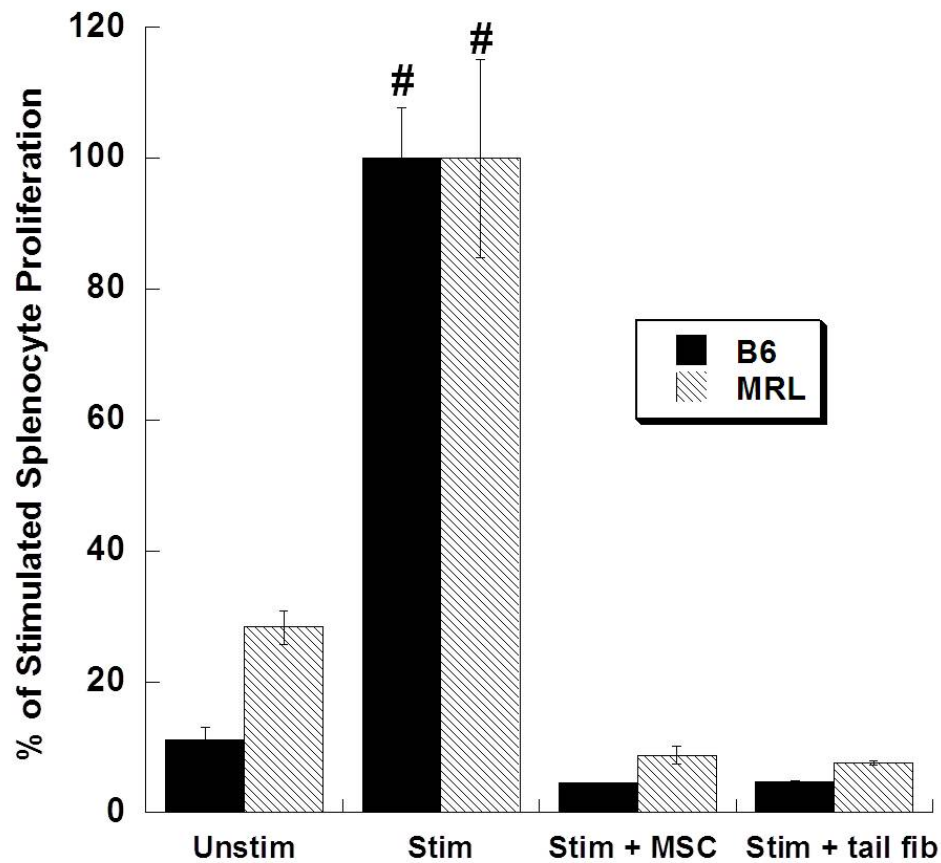
Figure 3-4: The effect of MSC co-culture on stimulated splenocyte proliferation. BrdU incorporation over the final 18 hours was assessed, normalizing to wells containing only stimulated splenocytes of the same mouse strain. ≥3 wells of one representative experiment. No statistically significant effect of mouse strain; pound indicates stimulated splenocytes different to all other groups except each other, $p < 0.05$.

3.3.6 Effect of oxygen tension on the proliferation of tail fibroblasts

The proliferation of B6 and MRL tail fibroblasts from two different isolation methods was assessed under normoxic and hypoxic conditions in a trial experiment. B6 and MRL strains showed increased proliferation at 2% O_2, and B6 tail fibroblasts demonstrated greater expansion by the end of five passages (Figure 3-5). The trends of

mouse strain and oxygen tension were similar between the collagenase method and the

outgrowth method, but expansion was greater in the collagenase digested cells.
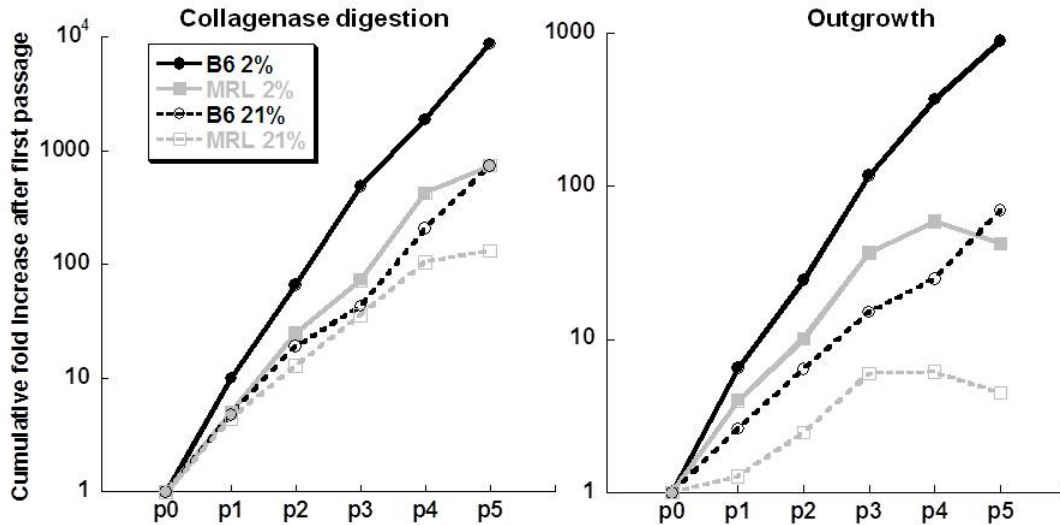
Figure 3-5: Effect of hypoxia on tail fibroblast proliferation. Tail fibroblasts from B6 and MRL mice isolated by two different methods were expanded under 2% and 21% oxygen for five passages in one trial experiment.

3.4 Discussion

Due to the development of well characterized inbred strains and the technologies

of genetic manipulation, mouse models have provided rich opportunities to study a

wide variety of human diseases as well as providing insight into normal biological

processes (Peters et al., 2007). However, the challenges associated with isolating a pure

murine MSC population and expanding those cells in vitro has limited investigations

into the relationship between stem cell function and specific phenotypic features of mice.

To explore how MSCs may contribute to an exceptional regenerative phenotype, we

developed a method for the robust expansion of a pure MSC population and characterized MSCs from B6 and "superhealer" MRL mice.

Unlike human MSCs, plastic adherence and serial passaging are insufficient to purify murine MSCs and the resulting adherent population contains contaminating cells as illustrated by the ability to fully reconstitute the hematopoietic system of irradiated mice (Phinney, 2008). Purification by depleting undesirable cells after initial in vitro culture can improve the homogeneity of MSCs but does not allow for identification of the in situ location of the cells. In contrast, positive selection of a rare population at the time of isolation results in MSCs with in vitro characteristics that can be linked to in situ properties and endogenous stem cell function (Morikawa et al., 2009; Short et al., 2009; Taichman et al., 2010). PDGFRα^+/Sca-1$^+$ cells reside in the perivascular space near the inner surface of cortical bone (Morikawa et al., 2009), consistent with the recent proposal that human MSCs are perivascular cells that associate with endothelial cells around small blood vessels in a wide range of human tissues including bone marrow, fat, muscle, and placenta (Crisan et al., 2008; da Silva Meirelles et al., 2008; Sacchetti et al., 2007; Zannettino et al., 2008). Isolated and labeled PDGFRα^+/Sca-1$^+$ cells delivered to recipient mice still demonstrated multipotent differentiation at a clonal level after secondary isolation 16 weeks later, confirming these rare cells are self-renewing MSCs (Morikawa et al., 2009).

This study confirmed previous observations (Morikawa et al., 2009) that prospective isolation of PDGFRα^+/Sca-1$^+$ cells from collagenase-digested bone results in a pure population of MSCs. The CFU-F assay has commonly been used as a means of assessing the frequency of MSCs, as clonogenic growth at low density is a hallmark of progenitor cells (Bianco et al., 2010). Typically, mouse bone marrow contains CFU-F at a frequency of approximately one in one million cells (Phinney et al., 1999). The cell sorting strategy using PDGFRα^+/Sca-1$^+$ resulted in a significant enrichment of CFU-F, with approximately one out of every twenty cells being clonogenic.

The sufficient expansion of murine MSCs for in vitro studies can be problematic due to the rarity of the population and slow growth. Prolonged expansion over several months can generate a large number of marrow derived cells, but extensive manipulation in culture alters the cell properties in such a way that they may no longer be representative of in situ function (Phinney et al., 2006). In this study, employing 2% oxygen culture substantially reduced the required culture time for expansion and provided oxygen tension levels that are more representative of the in situ bone marrow microenvironment (Ivanovic, 2009). In just 3 weeks, MSCs from B6 mice expanded greater than 100,000 fold. This is a significant improvement from the three month culture required to achieve only a 10,000 fold increase when MSCs were expanded at an atmospheric oxygen tension of 21% (Morikawa et al., 2009). This observation is in line with previous studies showing low oxygen tension facilitates human, rat, and mouse

65

MSC expansion (Das et al., 2010; Grayson et al., 2007; Lennon and Caplan, 2006b; Short et al., 2009). The effect of low oxygen on proliferation was not limited to MSCs, as a trial experiment indicated that the proliferation of tail fibroblasts from B6 and MRL mice was also enhanced at 2% O_2. Interestingly, B6 tail fibroblasts demonstrated enhanced proliferation, similar to the results seen with MSCs from the two strains.

Our hypothesis was that MSCs isolated from MRL mice would demonstrate distinct in vitro characteristics when compared to B6 MSCs. We found that although MRL MSCs have a higher frequency of clonogenic cells, these cells have lower expansion rates as compared to B6 MSCs. This was surprising given that Alfaro et al showed enhanced proliferation of MSCs from MRL mice (Alfaro et al., 2008). This may be due to differences in methodology, as we used prospective isolation of MSCs from collagenase-digested bone as opposed to whole bone marrow plating and subsequent immunodepletion, and we used 2% O_2 without growth factors instead of 21% O_2 with PDGF-BB for expansion. Regardless, the relationship between in vitro proliferation rates and in vivo functionality is unclear. While rapid expansion of MSCs is desired for in vitro studies, MSCs are typically quiescent in vivo until activated in response to specific signals (Baksh et al., 2004; Gronthos et al., 2003; Kolf et al., 2007). Indeed, 71% of freshly isolated PDGFRα^+/Sca-1$^+$ MSCs were found to be in the G0 phase (Morikawa et al., 2009).

The MSCs from both strains displayed cell surface markers consistent with previous MSC isolation strategies, showing MSCs to be positive for the HA receptor

CD44 and the hematopoietic stem cell marker Sca-1, while being negative for the

macrophage marker CD11b and pan-hematopoietic marker CD45 (Alfaro et al., 2008;

Soleimani and Nadri, 2009). The continued presence of PDGFRα after passaging may

indicate the maintenance of undifferentiated status, as progenitor cells lose PDGFRα

expression with differentiation to muscle cells or adipocytes (Ball et al., 2007; Uezumi et

al., 2010). We also assessed cell surface molecules known to be important in MSC

homing (Granero-Molto et al., 2009; Ip et al., 2007; Kumar and Ponnazhagan, 2007) and

found that MSCs expressed CD29 but not the companion integrin subunit CD49d or

CXCR4, which is the receptor for the chemokine stromal cell-derived factor 1 (SDF-1).

Tail fibroblasts were mostly indistinguishable from MSCs, emphasizing that cell surface

marker expression alone is insufficient to characterize MSCs due to the lack of specific

markers.

The in vitro expansion of MSCs does affect in vivo homing and engraftment,

possibly as a result of the downregulation of chemokine receptors such as CXCR4

(Granero-Molto et al., 2009; Morikawa et al., 2009; Rombouts and Ploemacher, 2003).

However, chemotaxis assays have been used successfully on cultured cells to provide

insight into how cells respond to chemoattractants, an important feature of endogenous

stem cells after injury or in cell therapy applications (Richter, 2009; Ringe et al., 2007).

The serum dose response provides validation of the sensitivity of the method as well as

demonstrating the migration of cells to a non-specific stimulus containing a complex

milieu of growth factors. PDGF-BB was a logical chemoattracant to use, as several

studies testing a range of growth factors showed that PDGF-BB is very potent for human

MSC chemotaxis (Fiedler et al., 2002; Mishima and Lotz, 2008; Ozaki et al., 2007) and the

murine MSCs used in this study were initially sorted for expression of a PDGF-BB

receptor and cells maintained expression at passage 3. A maximal response was noted

at 10 ng/ml PDGF-BB, but the chemotactic index at this concentration was lower than the

high doses of serum. While MRL MSCs appeared to demonstrate a trend toward greater

chemotaxis than B6 MSCs in both the serum and PDGF-BB experiments, MRL tail

fibroblasts also showed high chemotaxis and therefore this may not be a specific feature

of MSCs.

The ability to differentiate into cells with the properties of adipocytes,

osteoblasts, and chondrocytes is one of the defining properties of MSCs (Dominici et al.,

2006). Observations such as MRL mice filling cartilage defects with neotissue to a

greater degree than B6 mice only if the injury extended through the subchondral bone

(Fitzgerald et al., 2008) led us to hypothesize that superior differentiation of MRL MSCs

may be the cause of their unique regenerative potential. Contrary to this hypothesis, B6

MSCs displayed more robust differentiation down the adipogenic, osteogenic, and

chondrogenic lineage than MRL MSCs. The osteogenic and chondrogenic potential seen

in tail fibroblasts, especially of the MRL strain, may be due to the inherent heterogeneity

in using collagenase digestion of tails containing multiple cell types, or an example of

the plasticity seen in many tissue sources including skin (Huang et al., 2010; Yin et al., 2010).

Interestingly, differentiation of MSCs likely plays a secondary role in their contribution to healing. Due to the rarity of MSCs and the traditional lack of specific cell surface makers, assessing MSC contributions in homeostasis and injury response has been challenging (da Silva Meirelles et al., 2008; Uccelli et al., 2008; Valtieri and Sorrentino, 2008). However, improvements in identifying MSCs in situ (Crisan et al., 2008; da Silva Meirelles et al., 2008; Sacchetti et al., 2007; Zannettino et al., 2008) and the success of cell therapy in animal models without significant engraftment or differentiation (Gnecchi et al., 2008; Granero-Molto et al., 2009; Lee et al., 2009; Murphy et al., 2003; Nemeth et al., 2009; Ortiz et al., 2007) have established that a primary mechanism of MSC function is modulating cells of the immune system.

The mixed lymphocyte reaction (MLR) and splenocyte stimulation assays have been used as in vitro measures of immunomodulation and have demonstrated that human and mouse MSCs are able to inhibit the proliferation of stimulated T cells through secreted factors and cell-cell contact (Abdi et al., 2008; Aggarwal and Pittenger, 2005; English et al., 2007; Ghannam et al., 2010; Le Blanc et al., 2003; Ren et al., 2008; Sotiropoulou and Papamichail, 2007). The immunomodulatory properties of MSCs have also been effective in clinical trials treating severe graft-versus-host disease (Le Blanc et al., 2004). In this study, both B6 and MRL MSCs dramatically reduced the proliferation

of splenocytes stimulated with ConA and PHA, confirming their immunomodulation. However, this effect was not specific to MSCs, as similar results were seen with tail fibroblasts from both strains. This finding was consistent with data showing that human fibroblasts demonstrate an immunomodulatory effect in vitro (Cappellesso-Fleury et al., 2010; Haniffa et al., 2007).

While in vitro characterization provides an important first step for investigating the relationship between MSCs and healing in the MRL mouse, there are limitations to this work. One is that the complexity of cellular interactions that occur during the injury response cannot be reproduced in vitro, limiting the assays employed to specific aspects of MSCs that may play a role such as differentiation or immunomodulation. Additionally, it is known that some features of MSCs are "activated" by specific signals that would occur during injury (Ren et al., 2008) and therefore distinctions between B6 and MRL MSCs essential to determining the regenerative outcome may not be detected outside the context of this activation. To address these aspects, future work will apply B6 and MRL MSCs as cell therapy agents in an injury model.

3.5 Summary

We demonstrated the rapid expansion of a pure population of murine MSCs by prospective isolation from bone using PDGFRα/Sca-1 expression and subsequent culture at 2% O_2. Contrary to our hypothesis, MSCs isolated from control B6 mice displayed

faster expansion and more extensive differentiation as compared to MSCs from

MRL"superhealer" mice.

4. Mesenchymal stem cell therapy for the prevention of post-traumatic arthritis after intra-articular fracture in mice

4.1 Introduction

An estimated 27 million Americans have clinical osteoarthritis (OA) (Lawrence et al., 2008), and the risk of OA increases 10- to 20-fold following joint trauma such as ligament injury, meniscal tear, or intra-articular fracture (Anderson et al., 2011). Post-traumatic arthritis (PTA) represents 12% of lower-extremity OA cases and causes a large economic burden due to the young age of the PTA population (Brown et al., 2006). The presence of inflammatory cytokines such as interleukin-1 (IL-1) and tumor necrosis factor α (TNF-α) in the joint fluid, synovium and other joint tissues has emerged as an important contributor to the pathogenesis of both idiopathic and secondary OA (Bondeson et al., 2010; Denoble et al., 2011; Furman et al., 2006; Goldring and Otero, 2011; Guerne et al., 1989; Guilak et al., 2004). Furthermore, the rapid development of OA after closed-joint intra-articular fracture of the mouse knee has confirmed the central role of inflammation and provides a model system for examining the effects of different therapeutic approaches to prevent the onset or progression of PTA (Furman, 2009; Furman et al., 2007; Lewis, 2010).

The delivery of mesenchymal stem cells (MSCs) has been proposed as a regenerative therapy for a wide range of disease states. An emerging paradigm suggests that long-term engraftment and differentiation may not be the primary regenerative

mechanisms of exogenously delivered MSCs. Instead, MSCs modulate inflammation

and provide a regenerative environment either by direct secretion of bioactive factors, or

by altering the cytokine and growth factor production of endogenous cells (Caplan and

Dennis, 2006; Iyer and Rojas, 2008; Phinney and Prockop, 2007; Prockop and Youn Oh,

2011). While stem cell based solutions have been studied for musculoskeletal repair and

regeneration (Arthur et al., 2009; Lee et al., 2007; Murphy et al., 2003; Toghraie et al.,

2011), MSC therapy for the prevention of PTA after closed intra-articular fracture has not

been investigated.

Different mouse strains possess significantly different regenerative phenotypes,

suggesting that their MSCs may have different therapeutic effectiveness. For example,

the MRL/MpJ (MRL) "superhealer" inbred mouse strain has shown enhanced

regeneration after injury in a variety of tissues such as the ear, cornea, heart, digit tips,

and articular cartilage (Chadwick et al., 2007; Clark et al., 1998; Fitzgerald et al., 2008;

Leferovich et al., 2001; Ueno et al., 2005). Of particular interest was the observation that

MRL mice were protected from PTA after intra-articular fracture (Ward et al., 2008).

Regeneration in MRL mice is correlated with a reduced inflammatory signature after

injury (Furman, 2009; Gourevitch et al., 2003; Hunt et al., 2011; Li et al., 2001), suggesting

an altered transition from the acute inflammatory phase to a resolution phase that

allows for regeneration. The contribution of MSCs to this transition is unknown, but

bone-marrow derived MSCs from MRL mice exhibit enhanced engraftment, deposition

of granulation tissue, and functional improvement in a model of myocardial injury (Alfaro et al., 2008).

We hypothesized that the delivery of MSCs directly to the joint space after fracture would prevent the development of PTA by altering the inflammatory environment. Additionally, we used this model system to compare the regenerative capabilities of MSCs isolated from control C57BL/6 mice and MRL/MpJ "superhealer" mice.

4.2 Materials and Methods

4.2.1 Intra-articular fracture

All procedures were performed in accordance with a protocol approved by the Duke University Institutional Animal Care and Use Committee. B6 mice at the skeletally mature age of 16 weeks were used for a closed tibial plateau fracture model of PTA as described previously (Furman et al., 2007; Ward et al., 2008). Briefly, the sedated mouse was fit into a custom cradle so that the left hind limb was at neutral position under a 10 N preload, which was applied using a wedge-shaped indenter attached to a materials testing system (ElectroForce ELF3200). Compression force was applied until -2.7 mm displacement at a rate of 20 N/s in load control. Each fracture was confirmed using high resolution digital X-ray (MX-20, Faxitron). Right hind limbs were not fractured and served as contralateral controls.

4.2.2 Stem cell injection

MSCs were isolated and expanded according the method developed in chapter 3 of this dissertation. Passage 3 MSCs isolated from B6 or MRL mice were delivered immediately after fracture. The sedated mice were injected with either sterile saline only (Hospira Inc) or 10,000 MSCs in 6 µl saline using a specialty syringe (catalog #80401, Hamilton Company) and 30 ga ½ needle (BD). The mouse was positioned for lateral entry with the left hind limb extended to facilitate injection of 6 µl into the joint space through the patellar tendon. This delivery technique does not result in initiation of osteoarthritis (van der Kraan et al., 1990). To allow for cell tracking, some MSCs were first treated with 4 µM of the membrane dye chloromethylbenzamido (CM-DiI, Sigma-Aldrich) for 5 minutes and washed before injection.

4.2.3 Serum and synovial fluid analysis

At the time of sacrifice (day 1, day 3, day 7, or 8 weeks after fracture and injection), retro-orbital bleeding and cardiac stick were used to collect blood. After clotting, samples were centrifuged at 3500 rpm for 15 minutes and serum was transferred to -80 °C. At the same time points, synovial fluid from fractured and contralateral limbs was isolated from the exposed joint space as described previously (Seifer et al., 2008). Briefly, the synovial fluid was absorbed onto a Melgisorb pad and this was dissolved with alginate lyase and sodium citrate. Serum and synovial fluid from the fractured knee were analyzed for the presence of the following cytokines by

ELISA utilizing the manufacturer's instructions and a 1:5 dilution for synovial fluid samples (R&D Systems): IL-1β (cat #MLB00C), interleukin-1 receptor antagonist (IL-1ra, cat #MRA00), and interleukin-10 (IL-10, cat #M1000, serum only). Samples that were undetectable were assigned a value of one half of the lower limit of quantification for analysis.

4.2.4 Gene expression in joint capsule

At the time of sacrifice (day 1, day 3, or day 7 after fracture and injection), joint capsule tissue was isolated from both hindlimbs as described previously (Van Meurs et al., 1997). Briefly, the joint capsule was released from the knee and 3 mm biopsy punches from either side of the patella were transferred to RNALater (Qiagen). Tissue from three mice per group was combined and homogenized. RNA was isolated with Trizol (Invitrogen) and RNeasy columns (Qiagen). RNA was reverse transcribed and distributed in duplicate across wells of a custom SA Biosciences PCR array (Qiagen) containing the following genes (abbreviations follow SA Biosciences nomenclature): Interleukin-1β (Il1b), interleukin-1α (Il1a), tumor necrosis factor (Tnf), interleukin-10 (Il10), interferon gamma (Ifng), chemokine C-X-C motif ligand 5 (Cxcl5), chemokine C-C motif ligand 2 (Ccl2), chemokine C-X-C motif ligand 10 (Cxcl10), chemokine C-C motif ligand 12 (Ccl12), interluekin-1 receptor antagonist (Ilrn), interluekin-6 (Il6), heat shock protein 90 kDa (Hsp90ab1, housekeeping gene). The fold change of genes relative to the pre-fractured state was calculated using the $2^{-\Delta\Delta Ct}$ method (Livak and Schmittgen, 2001).

4.2.5 Analysis of mouse joints

Fractured and contralateral control limbs were fixed in neutral alignment using 10% neutral buffered formalin for 48 hours. Joints were transferred to 70% ethanol and analyzed with micro-CT (μCT 40, Scanco Medical) as described previously (Furman et al., 2007; Ward et al., 2008). Briefly, transverse slices of 16 μm were used to generate 3D reconstructions for bone density and bone volume analysis in 3 regions: cancellous bone of the distal femoral condyles, tibial plateau distal to subchondral plate, and metaphyseal region of tibial plateau. After micro-CT analysis, the limbs were decalcified and processed for histology using an increasing ethanol series, xylenes, and paraffin steps in an automated tissue processor (ASP300S, Leica Microsystems).

Coronal plane sections of 8 μm were taken for histology and stained with Safranin-O/Fast Green/Hematoxylin for analysis of cartilage degradation. Modified Mankin grading of OA features including cartilage structure was performed by three blinded graders and used to calculate a score with a maximum of 30 for both the medial and lateral aspects of the femur and tibia (Ward et al., 2008). Sections were stained with Harris hematoxylin and eosin (H&E) for assessment of synovitis by three blinded graders as described previously (Lewis et al., 2011). Selected joints were analyzed with immunohistochemistry for activated macrophages using a monoclonal antibody against F4/80 (Clone BM8, Biolegend). Antigen retrieval was aided by 0.05% Proteinase K (Sigma-Aldrich) and heated citrate buffer extraction. Chromogen detection was carried

out with the Vectastain system (Vector Laboratories).   Sections analyzed for CM-DiI cell

tracking were cleared with xylenes and excited with a 543 nm laser using confocal

microscopy (LSM510, Zeiss).

4.2.6 Statistical analysis

Statistical analysis was carried out using a t-test for comparison of two groups

and analysis of variance (ANOVA) for comparison of multiple groups, with repeated

measures ANOVA on control and fractured limbs for modified Mankin scoring. Fisher's

LSD post-hoc analysis with α=0.05 was used. Normality was tested and data log-

transformed before analysis if necessary. For non-parametric analysis of cytokine data,

Kruskal-Wallis Median test was used and undetectable values were assigned the value

of one half of the lower limit of detection for analysis. Data are presented as mean ±

standard error of the mean (SEM).
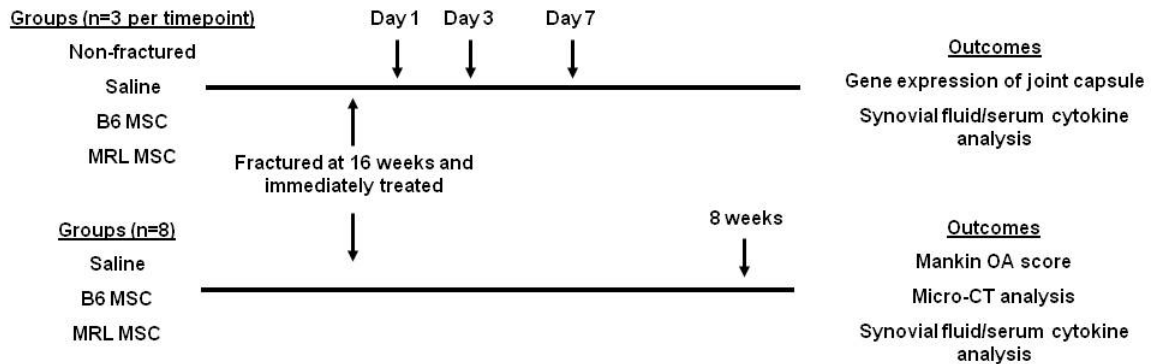
Figure 4-1: Experimental design. Groups, time points, and outcomes.

4.3 Results

4.3.1 Prevention of post-traumatic arthritis by stem cell therapy

Fracture of the left hind limb treated with only a control saline injection resulted in a significantly higher modified Mankin osteoarthritis score as compared to the contralateral control limb, indicating the presence of PTA in this group of mice (Figure 4-2A). Direct intra-articular delivery of either B6 or MRL MSCs immediately after fracture eliminated the difference in total joint modified Mankin score between the fractured limb and the control limb, showing MSC therapy was able to mitigate the development of PTA. Due to the location of the fracture, degeneration was most severe at the lateral tibia and the protective effect of the MSC therapy was most apparent on the lateral side of the joint (Figures 4-2B). A small number of MSCs were detected in various joint structures at days 1, 3, 7 as well as 8 weeks (Figure 4-3).
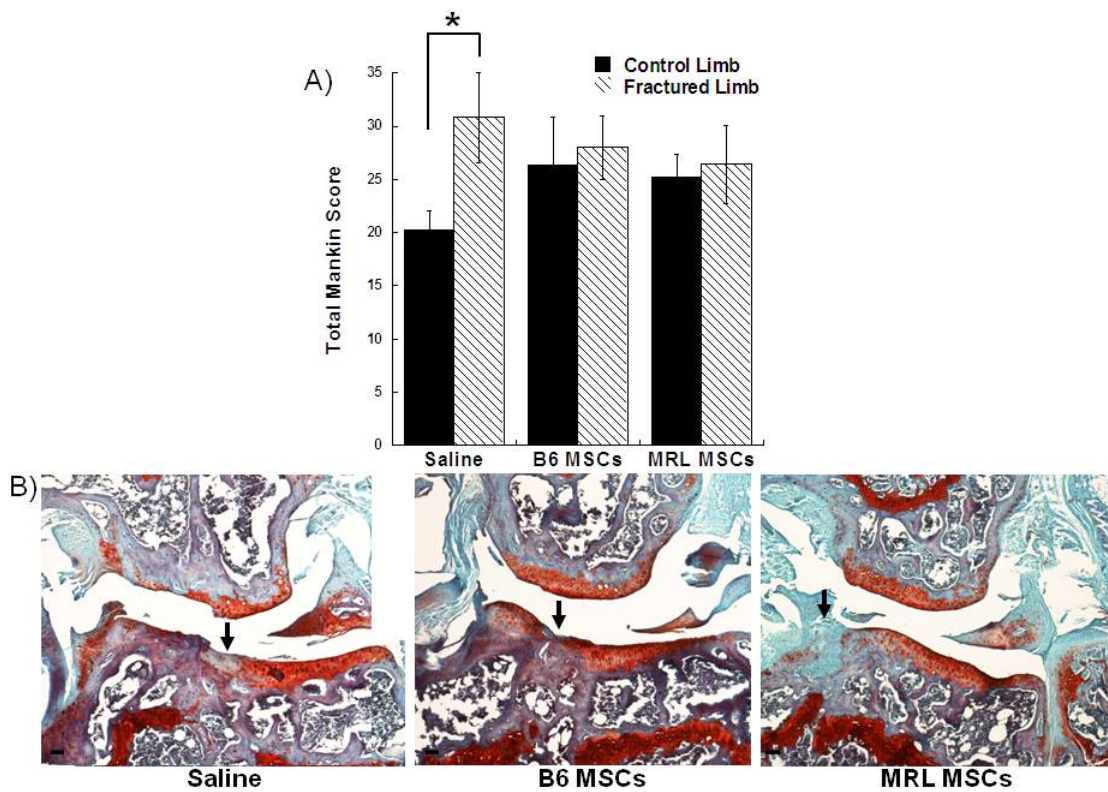
Figure 4-2: Evaluation of post-traumatic arthritis. A) Total joint modified Mankin score of joint degeneration, average of ≥7 joints per group with SEM displayed. Asterisk indicates significance. **B-D)** Safranin-O/Fast-Green/Hematoxylin staining 8 weeks after fracture. Joint with the highest structural Mankin scores on lateral side shown. Scale bar = 100 μm, arrow indicates fracture site.
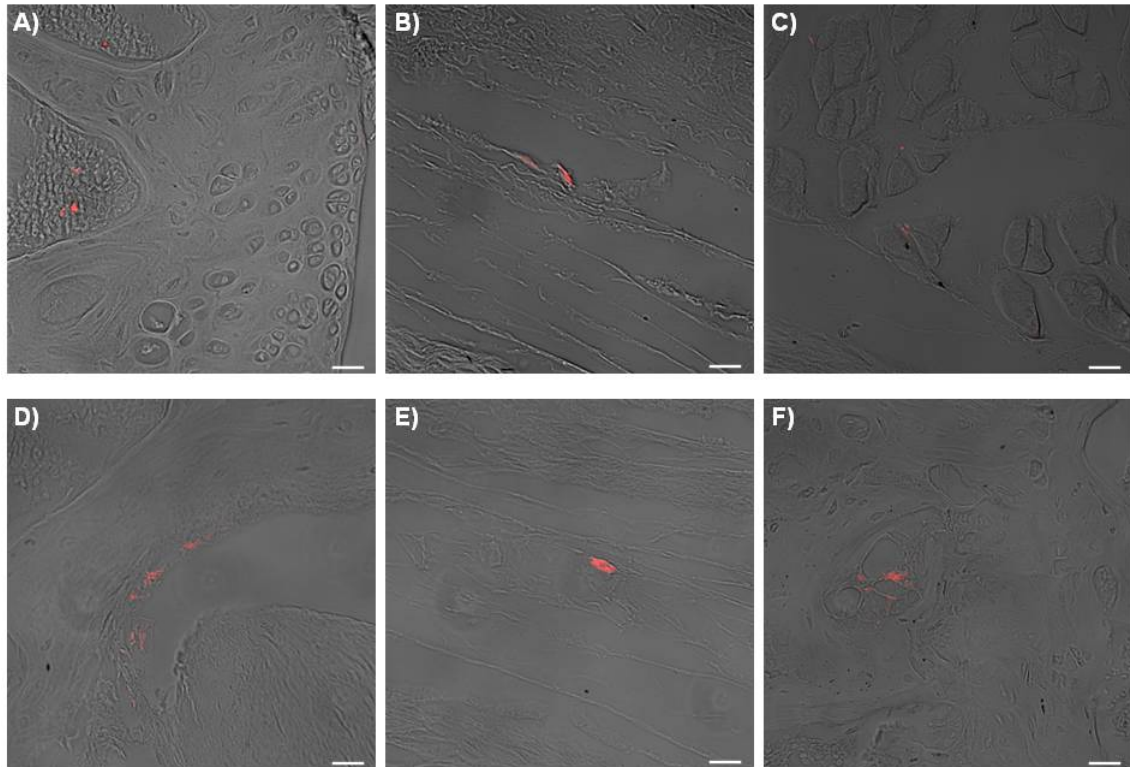
Figure 4-3: Cell tracking. MSCs were labeled with CM-DiI before injection. B6 MSCs at day 1 were found in A) bone marrow, B) synovium, and C) muscle. B6 MSCs also found D) day 3 in the lateral femoral synovium, E) day 7 near lateral ligamentous tissue, and F) 8 weeks in the tibial subchondral bone.

4.3.2 Serum and synovial fluid analysis

The level of IL-1β in serum was increased at early time points after fracture and

returned towards the pre-fracture values after 8 weeks in all groups with no significant

effect of treatment (Figure 4-4A). The treatment group did have a significant effect on

synovial fluid levels of IL-1β at day 3 and at 8 weeks, with MSC treatment being

associated with higher values at day 3 but reduced levels at 8 weeks (Figure 4-4B).

Serum levels of IL-1ra were affected by the treatment group at 8 weeks, with elevated

IL-1ra in the B6 MSC treatment group (Figure 4-4C), and all groups demonstrated a

trend towards increased synovial fluid IL-1ra 7 days after fracture (Figure 4-4D). The

treatment group significantly affected the serum levels of IL-10 at days 3 and 7 after

fracture, with higher values in the MSC treated groups (Figure 4-4E).
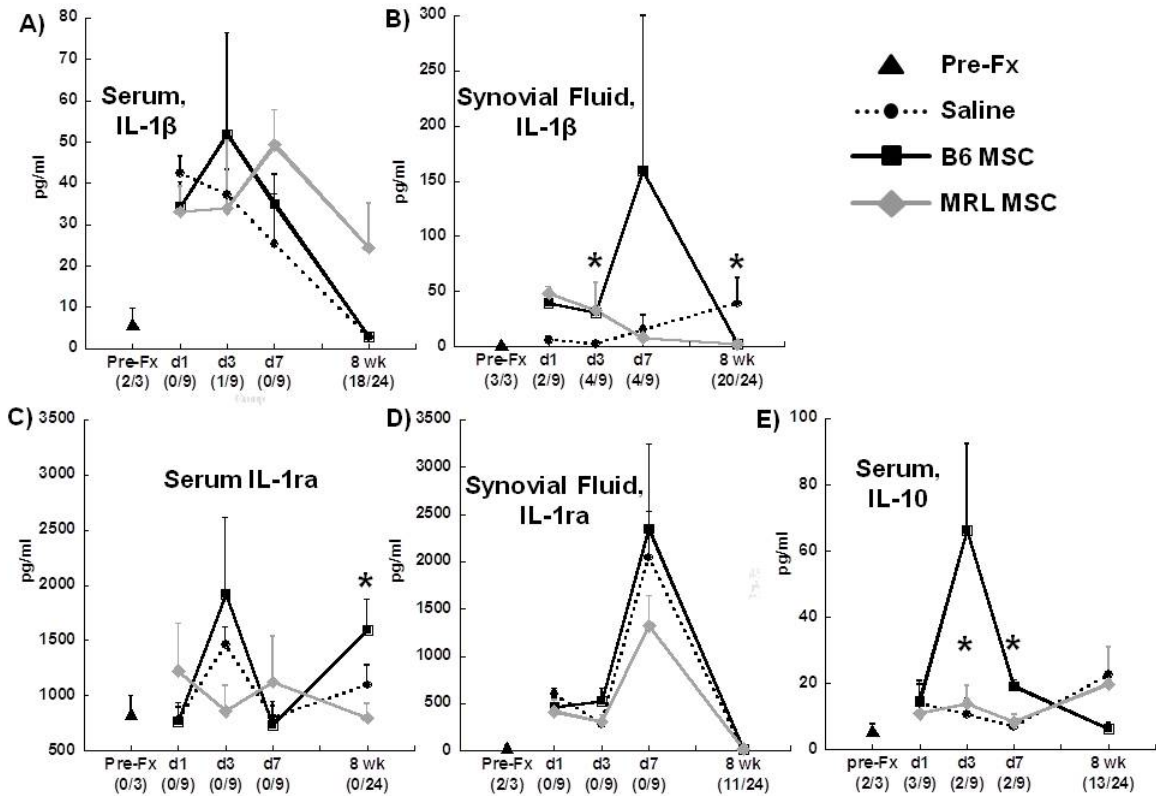
Figure 4-4: Systemic and local cytokine concentrations. Serum and synovial fluid from fractured knees analyzed for A,B) Interleukin 1β (IL-1β); C-D) Interleukin 1 receptor antagonist (IL-1ra); E) serum interleukin 10 (IL-10). Number of undetectable samples in parentheses; asterisk indicates significant effect of treatment group at that time point. Mean ± SEM shown at days 1, 3, 7 (n=3), and 8 weeks (n=8) after fracture.

4.3.3 Synovial inflammation and macrophage immunohistochemistry

The inflammation of the synovium 8 weeks after fracture was measured by a

synovitis score that assesses the thickening of the synovial lining as well as the

cellularity of the surrounding stroma. Fracture clearly increased the degree of synovitis

in all treatment groups as compared to the contralateral control and MRL MSCs resulted

in more inflammation than B6 MSCs (Figure 4-5A). An antibody against F4/80, used to

identify activated macrophages, demonstrated that some of the cells contributing to the

synovial response are macrophages (Figure 4-5C). Gene expression of the joint capsule

indicated the presence of inflammatory cytokines at early time points after fracture

(Table 4-1).
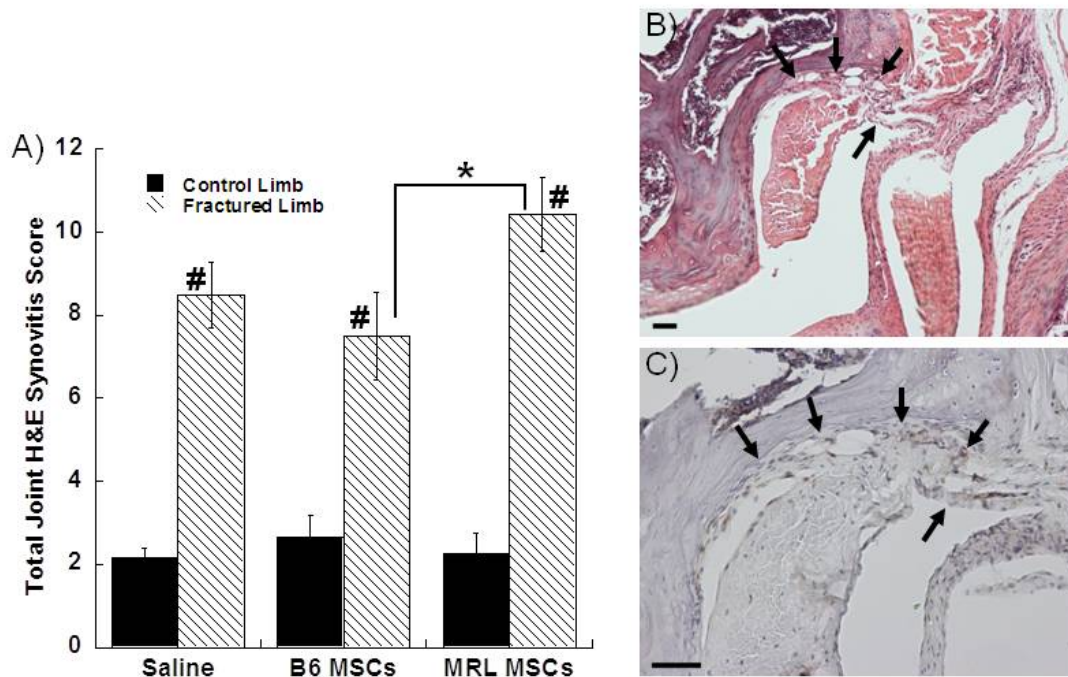
Figure 4-5: Synovial response to fracture. A) Total joint synovitis score, ≥7 joints per group, mean ± SEM. Asterisk indicates significance; pound symbol indicates significance to all control groups. B) Hematoxylin/Eosin staining of lateral femur 8 weeks after fracture and injection of B6 MSCs. Scale bar = 50 μm and arrows indicate synovium. C) F4/80 staining for macrophages, scale bar = 50 μm.

Table 4-1: Joint capsule gene expression at early time points after fracture (fold upregulation from pre-fracture levels)

Cytokine	Treatment	Day 1	Day 3	Day 7
Il1b	Saline	21.11	1.52	284.05
	B6 MSCs	16.56	1.80	168.90
	MRL MSCs	6.73	9.19	11.71
Il1a	Saline	1.57	0.54	4.59
	B6 MSCs	0.57	0.33	3.03
	MRL MSCs	0.64	1.52	0.68
Tnf	Saline	8.00	8.28	40.79
	B6 MSCs	5.86	17.75	40.79
	MRL MSCs	2.93	8.00	2.55
Il10	Saline	1.00	4.00	3.86
	B6 MSCs	0.84	0.93	2.46
	MRL MSCs	0.44	1.62	0.76
Ifng	Saline	0.71	0.90	13.00
	B6 MSCs	1.41	1.32	13.00
	MRL MSCs	0.87	1.00	1.27
Cxcl5	Saline	989.12	24.25	3444.31
	B6 MSCs	247.28	13.93	1606.83
	MRL MSCs	73.52	107.63	64.00
Ccl2	Saline	32.00	6.28	21.11
	B6 MSCs	10.56	4.29	9.19
	MRL MSCs	5.28	4.29	2.55
Cxcl10	Saline	3.61	4.00	38.05
	B6 MSCs	5.28	2.46	21.86
	MRL MSCs	2.73	2.73	1.57
Ccl12	Saline	3.03	0.90	6.28
	B6 MSCs	0.81	0.06	2.30
	MRL MSCs	1.07	1.07	0.87
Ilrn	Saline	16.00	2.83	46.85
	B6 MSCs	8.00	1.46	42.22
	MRL MSCs	7.21	10.56	9.51
Il6	Saline	6.96	0.44	84.45
	B6 MSCs	6.06	0.44	26.91
	MRL MSCs	2.83	2.22	3.03

4.3.4 Morphologic bone changes

Micro-computed tomography (micro-CT) analysis of morphologic bone changes showed increased bone volume and decreased bone density in the tibia and tibial metaphysis of the fractured limb as compared to the contralateral control limb (Figure 4-6A-D). The stem cell groups appeared to contribute to a larger bone volume, with the fractured limbs receiving MRL MSCs having a significantly larger volume than all

control limbs in the tibial metaphysis (Figure 4-6C). In the femur, the saline group

showed significantly lower cancellous bone fraction (bone volume / total volume) in the

fractured limb compared to the control limb and compared to both MSC therapy groups

(Figure 4-6E). With MSC treatment, there was no significant decrease in cancellous bone

fraction following fracture as compared to the contralateral control limbs.
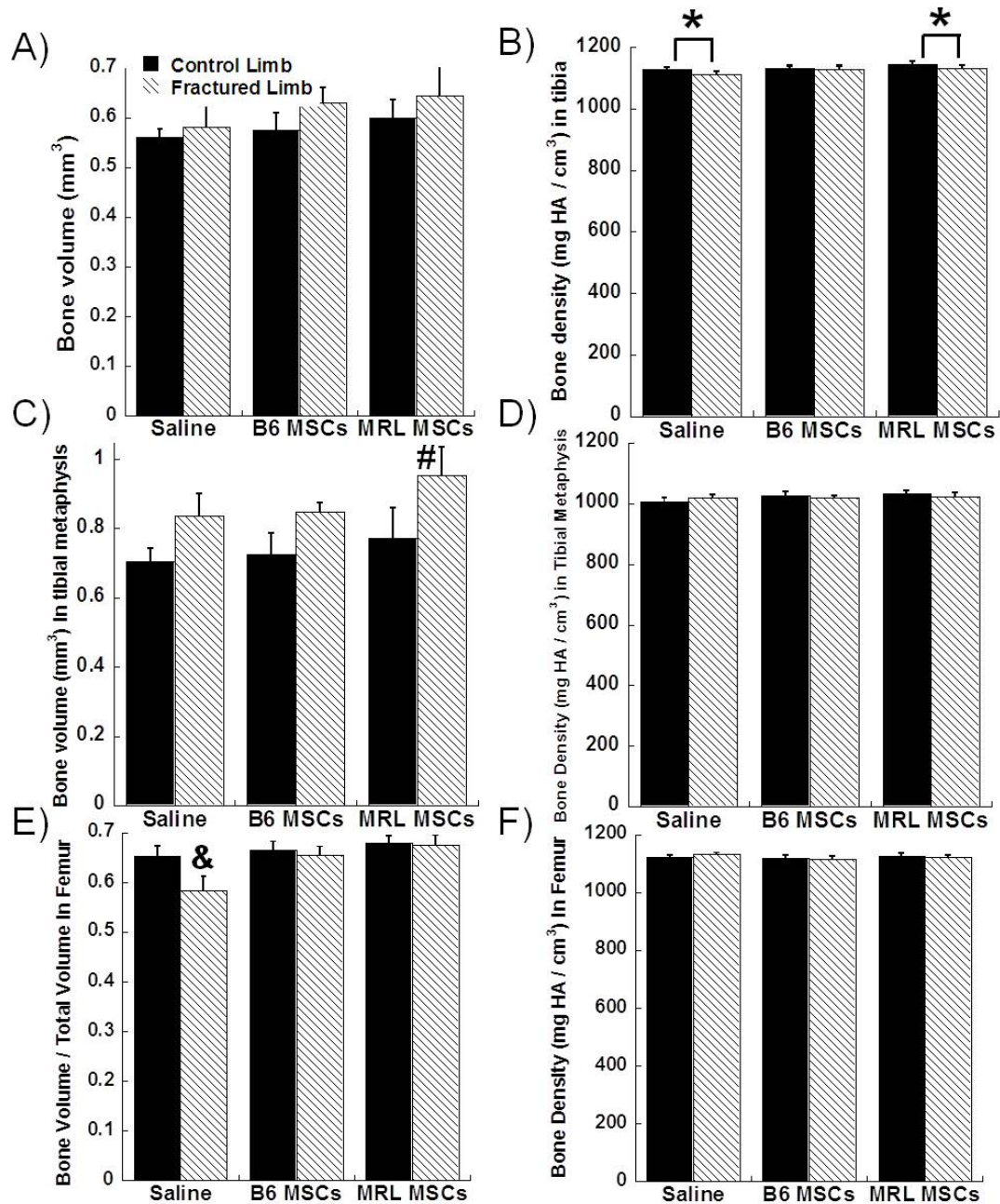
Figure 4-6: Morphological bone changes. A) Tibial bone volume; B) Tibial bone density; C) Bone volume in tibial metaphysis; D) Bone density in tibial metaphysis; E) Femoral bone volume / total volume; F) Femoral bone density. Significance to contralateral control (asterisk), all control groups (pound), or all groups (ampersand) noted; 8 joints per group. Mean ± SEM shown.

4.4 Discussion

The goal of this study was to prevent the development of OA after intra-articular

fracture using a single injection of expanded MSCs directly into the murine knee joint.

Our findings show that an allogeneic stem cell based therapy can prevent the

degenerative changes following joint trauma, and similar protective effects were

observed using either B6 or MRL MSCs. The modified Mankin score of the fractured

joint was significantly higher than the control joint when only saline was used as the

treatment, indicative of PTA. However, intra-articular injection of 10,000 B6 or MRL

MSCs after fracture eliminated the difference between control and fractured limbs.

Establishing treatment options for PTA is particularly promising because, in contrast to

idiopathic OA, the clear initiating event allows for early intervention before excessive

degradation occurs (Anderson et al., 2011).

The use of cellular therapy or cell-based tissue engineering for the regeneration

of cartilage after joint injury has generated promising pre-clinical and case study results.

With regard to PTA, the intra-articular delivery of MSCs has been shown to lessen the

degree of OA in goat knees after meniscectomy and ACL resection, potentially through

partial regeneration of the resected meniscus (Murphy et al., 2003). Recent studies have

also shown a protective effect of infrapatellar fat pad cells injected in the rabbit knee

following transection of the ACL (Toghraie et al., 2011). Furthermore, a series of studies

in mice and rats demonstrated that delivery of BMP-2 overexpressing stem cells

contributed to fracture healing and cartilage repair after open osteotomy of the hind limb (Zachos et al., 2007a; Zachos et al., 2007b). Clinical case studies using MSCs to repair cartilage defects have illustrated the production of neotissue (Matsumoto et al., 2010; Wakitani et al., 2002) and there are currently 8 clinical trials investigating the use of MSCs for osteoarthritis (Maumus et al., 2011), including a phase I/II clinical trial to prevent OA after meniscal tear (http://clinicaltrials.gov, #NCT00702741).

The concept that MSCs may prevent PTA after intra-articular fracture is consistent with the role of endogenous stem cells after bone and cartilage injury. After long-bone fracture, MSCs arrive at the fracture site to instigate endochondral ossification as part of the repair process (reviewed in (Marsell and Einhorn, 2011)). A similar mechanism is likely to occur after intra-articular fracture, as a multipotent MSC population was derived from hemarthrosis in joints after fracture (Lee et al., 2008). Indeed, treatment of chondral defects with microfracture or other marrow stimulating techniques relies on accessing the subchondral bone marrow to allow infiltration of progenitor cells (Frisbie et al., 2003; Kramer et al., 2006; Richter, 2009).

Cytokines such as IL-1β are upregulated with joint trauma (Irie et al., 2003; Pickvance et al., 1993) and result in cartilage degradation by suppressing matrix synthesis and inducing catabolic matrix metalloproteinase (MMP) activity (Fernandes et al., 2002; Goldring and Otero, 2011). In contrast, increased levels of IL-1ra systemically or in the joint may disrupt the inflammatory cascade by preventing IL-1 from binding to

88

its cell receptor (Caron et al., 1996; Lawrence et al., 2011). Similarly, IL-10 has been

identified as an important anti-inflammatory molecule that shows a chondroprotective

role in several settings of joint disease (reviewed in (Schulze-Tanzil et al., 2009)). We

hypothesized that MSC therapy would preserve cartilage by altering the balance of these

pro-inflammatory and anti-inflammatory cytokines in the joint after injury. In studies

using other injury models, MSCs decreased the systemic level of IL-1β after long-bone

fracture (Granero-Molto et al., 2009), protected the lung from injury by secreting IL-1ra

(Ortiz et al., 2007), and reprogrammed macrophages to increase IL-10 secretion in a

sepsis model (Nemeth et al., 2009). In this study, stem cell treatment altered the time

course of IL-1β in the synovial fluid and B6 MSCs increased the presence of IL-10 in the

serum at several time points.

The synovium is a likely target for the therapeutic effects of MSCs because it

exhibits significant cellular activity in response to injury. However, the relationship

between stem cells and the synovium is complex, as endogenous MSCs in the mouse

synovium contribute to a regenerative response through chondrogenic differentiation

after cartilage injury (Kurth et al., 2011), but a significant inflammatory environment can

alter the differentiation of progenitors in the synovium and cause a pannus-like invasion

(Li and Makarov, 2006). Inflammation of the synovium after injury is correlated to

negative outcomes in clinical studies of meniscal injury (Scanzello et al., 2011). Synovitis

was clearly caused by fracture in this study, but stem cell therapy improved OA scores

without reducing the degree of synovial hyperplasia after fracture. Since macrophages have been implicated as producers of inflammatory cytokines and other destructive molecules such as MMPs (Bondeson et al., 2010), we performed immunohistochemical staining for activated macrophages. Similar to the overall synovial inflammation, delivery of MSCs did not appear to mitigate the presence of activated macrophages in the synovium.

Bone is a joint tissue with high turnover and the capacity to respond to MSC delivery. In a long-bone fracture model, systemically delivered MSCs produced BMP-2 at the fracture site and caused an increase in callus strength, total volume, and mineralization content (Granero-Molto et al., 2009). In this study, MSCs directly delivered to the joint increased several measures of bone volume. Exogenously delivered MSCs may therefore contribute to the prevention of PTA by providing additional cells for earlier and more robust stabilization of the joint. The differentiation of endogenous MSCs to an osteoblastic lineage is essential to bone repair and is organized by multiple waves of biochemical signals such as IL-1 and TNFα (Marsell and Einhorn, 2011). Since these inflammatory cytokines are essential to early fracture healing but may be catabolic for cartilage at later times, the timing and dose of MSCs or other agents that may affect cytokine levels will need to be considered for optimal fracture repair and protection from PTA.

There is controversy in the literature about the extent of MSC engraftment when used in injury models, with some studies showing significant engraftment and differentiation but most demonstrating functional improvements with few cells remaining at the site of cell delivery (reviewed in (Prockop, 2007)). With systemic delivery, MSCs get trapped in the lungs before distribution to organs such as the liver and spleen (Gao et al., 2001). However, intra-articular delivery of stem cells to the knee has resulted in some engraftment in joint structures (Horie et al., 2009; Lee et al., 2007; Murphy et al., 2003). For cell tracking experiments, we labeled cells with CM-DiI, which is a lipophilic carbocyanine membrane dye that has been used effectively for tracking cells in vivo in the context of bone (Ferrari et al., 2001). Consistent with previous studies, we observed a relatively small fraction of fluorescent cells in various tissues of the joint throughout the time course studied. However, quantification was not possible due to the challenges associated with discriminating between infrequent positive cells and background fluorescence (Brazelton and Blau, 2005) and the possibility of membrane dyes transferring to other cells over a period of time (Kruyt et al., 2003). New methods for quantifying the rate of engraftment and longitudinally tracking the fate of delivered cells will be an important aspect for the future development of cellular therapies (de Almeida et al., 2011).

The identification of MSCs with exceptional properties can help elucidate how the cells contribute to healing and may provide a pathway to modify MSCs for enhanced

function. Because MRL "superhealer" mice may derive some of their regenerative

capabilities from altered stem cell function (Alfaro et al., 2008), MSCs from both control

B6 and MRL mice were compared in this model system. However, differences between

the strains were difficult to assess because delivering exogenous stem cells of either

strain to the B6 knee after fracture was sufficient to prevent the primary endpoint of

PTA. In this way, MSC therapy may have created a B6 joint environment that is more

similar to that found in the MRL mouse knee after fracture, which is also protected from

PTA (Furman, 2009; Ward et al., 2008). A defining feature of the MRL joint environment

after fracture is reduced inflammation, as seen in work showing that MRL mice had

different serum and synovial fluid IL-1β profiles after fracture (Furman, 2009) and that

macrophages from MRL mice have lower upregulation of inflammatory cytokines

(Kench et al., 1999). Indeed, further support for the effect of local inflammation on

healing in the MRL has come from experiments demonstrating that the regenerative

phenotype of MRL mice is lost when the inflammatory environment is changed due to a

secondary injury (Zins et al., 2010).

4.5 Summary

We demonstrated that a single intra-articular injection of MSCs from either

control B6 or MRL "superhealer" mice prevented the development of post-traumatic

arthritis 8 weeks after intra-articular fracture of the knee. MSCs did not reduce synovitis

or the presence of activated macrophages in the synovium, but did alter cytokine levels

and the bone healing response. This work suggests that stem cell therapy is a promising

treatment for preventing PTA and could possibly be extended to explore other biologic

interventions after joint injury before extensive osteoarthritis has occurred.

5. Chondrogenic differentiation of murine induced pluripotent stem cells

5.1 Introduction

The poor healing capacity of cartilage has limited the success of treatments for focal cartilage defects, and many patients progress to widespread osteoarthritis (OA) requiring total joint replacement (Hunziker, 2002). Cartilage tissue engineering seeks to provide a biological replacement tissue, which requires an adequate cell source (Guilak et al., 2001; Solchaga et al., 2001; Song et al., 2004). Autologous chondrocytes have been used for focal defect repair (Brittberg et al., 1994), but the harvest procedure requires an additional surgery and may cause complications at the donor site (Lee et al., 2000). Adult stem cells are a promising alternative cell source due to their minimally invasive isolation and chondrogenic potential (Guilak et al., 2010; Johnstone et al., 1998; Mackay et al., 1998; Noth et al., 2008; Zuk et al., 2001), but these cells also have limitations. The frequency of mesenchymal stem cells (MSCs) in bone marrow is low (Pittenger et al., 1999), and the more abundant adipose-derived stem cells (ASCs) have shown a reduced chondrogenic potential as compared to MSCs (Diekman et al., 2010; Hennig et al., 2007; Huang et al., 2005). Additionally, the adult stem cells of patients most likely to need therapy may be unfit for use, as some studies have shown a reduced MSC yield with age (Muschler et al., 2001) and a reduced chondrogenic ability with OA (Murphy et al., 2002).

Induced pluripotent stem cells (iPSCs) have the potential to overcome the current

cell source limitations, as large numbers of patient-matched cells with chondrogenic

potential can be derived from a non-invasive starting cell population.   Induced

pluripotent stem cells are somatic cells that have been genetically reprogrammed to a

pluripotent state, similar to that of embryonic stem cells (ESCs) (Takahashi et al., 2007;

Takahashi and Yamanaka, 2006; Yu et al., 2007). Pluripotent cells demonstrate indefinite

expansion in culture without the loss of differentiation potential. However, conditions

for the specific and robust chondrogenic differentiation of iPSCs must be established in

order for them to be used as a cell source for cartilage tissue engineering applications.

Chondrogenic differentiation of murine and human ESCs is regulated by growth

factors such as the bone morphogenetic proteins (BMPs) (Kramer et al., 2000; Nakayama

et al., 2003) and transforming growth factor-beta (TGF-β) (Hwang et al., 2006a; Koay et

al., 2007) . While the expression of chondrogenic genes can be induced in monolayer

culture (Oldershaw et al., 2010; Waese and Stanford, 2011), chondrogenesis is typically

enhanced by recapitulating mesenchymal condensation using three-dimensional culture

systems such as embryoid bodies (Toh et al., 2007), micromasses (Gong et al.; Yamashita

et al., 2010), pellets (Nakagawa et al., 2009), or scaffolds (Fecek et al., 2008; Hwang et al.,

2006b; Yeung et al., 2009). Initial studies with mouse and human iPSCs have indicated

that chondrogenesis can be achieved using similar strategies to ESCs (Kim et al., 2011;

Medvedev et al., 2011; Teramura et al., 2010; Wei et al., 2012). The hypothesis of this

95

study is that forced aggregation and culture with TGF-β superfamily proteins will induce chondrogenesis in a subset of mouse iPSCs, which can be identified by type II collagen gene expression and subsequent production of cartilaginous matrix in pellet culture.

5.2 Materials and Methods

5.2.1 Induced pluripotent stem cell derivation and culture

All procedures were performed in accordance with a protocol approved by the Duke University Institutional Animal Care and Use Committee. Tail fibroblasts from C57BL/6 mice were isolated by removing the outer layer of skin, mincing the tissue, and digesting overnight in 0.2% collagenase type I (Worthington Biochemical). Digested cells were passaged several times in DMEM-LG (Sigma-Aldrich) with 15% fetal bovine serum (FBS, Sigma-Aldrich) and 1% penicillin-streptomycin-fungizone (P/S/F, Gibco). Mouse embryonic fibroblasts (MEFs, Millipore) were treated with 10 μg/ml mitomycin-C (Sigma-Aldrich) for 2-3 hours to prevent proliferation and then cultured on 0.1% gelatin coated dishes at confluence to provide a feeder layer. Tail fibroblasts were transduced with a single doxycycline-inducible lentiviral vector controlling the transgenic expression of mouse cDNAs for Oct4 (also known as Pou5f1), Sox2, Klf4, and c-Myc (Carey et al., 2009) for 24 hours. Tail fibroblasts were then cultured on a MEF feeder layer in iPSC media containing DMEM-HG (Gibco), 20% lot-selected FBS (Atlanta Biologicals), 100 nM MEM non-essential amino acids (NEAA, Gibco), 55 μM 2-

96

mercaptoethanol (2-me, Gibco), 25 ng/ml gentamicin (Gibco), 1000 U/ml mouse

leukemia inhibitory factor (LIF, Millipore ESGRO), and 10 µg/ml doxycycline (Sigma-

Aldrich). After approximately 2 weeks, individual colonies were manually selected

based on morphology and colonies were maintained on feeder cells in iPSC media

without doxycycline.

For some of the trials, iPSCs were derived from different cell sources or using a

different reprogramming vector, but were cultured in the same fashion. In the

experiment that investigating iPSCs in cartilage-derived matrix (CDM) scaffolds,

fibroblasts derived from the joint capsule of C57BL/6 (B6) and MRL/MpJ (MRL) mice

were reprogrammed with the doxycycline inducible system. However, individual

colonies were not selected so some non-reprogrammed cells were present. In the

experiment that compared chondrogenic differentiation in monolayer and micromass

culture, the iPSCs were derived from PDGFRα+/Sca-1+ MRL MSCs (methods for

isolation are described in chapter 3) and colonies were selected for expansion. The

pWPXL lentiviral vector (Addgene) used for reprogramming has the potential to be

excised after pluripotency has been achieved, but this was not done and so there was

potential for continued expression of the transgenes. In experiments investigating the

timing of growth factor delivery, MEFs were used as the starting cell source for

doxycycline-inducible reprogramming with colony selection.

5.2.2 Three-dimensional culture of undifferentiated iPSCs

Undifferentiated iPSCs were cultured in CDM, 2% agarose, or 10% poly (ethylene glycol)-diacrylate with 2.5 mM tyrosine-arginine-glycine-aspartate-serine (PEG-RGD) environments. CDM scaffolds were generated from native porcine cartilage tissue as described in chapter 2. To seed scaffolds, 1×10^6 cells in 30 μl were allowed to attach to dry scaffolds for 1 hour before adding additional media. Pellets containing 1×10^6 iPSCs were generated by centrifuging cells in 15 ml conical tubes (Corning) at 200 xg for 5 minutes and culturing with a loosened cap. For agarose culture, iPSCs were directly resuspended in a solution of 2% Agarose (Type VII, Sigma-Aldrich) in PBS. Molds were filled with 60 μl molten agarose containing 1×10^6 cells were allowed to harden for 10 minutes before transferring to low-attachment plates (Corning) for culture. PEG-RGD hydrogels were generated following described methods with slight modifications (Hwang et al., 2006b). Briefly, the photo-initiator Irgacure 2959 was added at 0.1% final concentration to 1:1 solutions of 2x polymer and cell suspensions. The solution containing 1×10^6 cells in 60 μl was pipetted to a mold and photopolymerized using 365 nm light at 3 mW/cm^2 for 10 minutes. Constructs were then transferred to low-attachment plates.

Chondrogenic differentiation was performed for 21 or 28 days in serum-free chondrogenic differentiation medium containing DMEM-HG, ITS+ premix (BD), penicillin-streptomycin (P/S, Gibco), 37.5 μg/ml L-ascorbic acid 2-phosphate (Sigma-

Aldrich), 50 μg/ml L-proline (Sigma-Aldrich), 100 nM NEAA, 55 μM 2-me, and 100 nM

dexamethasone (DEX, Sigma-Aldrich). In the CDM experiment, DEX was not provided

for the control conditions and NEAA and 2-me were not included. Growth factor

supplementation of 10 ng/ml TGF-β3 (R&D Systems), 50 ng/ml BMP-4 (R&D Systems),

or 500 ng/ml BMP-6 (R&D Systems) was used for chondrogenic induction.

5.2.3 Chondrogenic induction in monolayer culture

Feeder layer cells were removed using two subtraction steps of 45 minutes on

tissue culture plastic separated by a day of culture on 0.1% gelatin. Cells were then

plated in 0.1% gelatin coated plates at 2.5×10^5 per well of a 6 well plate in iPSC media

containing the following media conditions: Serum-free control, 10% serum control, 1%

serum control, or 1% serum plus 50 ng/ml BMP-2, BMP-4, BMP-6, platelet-derived

growth factor (PDGF-BB), or 10 ng/ml TGF-β3. Monolayer wells were passaged upon

confluence at days 3 and 10 to prevent overgrowth, and replated at approximately 2×10^6

cells per well.

5.2.4 Chondrogenic induction in micromass culture

Feeder-subtracted cells were resuspended at a concentration of 2×10^7 cells/ml,

and micromasses were established by plating 10 μl droplets with 2×10^5 iPSCs into

individual wells of 48 well plates (Corning) or as a set of 30 micromasses in a 10 cm dish

(BD). After 2-3 hour incubation, additional 10% serum iPSC media without LIF was

added. Twenty-four hours after establishing micromasses, the media was switched to

serum-free chondrogenic differentiation medium. At 48 hours, media was switched to

serum-free chondrogenic media containing growth factors and DEX. Micromasses were

fed every 2-3 days until analysis at days 5, 10, or 15, using a range of growth factors to

induce chondrogenesis: 50 ng/ml BMP-2, BMP-4, BMP-6, PDGF-BB, 30 ng/ml Activin A,

or 10 ng/ml TGF-β3. In some experiments, the effect of DEX and the timing of BMP-4

and ascorbate/proline delivery were investigated.

For Alcian blue staining, micromasses were washed with PBS, stained for 20

minutes at room temperature with 4% PFA, washed with PBS, equilibrated with 0.1N

HCl for 5 minutes, stained for 30 minutes with 1% Alcian blue (Acros Organics) in 0.1N

HCl, and washed twice with 0.1N HCl before imaging.

5.2.5 Chondrogenic induction in embryoid body culture

Embryoid bodies (EBs) were formed using the hanging drop method with

undifferentiated iPSCs resuspended at 40,000 cells/ ml of 20% iPSC media without LIF.

One-hundred droplets of 20 μl containing ~800 cells each were placed onto the lid of a 15

cm dish (BD) that was then cultured over the dish containing 40 ml of sterile dH_20. After

3 days of hanging drop culture, the droplets were washed and transferred to a 10 cm

dish that had been pretreated with polyHEMA (Sigma-Aldrich) to prevent attachment.

EBs were cultured in liquid suspension culture for 3 days with 20% serum media with or

without 50 ng/ml BMP-4. EBs were collected from suspension with a pipette and

approximately 10 EBs were transferred to gelatin coated wells of 48 well plates for

outgrowth culture. In outgrowth culture, EBs were fed with serum-free media until harvest at day 15 or day 27, with some wells receiving media containing BMP-4 for days 6 through 10 only and other wells receiving control media for the duration of culture.

5.2.6 Cell sorting based on Col2-GFP expression

To provide a fluorescent marker for the cell sorting of chondrocyte-like cells, a construct was used that contains the promoter/enhancer of murine type II collagen (Col2) driving expression of green fluorescent protein (GFP) (Grant et al., 2000). The Col2-GFP construct was introduced into undifferentiated iPSCs using nucleofection (Lonza) and colonies were selected for further study based on a specific increase in GFP+ percentage after chondrogenic induction in micromass culture. Micromasses were digested for 1 hour using 0.4% collagenase type II (Worthington Biochemical), 1320 PKU/ml pronase (Calbiochem), and 10 µg/ml DNAse I (Worthington Biochemical). Cells were centrifuged, incubated with 0.25% tryspin-EDTA (Sigma-Aldrich) for 5 minutes, and resuspended in sort medium containing DMEM-HG, 2% FBS, DNAse I, 10 mM Hepes (Gibco), 2x P/S/F, and 33.3 nM propidium iodide (Biolegend) as a dead cell marker. Cells were sorted based on GFP expression using the 100 µM nozzle of a Cytomation MoFlo® sorter (Beckman Coulter). Micromasses from MEF-derived iPSCs without the Col2-GFP construct served as the control for setting flow cytometry gates.

5.2.7 Monolayer expansion and pellet culture of sorted cells

Cells sorted as GFP- or GFP+ were plated at 1×10^4 cells/cm^2 on 0.1% gelatin coated plates in chondrogenic expansion medium consisting of chondrogenic differentiation medium with the addition of 10% FBS and 4 ng/ml bFGF (Roche). Cells were passaged upon sub-confluence every 2-3 days using 0.05% trypsin-EDTA (Sigma-Aldrich). After each passage, some cells were used to form pellets by centrifuging 2.5×10^5 cells at 200 xg for 5 minutes in 15 ml tubes. Pellets were cultured in chondrogenic differentiation medium with the addition of either 10 ng/ml TGF-β3 or 50 ng/ml BMP-4 and for 21 days.

5.2.8 Immunocytochemistry, RT-PCR, histology, and immunohistochemistry

For gene expression analysis, cells were lysed and stored at -80 °C until RNA was isolated (Qiagen) and quantified (Nanodrop). Real time reverse transcription-PCR (RT-PCR) was carried out using SuperScript® VILO™ and Express Supermix (Invitrogen) with Taqman® assays (Applied Biosystems) for type II collagen (Col2, Mm01309565_m1), aggrecan (Acan, Mm00545807_m1), SRY-box containing gene 9 (Sox9, Mm00448840_m1), type X collagen (Col10, Mm00487041_m1), type I collagen (Col1, Mm01165187_m1), and the housekeeping gene 18s (Hs99999901_s1). The fold difference from undifferentiated iPSCs was calculated using the delta delta Ct (Livak and Schmittgen, 2001) method with efficiency curves. In some cases, the data were normalized to passage 1 GFP+ cells. After 21 days of culture, pellets were paraffin

102

embedded and sectioned for histology for Safranin-O (GAGs, red), Fast Green (collagen, green), and Hematoxylin (nuclei, blue) or immunohistochemistry for type II collagen (II-II6B3), type VI collagen (70R-CR009x, Fitzgerald), type X collagen (c7974, Sigma-Aldrich), and type I collagen (8D4A1, Chondrex) as described previously (Estes et al., 2010).

5.2.9 Statistical analysis

Statistical analysis was carried out using a t-test for comparison of two groups and analysis of variance (ANOVA) with Fisher's LSD post-hoc analysis for comparison of multiple groups, using α=0.05. Normality was tested and data log-transformed before analysis if necessary. Data are presented as mean ± standard error of the mean (SEM).

5.3 Results

5.3.1 Undifferentiated iPSCs in 3D culture

5.3.1.1: Cartilage-derived matrix scaffolds

Joint capsule fibroblasts from B6 and MRL mice were reprogrammed using the doxycycline-inducible system and $1x10^6$ undifferentiated iPSCs were seeded directly into CDM scaffolds. In serum-free control conditions, cells showed little cell attachment and proliferation, with no production of GAGs. When cultured with either 10 ng/ml TGF-β3, 500 ng/ml BMP-6, or both, some areas of the scaffold were filled with clusters of cells. Some of these areas showed robust staining for GAGs by Safranin-O staining (Figure 5-1).
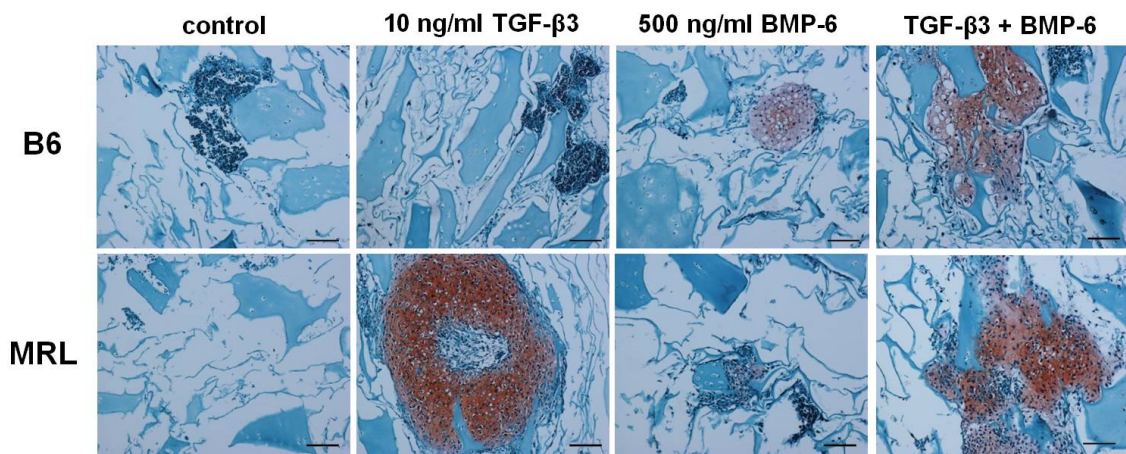
Figure 5-1: Histology of undifferentiated iPSCs in CDM scaffolds. Safranin-O/Fast Green/Hematoxylin staining of day 21 CDM scaffolds with 1x10⁶ undifferentiated iPSCs from B6 or MRL mice. Scale bar = 100 μm.

5.3.1.2: Pellet culture

Undifferentiated MEF-derived iPSCs were induced in pellet culture for 28 days. While there was significant GAG staining in serum-free pellets treated with 50 ng/ml BMP-4, this was abolished in the presence of 5% serum (Figure 5-2). Little GAG staining was seen in control or 10 ng/ml TGF-β3 pellets regardless of the presence of serum.
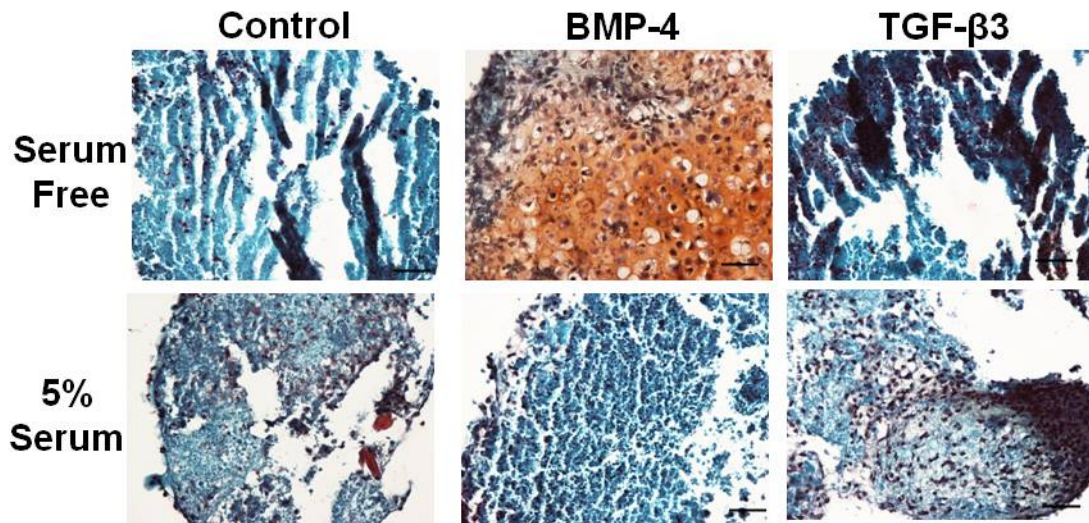
Figure 5-2: Effect of serum on chondrogenesis in pellet culture. Safranin-O/Fast Green/Hematoxylin staining of day 28 pellets with 1x10^6 undifferentiated iPSCs. Scale bar = 100 μm.

5.3.1.3: Agarose hydrogels

MEF-derived iPSCs were also induced in 2% agarose hydrogels for 21 days. Despite a seeding density of greater than 15 million cells per ml, cells were sparse and produced little matrix in serum-free conditions. With the presence of 5% serum, small pockets of cell clusters did appear, but only very faint GAG staining was seen in the presence of 50 ng/ml BMP-4 (Figure 5-3).
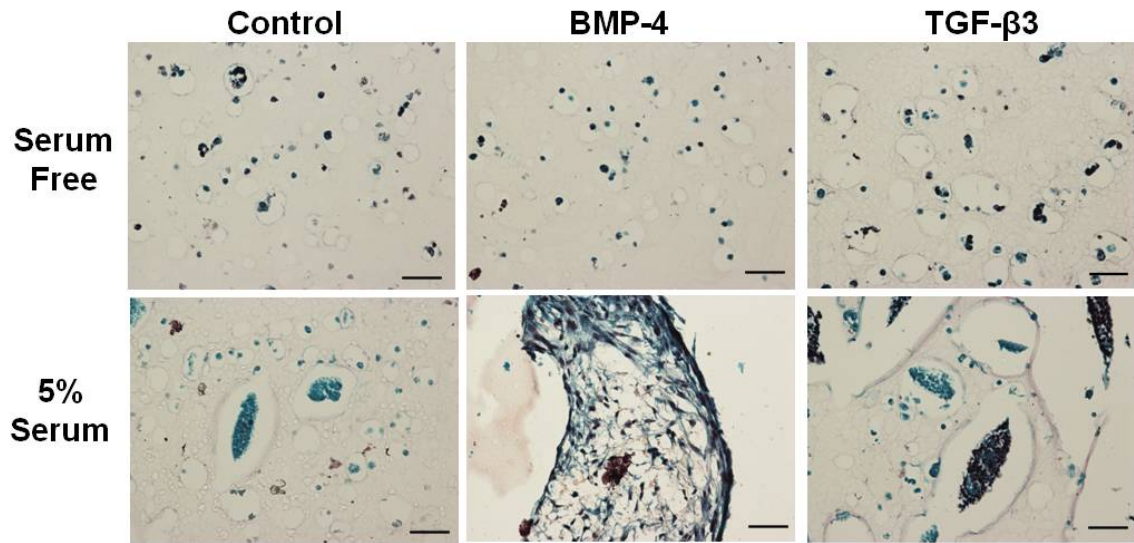
Figure 5-3: Effect of serum on chondrogenesis in agarose culture. Safranin-O/Fast Green/Hematoxylin staining of day 21 constructs with 1×10^6 undifferentiated iPSCs. Scale bar = 100 μm.

5.3.1.4: PEG-RGD hydrogels

To further investigate the effect of serum on chondrogenesis, B6 tail fibroblast-derived iPSCs (colony #7) were differentiated in PEG-RGD hydrogels for 21 days. Constructs in serum-free media showed little matrix production, whereas constructs in 5% serum media for the first 7 days or the all 21 days of culture showed areas of cell aggregation and/or proliferation (Figure 5-4). Some of these structures showed limited staining for GAGs by histology, especially when 50 ng/ml BMP-4 was provided in serum-free conditions.
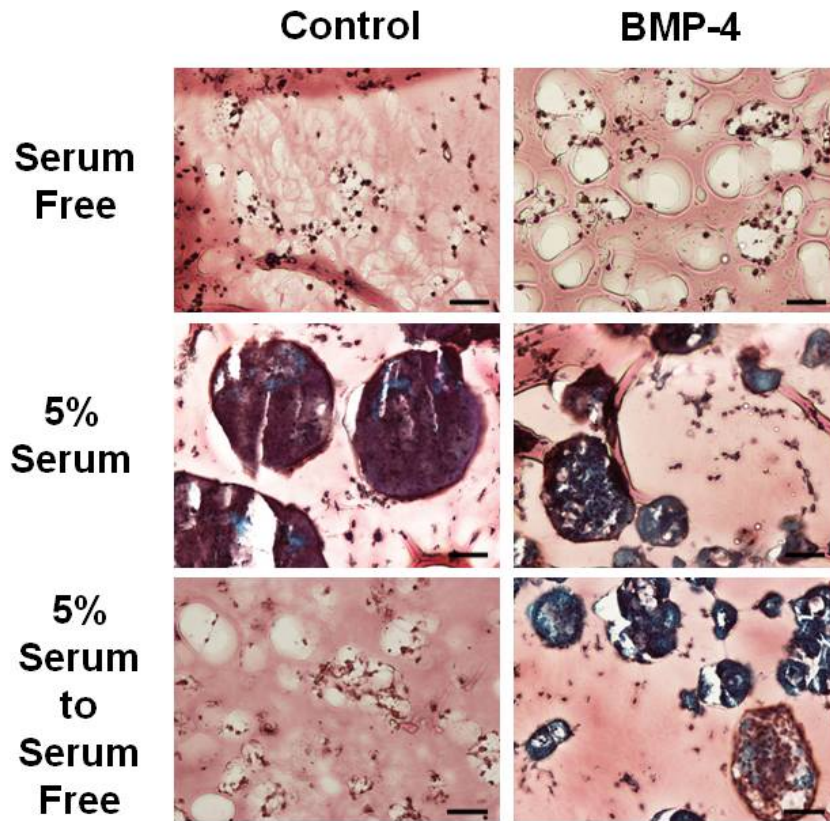
Figure 5-4: Effect of serum on chondrogenesis in PEG-RGD culture. Safranin-O/Fast Green/Hematoxylin staining of day 21 PEG-RGD constructs with 1x10^6 undifferentiated iPSCs. Scale bar = 100 μm.

5.3.2 Monolayer and micromass differentiation using growth factors

Monolayer (2.5x10^5 in a 6-well plate) and micromass (2x10^5 in 10 μl droplet)

differentiation were carried out on iPSCs derived from PDGFRα+/Sca-1+ MRL MSCs.

Nine different culture conditions were used: Serum-free control, 10% serum control, 1%

serum control, or 1% serum plus 50 ng/ml BMP-2, BMP-4, BMP-6, PDGF-BB, or 10 ng/ml

TGF-β3. The Col2 and Sox9 expression levels at day 15 were generally higher in

micromass culture as compared to monolayer culture. While BMP-2 and BMP-4

increased Sox9 expression above the 1% serum control in micromass culture, other

growth factors did not appear to increase the chondrogenic gene expression in either

monolayer or micromass culture. The highest values for both Col2 and Sox9 were found

in the serum-free control micromass group.
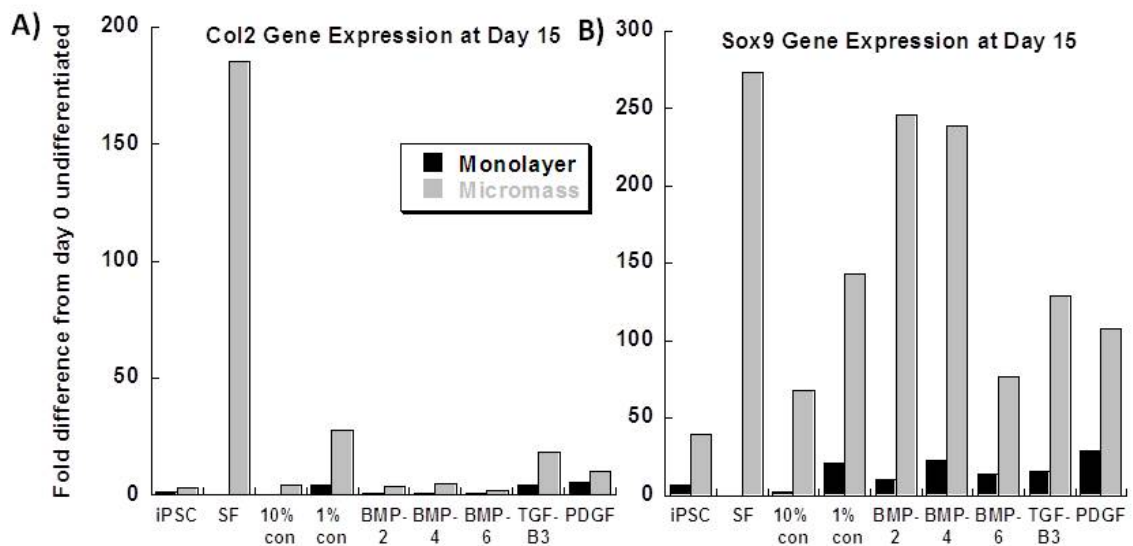
Figure 5-5: Monolayer and micromass gene expression. RT-PCR at day 15 for A) Col2 or B) Sox9 with controls of different serum concentrations or 1% serum plus growth factors. Fold difference from day 0 undifferentiated cells, one well or micromass per group.

5.3.3 Growth factor screen for serum-free micromass culture

MEF-derived iPSCs were used to investigate the effect of different growth factors

on chondrogenic induction in serum-free micromass culture. In addition to serum-free

chondrogenic differentiation media, groups had the following growth factors: 50 ng/ml

BMP-2, BMP-4, BMP-6, PDGF-BB, 10 ng/ml TGF-β3, 30 ng/ml Activin A, or 50 ng/ml

BMP-4 plus 10 ng/ml TGF-β3. After 10 days of culture, the degree of upregulation from

day 0 undifferentiated cells was different for each gene (Figure 5-6): Col2 (up to 500 fold), Sox9 (up to 20,000 fold), Acan (up to 9 fold), Col1 (up to 25 fold), and Col10 (up to 30 fold). Serum-free control conditions were the most effective at inducing chondrogenic differentiation as measured by Col2 and Acan expression, but BMP-2 and BMP-4 induced a greater upregulation of Sox9 expression. BMP-2 caused the upregulation of Col1 and Col10, and TGF-β3 induced the highest expression of Col10.

Additional information on the chondrogenic induction of growth factors was obtained by performing Alcian blue staining for GAGs on micromasses at day 10. While the control showed no staining and a smaller micromass, induction with BMP-2, BMP-4, or BMP-4 plus TGF-β3 demonstrated the presence of GAGs (Figure 5-7A). The Alcian blue staining results were confirmed for a second colony of iPSCs, indicating the most robust staining using BMP-4 treatment (Figure 5-7B).
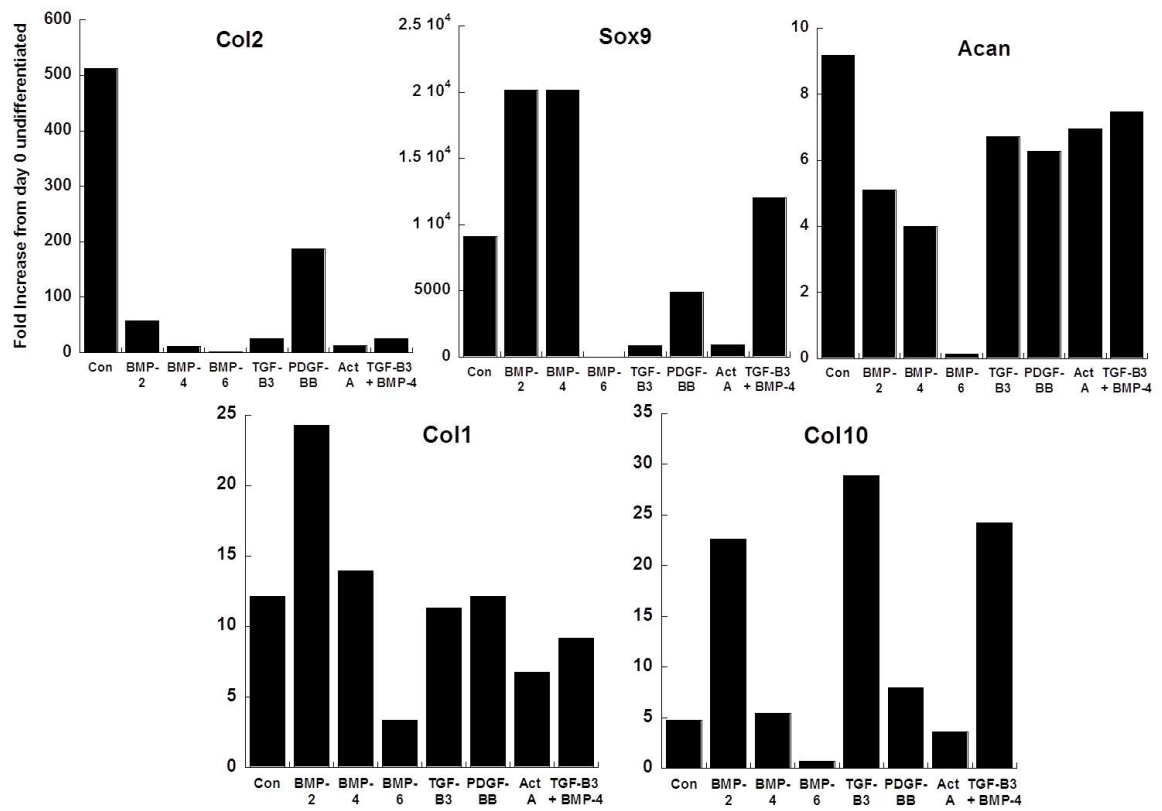
Figure 5-6: Gene expression for growth factor screen. RT-PCR at day 10. Fold difference from day 0 undifferentiated cells, one micromass per group.
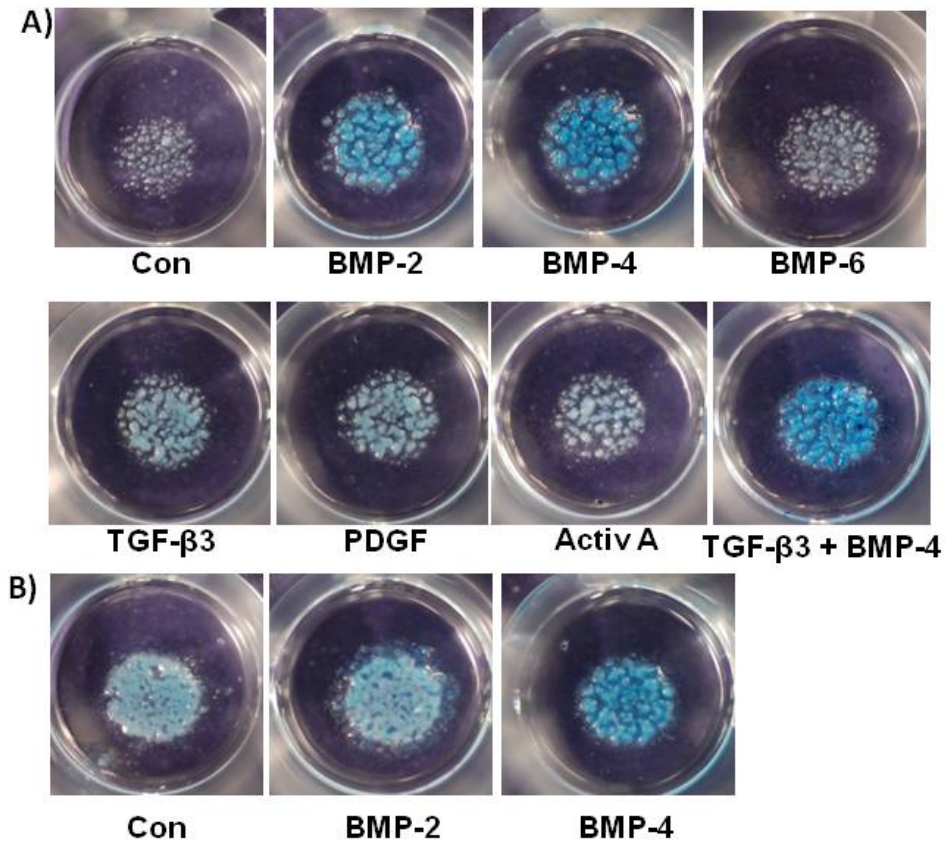
Figure 5-7: Alcian blue for growth factor screen. After 10 days, micromasses were stained for Alcian blue to indicate GAG accumulation using A) colony 1 or B) colony 2 of MEF iPSCs.

5.3.4 Effect of serum and timing of growth factor delivery in micromass culture

Micromasses from B6 tail fibroblast iPSC colony #7 were induced by BMP-4 for 15 days in the absence or presence of 1% serum. As measured by Col2, Sox9, and Acan gene expression, chondrogenesis was only induced by BMP-4 in serum-free conditions (Figure 5-8A). Additionally, the timing of BMP-4 was shown to be important. Continuous BMP-4 exposure increased Col2 expression over time up to 27 days as compared to control culture. However, the upregulation of Col2 was enhanced by

111

providing BMP-4 for only days 2-6 (short term) as opposed to continuously (Figure 5-8B). Short-term BMP-4 treatment also increased Sox9 and Acan expression while lowering Col10 expression as compared to continuous treatment (Figure 5-8C).
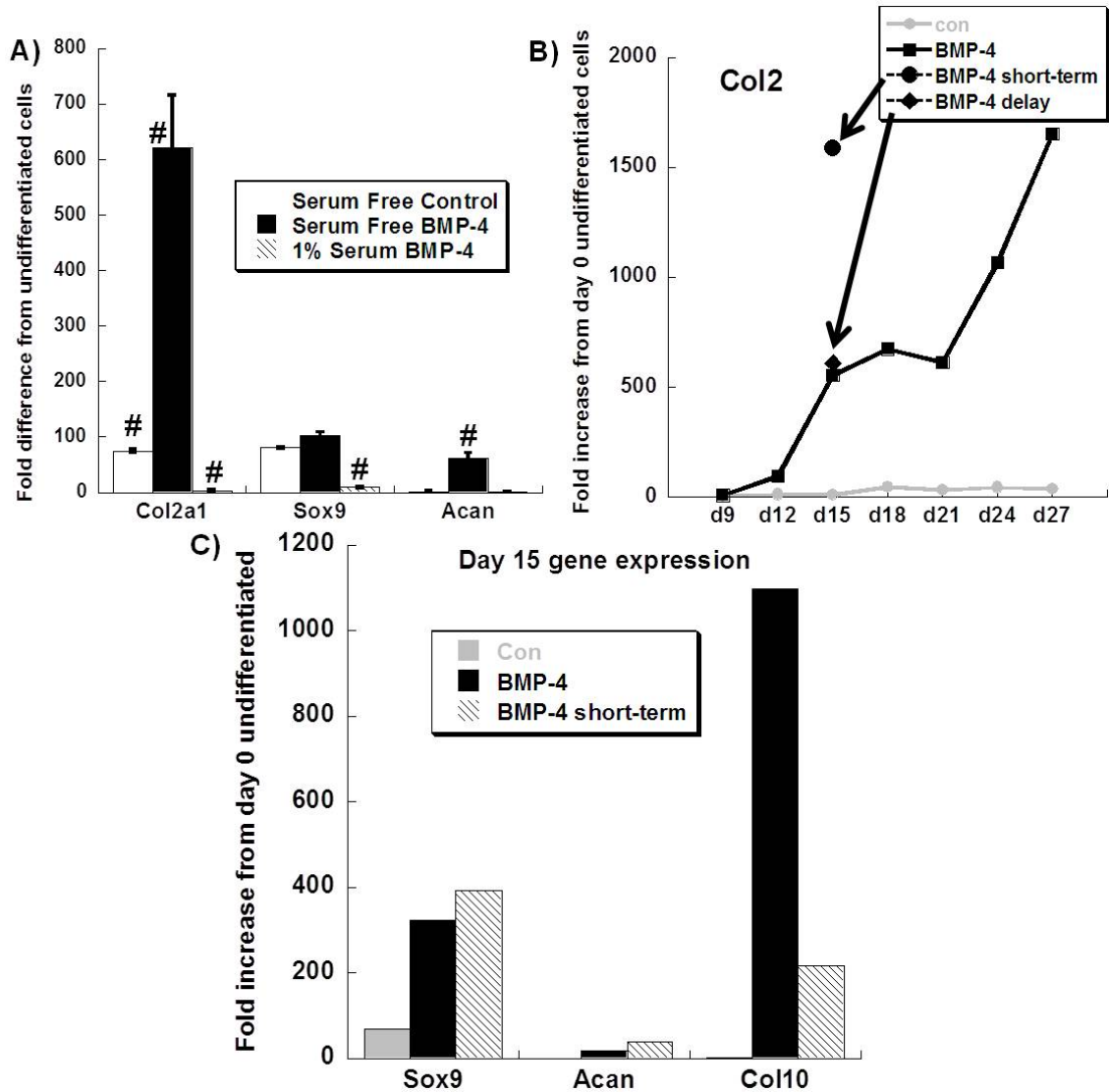
Figure 5-8: Effect of serum and growth factor timing in micromass culture. A) Chondrogenic gene expression of day 15 micromasses with BMP-4 in the presence or absence of serum, n=3. B) Col2 expression in micromasses over time in culture with BMP-4 continuously, for days 2-6 only (short term), or from day 4 on (delay). C) Gene expression at day 15 comparing continuous and short-term BMP-4 exposure.

5.3.5 Clone selection

In order to select clones with the successful integration of the Col2-GFP reporter construct, 12 clones from B6 and MRL iPSCs were screened to assess the specific increase in GFP expression with chondrogenic induction. Micromasses were cultured in serum-free continuous BMP-4 conditions and harvested at day 15 (B6) or day 17 (MRL) for cell sorting. The sort profiles of the clones that were selected for further analysis demonstrate the increase in GFP+ percentage with chondrogenic induction (Figure 5-9). The total yield of GFP+ cells also indicated an increase with BMP-4 culture in these clones (Table 5-1, selected clones highlighted).
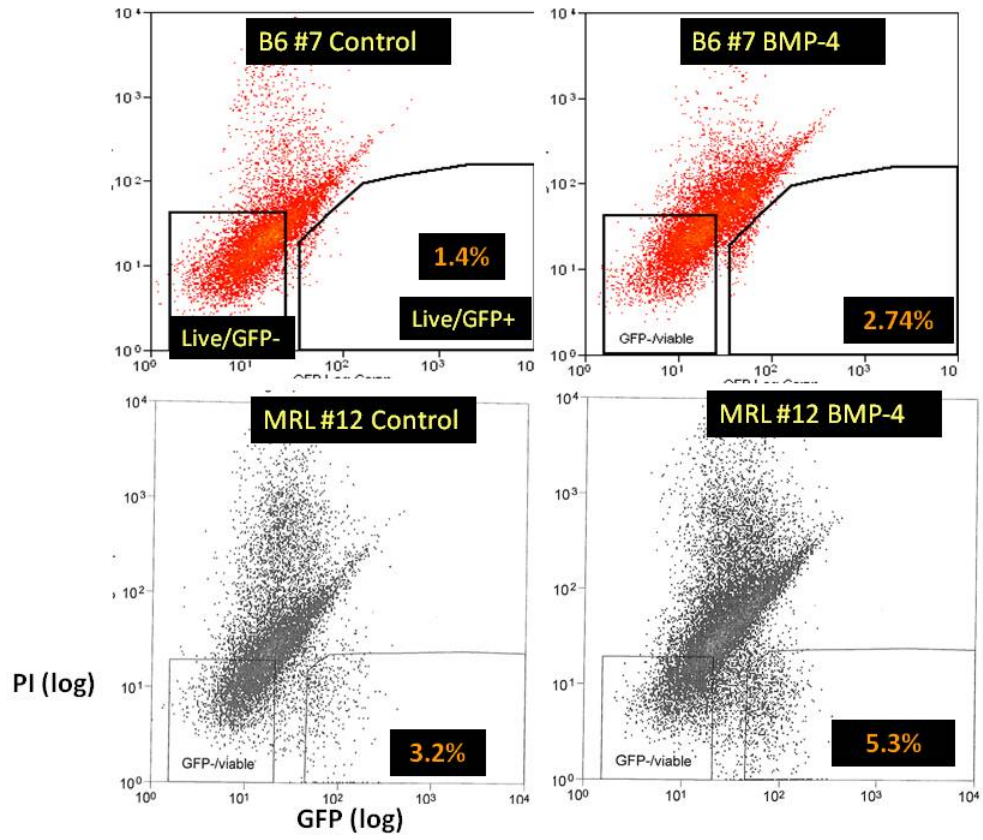
Figure 5-9: Sort profile for selected clones. The percentage of GFP+ cells in day 15 digested micromasses cultured in either control or BMP conditions.

Table 5-1: Clone selection based on increase in GFP+ cell yield with BMP-4

Clone	GFP+ yield: Control	GFP+ yield: BMP-4	Clone	GFP+ yield: Control	GFP+ yield: BMP-4
B6 #1	0	1	MRL #1	716	103
B6 #2	0	0	MRL #2	215	254
B6 #3	1	158	MRL #3	212	1
B6 #4	0	304	MRL #4	192	7
XXXX			XXXX		
B6 #6	0	0	MRL #6	0	0
B6 #7	47	567	MRL #7	116	0
B6 #8	0	3	MRL #8	532	1504
B6 #9	0	2	MRL #9	304	117
B6 #10	1	85	MRL #10	1646	1649
B6 #11	0	10	XXXX		
B6 #12	0	130	MRL #12	747	1301

5.3.6 Effect of culture duration and BMP-4 timing in micromasses

5.3.6.1: Effect of BMP-4 timing on gene expression

Optimization of the timing of BMP-4 delivery was investigated using B6 colony #7 iPSCs. Different short-term BMP-4 strategies were compared for gene expression at day 15 and day 27. These data showed that extended culture with BMP-4 yielded high Col2 and Acan expression, but also high Col10 expression. Delivering BMP-4 for days 2-3, 4-5, or 2-5 caused upregulation of Col2, Sox9, and Acan without high Col10 values (Figure 5-10).
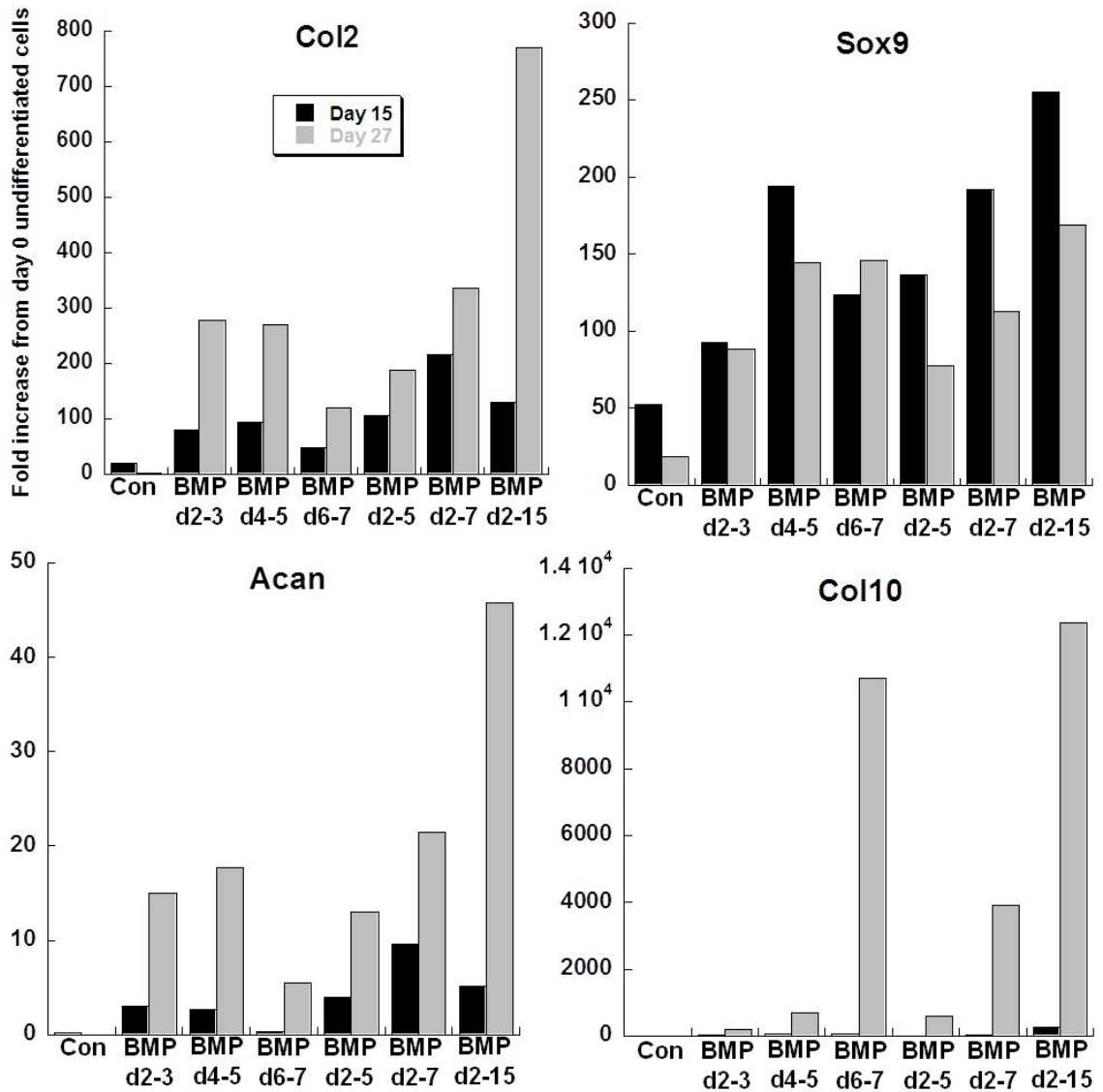
Figure 5-10: Timing of BMP-4 induction in micromass culture. Gene expression at days 15 and 27 after delivery of BMP-4 for different periods of time (as labeled). One micromass per group.

5.3.6.2: Effect of BMP-4 timing on yield of GFP+ cells

We utilized the Col2-GFP reporter construct to determine the yield of GFP+ cells in response to different timing strategies with BMP-4 (Table 5-2).   The highest yields of GFP+ cells were found when BMP-4 was given during days 4-5 or 2-5. Within these

groups, harvest of the micromasses at day 15 and day 27 yielded a similar number of

cells per micromass. The method of micromass digestion used for the timing

comparison was a combination of collagenase/pronase and trypsin. Additionally, extra

sets of micromasses fed with BMP-4 from days 2-5 showed that trypsin alone was

insufficient, but collagenase/pronase alone obtained a similar yield of cells at day 15 (400

cells trypsin, 10,500 cells collagenase/pronase, 11,200 cells both).

Table 5-2: Effect of BMP-4 timing on GFP+ cell yield

Group	GFP+ yield day 15: 5 micromasses	GFP+ yield day 27: 4 micromasses
Con	74	0
BMP d2-3	2,300	7046
BMP d4-5	10,800	8539
BMP d6-7	400	1
BMP d2-5	11,200	8996
BMP d2-7	4,800	7084
BMP d2-15	6,400	4167

5.3.6.3: Effect of additional culture factors on yield of GFP+ cells

An additional experiment explored the effects of adding DEX at various points

during differentiation, feeding ascorbate and proline at day 1 of micromass culture

instead of waiting until day 2, and providing BMP-4 from days 3-5 of micromass culture

on GFP+ cell yield (Table 5-3). The yield was greatly increased when feeding with

ascorbate and proline at day 1. The yield was also increased by either leaving DEX out

117

entirely or only providing DEX along with BMP-4. Feeding with BMP-4 beginning at

day 3 instead of day 4 also increased the yield of GFP+ cells. Culturing the

micromassess with 25 ng/ml BMP-4 instead of 50 ng/ml BMP-4 was not effective, and no

GFP+ cells were sorted when culturing the micromass at 2% O_2.

Table 5-3: Effect of DEX and other culture conditions on GFP+ cell yield

Group	GFP+ yield day 15: 2 micromasses
BMP d4-5, no asc/pro d1, dex all	23
BMP d4-5, asc/pro d1, dex all	353
BMP d4-5, asc/pro d1, dex d4 only	1336
BMP d4-5, asc/pro d1, no dex	1111
BMP d3-5, asc/pro d1, dex all	1847
25 ng/ml BMP d4-5, no asc/pro d1	0
BMP d4-5, no asc/pro d1, dex all, 2% O2	0

5.3.7 Embryoid body formation for chondrogenic induction

The formation of embryoid bodies was investigated for the ability to induce

chondrogenic differentiation. Embryoid bodies were formed using the hanging drop

method followed by liquid suspension culture and then outgrowth on gelatin coated

plates (Figure 5-10A). BMP-4 was provided either in the liquid suspension culture,

during the outgrowth monolayer phase, or both. The highest Col2 expression was seen

when BMP was provided during the liquid suspension phase but not during the

outgrowth phase (Figure 5-11B). These conditions also resulted in the highest yield of

GFP+ cells after 15 total days of culture, which corresponds to 9 days of outgrowth

culture. Col2 expression and GFP+ cell yields were higher at day 15 as compared to day

27.
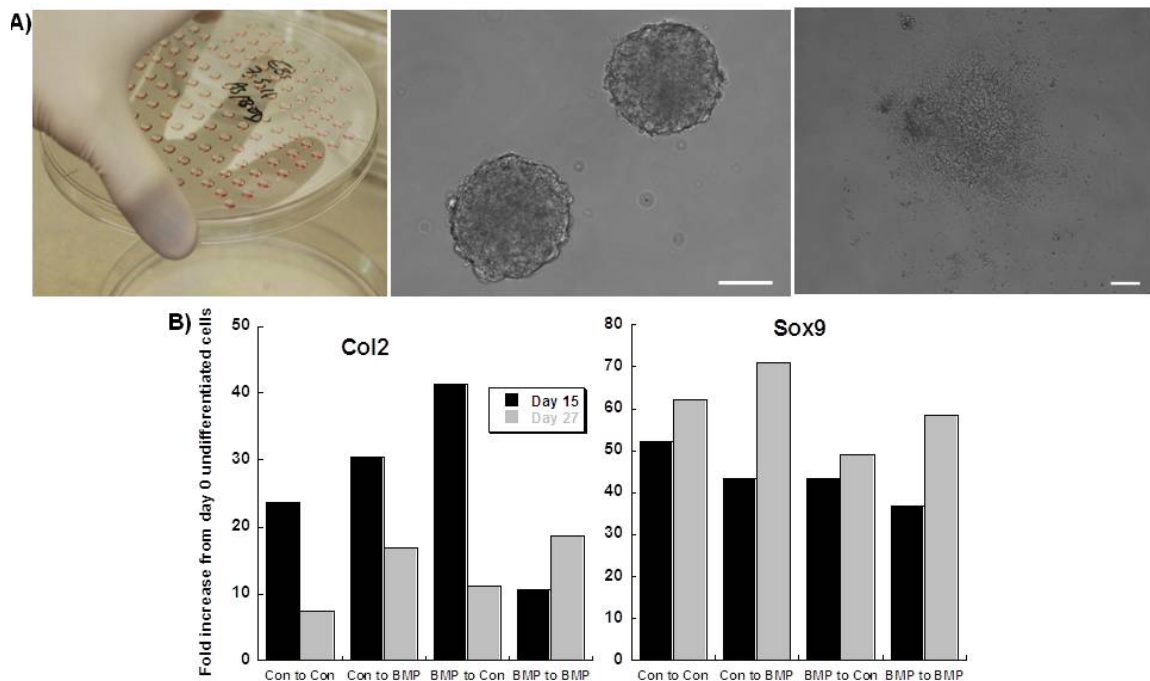
Figure 5-11: Embryoid body culture. A) Hanging drops were formed for 3 days (left), cultured in liquid suspension for 3 days with 20% serum (middle), then plated on gelatin coated plates for outgrowth (right), scale bars = 100 μm. B) RT-PCR at days 15 and 27; one well per group.

Table 5-4: Yield of GFP+ cells from embryoid bodies

Liquid Suspension	Outgrowth	GFP+ yield day 15	GFP+ yield day 27
Control 20% serum	SF control	677	578
Control 20% serum	SF BMP-4	341	200
BMP-4 20% serum	SF control	3,400	743
BMP-4 20% serum	SF BMP-4	640	234

5.3.8 Monolayer expansion of sorted cells

Cells sorted either as GFP+ or GFP- were plated in monolayer culture for expansion. Initial culture using B6 GFP+ cells indicated that 10% serum was more effective than 1% serum at promoting expansion of the cells, and that gelatin coated flasks resulted in better morphology and proliferation than standard tissue culture flasks. The default culture conditions were determined to be plating at 10,000 cells/cm^2 with 10% serum (same lot as for iPSC media), 4 ng/ml bFGF, and no DEX. Modifying any of these variables lowered the cumulative fold expansion over 3 passages in culture (Table 5-5).

Table 5-5: Effect of monolayer conditions on B6 GFP+ cell expansion

	Default	Different serum lot	20k/cm^2 density	No Dex No FGF	w/ Dex No FGF	w/ Dex w/ FGF
Fold Expansion (3 passages)	148	83	120	26	0.6	52

These monolayer conditions were used to compare the expansion of GFP+ and GFP- cells from B6 and MRL strains (Figure 5-12). The B6 cells showed rapid expansion, with GFP+ having greater expansion than GFP-. The MRL GFP- showed slower expansion than the B6 cells, and the MRL GFP+ cells did not expand in monolayer culture. This phenomenon was confirmed in a separate experiment.
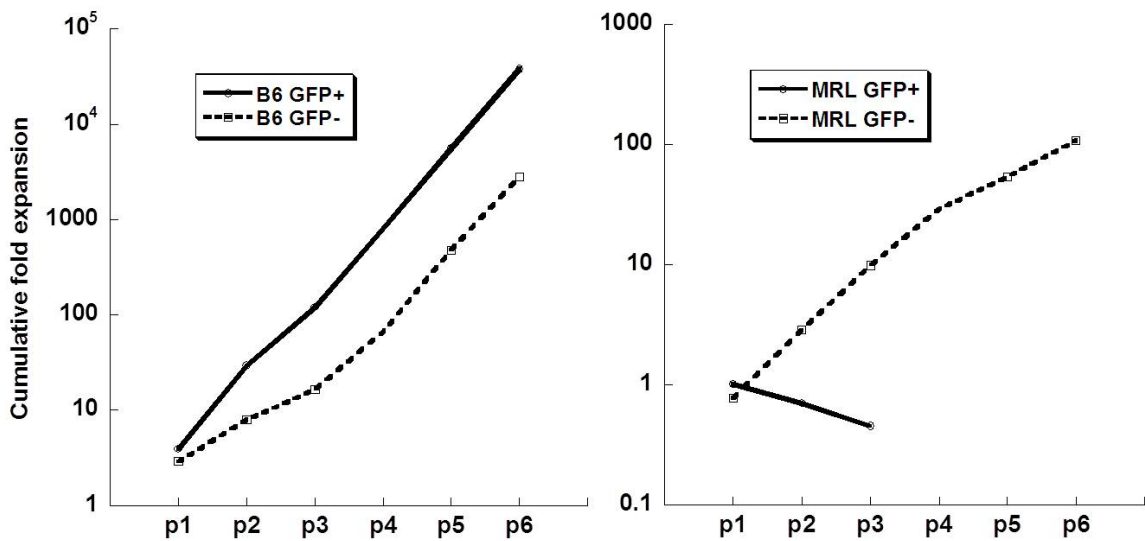
Figure 5-12: Expansion of B6 and MRL sorted cells. The cumulative fold expansion for B6 (left) and MRL (right) cells in monolayer with 10% serum and bFGF.

5.3.9 Growth factor induction in pellet culture

The capacity for sorted cells to form pellets and produce cartilaginous matrix was tested using B6 GFP+ cells sorted after 27 day micromass culture with BMP-4 provided from days 2-5. The GFP+ cells were expanded for 2 passages in 10% serum without bFGF or DEX before pellet culture with either 10 ng/ml TGF-β3 or 50 ng/ml BMP-4. While GAGs and type II collagen were produced in both conditions, more consistent matrix formation was seen with TGF-β3 induction (Figure 5-13).

121

Additionally, there was less staining for type X collagen with TGF-β3 as compared to

BMP-4.
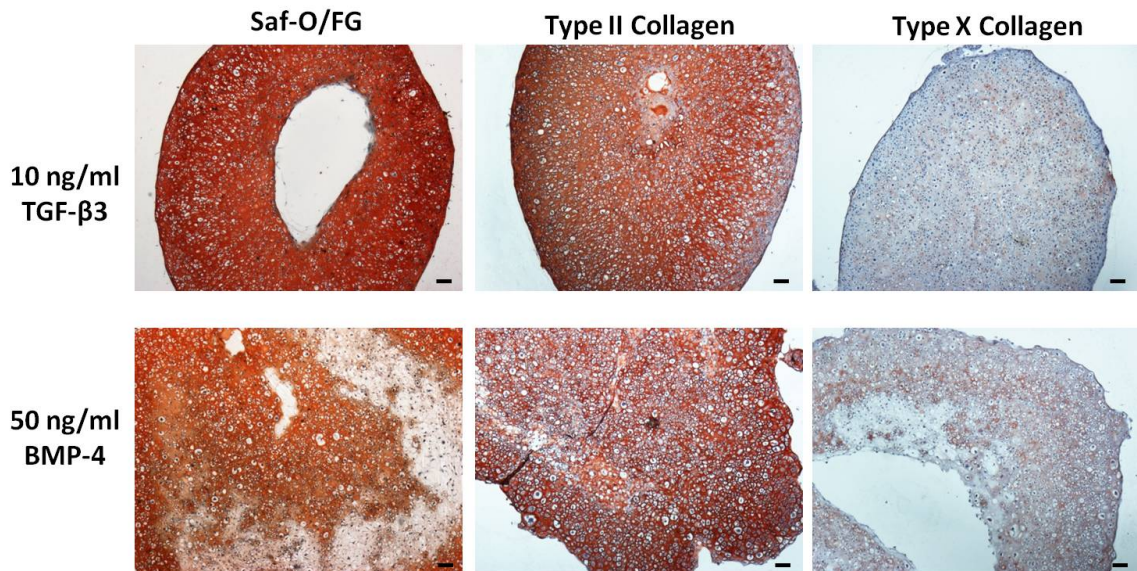
Figure 5-13: TGF-β3 and BMP-4 induction in pellet culture. Pellets were cultured for 21 days in the presence of TGF-β3 or BMP-4. Sections were stained with Safranin-O/Fast Green/Hematoxylin or processed for immunohistochemistry with antibodies to type II or type X collagen. Scale bar = 100 μm.

5.4 Discussion

There were numerous factors to investigate for determining the most effective

way to induce the chondrogenic differentiation of iPSCs. Key factors included the

culture system, the growth factors used, and the timing of growth factor delivery. The

expression of chondrogenic genes at different time points and histological staining of

cartilage matrix proteins were important for assessing the outcome of particular

conditions. Additionally, the yield of chondrogenically differentiated cells served as a

functional outcome of both cell survival and differentiation, important for the goal of

maximizing the number of cells with high chondrogenic potential for use in subsequent tissue engineering studies. Successful differentiation was assessed by selecting iPSC clones with stable and specific integration of GFP under the control of the Col2 promoter/enhancer and then using flow cytometry to sort for GFP+ cells.

To determine if iPSCs could be used to form tissue-engineered cartilage without pre-differentiation, we cultured undifferentiated cells in various 3D environments. In both agarose and PEG-RGD hydrogels, cells appeared to survive only if 5% serum was present. Even with serum, the cell proliferation and small amounts of matrix formation were found in cell clusters that displaced the surrounding hydrogel instead of uniformly populating it. In CDM scaffolds, undifferentiated iPSCs did not attach to the existing matrix in large numbers. The few areas that demonstrated a high cell density did produce GAGs in response to growth factors, indicating that cell-cell interactions are important for chondrogenesis at this stage. This concept is consistent with cartilage development, as condensation to form tightly interacting cells is the initiating event of chondrogenesis (Cancedda et al., 1995; Hall and Miyake, 2000). This was confirmed using pellet culture, as the forced aggregation in pellets was effective for inducing chondrogenesis of iPSCs as determined by histology for GAGs. Chondrogenic differentiation was noted in the presence of BMP-4 but not TGF-β3, and only in serum-free conditions. However, pellet culture did not reach the cartilage tissue engineering goal of a uniform GAG distribution.

Initial differentiation of iPSCs in a "pre-differentiation" system may be necessary to induce the early stages of chondrogenesis before culture in a 3D tissue engineering environment. We investigated monolayer culture, embryoid bodies, and micromass formation as possible systems for initial chondrogenic differentiation. Monolayer culture offers significant control and scalability, but may require a complex series of growth factor and matrix substrates to compensate for the lack of signals associated with aggregate culture (Oldershaw et al., 2010). Embryoid bodies have commonly been used for general differentiation of ESCs, and EB outgrowth cells can be used as the starting cell source for chondrogenic pellet or hydrogel culture with iPSCs (Kim et al., 2011; Medvedev et al., 2011; Teramura et al., 2010; Wei et al., 2012). However, EBs display unpredictable heterogeneous differentiation based on EB size (Nakagawa et al., 2009) and culturing in liquid suspension may present additional challenges. Finally, micromass culture of high density 2D culture provides a controlled system for aggregation that has been used successfully to initiate uniform chondrogenesis of limb bud cells (Ahrens et al., 1977).

Micromass culture was more effective at chondrogenic "pre-differentiation" than monolayer and EB culture under the conditions employed in this study. As compared to monolayer culture, micromass culture resulted in greater upregulation of Col2 and Sox9. The rapid proliferation of cells in monolayer may have inhibited differentiation to occur, and also presented the logistical challenge of frequent passaging to prevent

124

overgrowth.   Embryoid body formation was assessed for chondrogenic gene expression and yield of GFP+ cells. Delivering BMP-4 during the liquid suspension phase but not during the outgrowth phase maximized the Col2 expression and GFP+ cell yield at day 15. However, both chondrogenic gene expression and the yield of GFP+ cells were lower than corresponding micromass cultures. The value of EBs for generating large numbers of GFP+ cells would be inhibited by the requirement to provide BMP-4 in liquid suspension due to the large media requirements of this system.

Culture conditions such as the presence of serum had a large impact on the degree of differentiation and GFP+ cell yield in micromass culture. Serum was inhibitory to chondrogenesis, and the presence of just 1% serum dramatically reduced the Col2, Sox9, and Acan expression induced by BMP-4 at day 15.   Micromass culture of ESCs has been performed in both serum-free (Gong et al., 2010; Nakayama et al., 2003; Toh et al., 2007) and 1% serum conditions (Yamashita et al., 2010). Serum-free systems are preferable for recapitulating chondrogenesis and allow more exact characterization, but have the disadvantage of increased cell death and lower proliferation (Heng et al., 2004; Toh et al., 2007). Our results with micromass cultures were consistent with the results in pellet culture experiments, which indicated that BMP-4 mediated differentiation was abolished by the presence of 5% serum. Pellet culture of adult stem cells for chondrogenesis has also frequently been performed in serum-free culture conditions (Johnstone et al., 1998).

We then performed a growth factor screen using serum-free micromass cultures. Alcian blue staining confirmed strong GAG deposition in BMP-2 and BMP-4 treated micromasses. Gene expression was highly upregulated for Col2 and Sox9, with a moderate upregulation of Acan, Col1, and Col10 as well. While control conditions provided the highest Col2 and Acan upregulation, BMP-2 and BMP-4 provided the highest Sox9 values. An additional experiment using a different colony of MEF iPSCs confirmed these results and indicated that BMP-4 may be more consistent at inducing differentiation than BMP-2. The effectiveness of BMP-4 for chondrogenic differentiation of pluripotent cells (Kramer et al., 2000; Nakayama et al., 2003) is consistent with the growth factor's role in mediating both initial mesoderm formation (Zhang et al., 2008) and chondroprogenitor lineage determination (Hatakeyama et al., 2004).

The timing of growth factor administration is also an essential part of developing an effective differentiation protocol. For example, micromass culture of ESCs showed enhanced chondrogenesis by delaying the delivery of BMP-2 by a day (Gong et al., 2010). In this work, short-term delivery of BMP-4 was even more effective than continuous delivery at inducing expression of Col2, Acan, and Sox9. Importantly, shorter duration of BMP-4 delivery also reduced the dramatic Col10 upregulation that was seen with continuous BMP-4 culture. Further investigations were carried out by employing BMP-4 at different combinations for days 2-7 of culture. Feeding with BMP-4 for days 4-5 or days 2-5 was most effective at generating large numbers of GFP+ cells in

micromass culture. Additionally, culturing for 15 days gave yields as large as culturing for 27 days, despite the higher chondrogenic gene expression seen at the later time point. Final modifications to the culture conditions were made by an additional experiment showing that providing BMP-4 at day 3 instead of day 4 increased the yield of cells and that culturing with DEX only during BMP-4 induction enhances the number of GFP+ cells.

Despite a successful system for inducing expression of Col2 in micromass culture and the corresponding expression of GFP, the number of cells generated would be insufficient for future experiments. Additionally, cells that are digested from micromasses and immediately sorted may require time to recover before being used in pellet culture. Thus, conditions for expanding the cells in monolayer after sorting were investigated. Including 4 ng/ml bFGF and excluding DEX during expansion was ideal for rapidly expanding the sorted cells. Interestingly, while these conditions were sufficient for the expansion of B6 GFP-, B6 GFP+, and MRL GFP- cells, MRL GFP+ cells did not expand. This could be a result of the specific colony selected for use in this study, or it could also be a feature of chondrocyte-like cells from this particular mouse strain.

Pellet culture was used to distinguish the chondrogenic induction provided by TGF-β3 and BMP-4. For undifferentiated iPSCs, BMP-4 was effective at promoting matrix formation and TGF-β3 was not. After initial differentiation in micromass culture

127

and expansion of GFP+ cells, both growth factors were able to induce the production of cartilaginous matrix staining positive for GAGs and type II collagen. However, TGF-β3 provided more consistent differentiation across the pellet and also induced less deposition of the hypertrophic marker type X collagen. Insight into how the effect of BMP-4 and TGF-β3 change with the differentiation status of the cells can be gained from cartilage development, as both growth factors have specific chondrogenic effects in early and late differentiation. In initial differentiation, TGF-β is primarily responsible for the initiation of mesenchymal condensation whereas BMPs function in the transition to differentiation (Hall and Miyake, 2000; Roark and Greer, 1994). This could explain the greater effectiveness of the BMPs in micromass culture, as forced aggregation may obviate the need for initiation by TGF-β but rely on the transition to differentiation by BMP-4. In chondrocyte maturation, TGF-β can prevent hypertrophy (Yang et al., 2001) while BMPs are necessary for chondrocyte hypertrophy (Retting et al., 2009), supporting the type X collagen staining seen in pellets of pre-differentiated cells. Interestingly, the observation that TGF-β3 signaling induces less hypertrophy than BMP signaling has also been seen in the chondrogenic differentiation of adult stem cells (Hellingman et al., 2011).

5.5 Summary

The chondrogenic differentiation of pluripotent cells is regulated by the cell microenvironment and the timing of specific growth factors. To explore the effects of

the cell microenvironment on the differentiation of murine iPSCs, we cultured cells in

monolayer, micromass, and embryoid body systems. We determined that 15 day serum-

free micromass culture with BMP-4 and DEX present for days 3-5 only maximized the

yield of successfully differentiated cells based on sorting for Col2-GFP+. For

undifferentiated iPSCs, serum-free pellet culture with BMP-4 was effective at inducing

non-uniform matrix production, whereas hydrogel and CDM scaffolds were insufficient.

The number and chondrogenic capacity of the starting cells was enhanced by pre-

differentiating the cells in micromass culture, sorting based on GFP expression, and

expanding in monolayer with bFGF. Subsequent pellet with TGF-β3 and to a lesser

extent BMP-4 resulted in robust matrix production. This multi-stage system for

chondrogenic induction of pluripotent cells can be used to generate pellets with rich

cartilage-like matrix.

6. Cartilage tissue engineering using differentiated and purified induced pluripotent stem cells

6.1 Introduction

Tissue engineering has shown promise as a regenerative therapy for cartilage injury, but these strategies require a sufficient cell source (Song et al., 2004). Genetic reprogramming of somatic cells into induced pluripotent stem cells (iPSCs) (Takahashi and Yamanaka, 2006) can generate large numbers of patient-matched cells with chondrogenic potential. In addition to providing a novel source of cells for therapy applications, a second important use of iPSC technology is to create cell and tissue models from specific patients for study and drug screening (Ebert et al., 2009; Israel et al., 2012; Park et al., 2008; Quarto et al., 2012; Saha and Jaenisch, 2009). We propose that this principle can be used to create cartilage constructs from specific mouse strains for the mechanistic study of cartilage development, repair, and OA. However, one of the major challenges with using iPSCs for cell therapy and in vitro modeling is the difficulty in achieving uniform differentiation to the cell type of interest (Yoshida and Yamanaka, 2010). A non-uniform cell population limits the effectiveness of the therapy or model, and also increases the risk for undifferentiated cells contained in the population to contribute to teratoma formation during in vivo studies (Blin et al., 2010).

The goal of this study was to create tissue-engineered cartilage constructs from purified iPSCs. To select for cells successfully differentiated toward the chondrogenic lineage, we performed micromass differentiation with bone morphogenetic protein-4

130

(BMP-4) and used flow cytometry to sort cells expressing green fluorescent protein

(GFP) under control of the chondrocyte-specific type II collagen (Col2)

promoter/enhancer (Grant et al., 2000). The potential of differentiated and purified

iPSCs to be used for cartilage repair was investigated using an in vitro cartilage defect

model system.

6.2 Materials and Methods

6.2.1 Analysis of pluripotency and karyotype

Tail fibroblasts from C57BL/6 (B6) mice were reprogrammed to pluripotency

using a single doxycycline-inducible lentiviral vector controlling the transgenic

expression of mouse cDNAs for Oct4 (also known as Pou5f1), Sox2, Klf4, and c-Myc

(Carey et al., 2009) and cultured as described in chapter 5. The Col2-GFP construct was

introduced into undifferentiated iPSCs using nucleofection (Lonza) and B6 clone #7 was

selected for further analysis based on a specific increase in expression of GFP after

chondrogenic induction in micromass culture.

Undifferentiated iPSCs on feeder cells were analyzed for alkaline phosphatase

activity (Stemgent) or fixed with 4% paraformaldehyde (PFA, Electron Microscopy

Sciences), permeabilized with 0.2% Triton X-100 (Sigma-Aldrich), and stained using

DAPI or primary antibodies to Nanog (Abcam #21603), Oct4 (Abcam #19857), and

SSEA1 (MC-480, Developmental Studies Hybridoma Bank) for immunofluorescence.

Teratoma formation analysis (Applied Stem Cell) was performed by injecting 0.5-

2x10^6 undifferentiated iPSCs with 30% Matrigel into the kidney capsule and testis of 6

week-old SCID mice. After approximately 5 weeks, tumors were removed and analyzed

by histology for the presence of tissues from all three germ layers. Additionally,

chromosome counting and G banding were used to analyze the karyotype of the iPSCs

(Applied Stem Cell).

Undifferentiated iPSCs, passage 2 GFP+, passage 2 GFP-, and passage 2 unsorted

cells, as well as tail fibroblasts before reprogramming, were analyzed using RT-PCR.

The expression of Oct4/Pou5f1, Sox2, Klf4, and c-Myc was assessed using primers that

recognized either endogenous copies only, or both endogenous and exogenous copies.

Nanog was also analyzed for endogenous expression. Primer sequences are found in

Table 6-1.

Table 6-1: Primers for RT-PCR of pluripotency genes

Target	Forward	Reverse
Nanog	AAAAAGCAGGCTCTGACATGAGTGTGGGTCTT	AGAAAGCTGGGTAAGTCTCATATTTCACCTGG
Oct4 (Endo/Exo)	CCCCATGTCCGCCCGCATAC	TGCTCCTGCCTGGCCCTCAG
Oct4 (Endo)	CTGCCCCCAGGTCCCCACTT	AGCATCCCCAGGGAGGGCTG
Sox2 (Endo/Exo)	GGGGGCAGCGGCGTAAGATG	CCCGCTCGCCATGCTGTTCC
Sox2 (Endo)	CCGAGGAGGAGAGCGCCTGT	GCGGCTTCAGCTCCGTCTCC
Klf4 (Endo/Exo)	GCCTGCCTCTTCCCCCAGGA	TTGGGCTCCTCTGGCAGGCA
Klf4 (Endo)	AGTCCCCAGGACTCCGCACC	TCAGCAGTGTCCCCCACCGT
c-Myc (Endo/Exo)	CCTCCGAGTCCTCCCCACGG	GGGTGCGGCGTAGTTGTGCT
c-Myc (Endo)	CCCATTGCAGCGGGCAGACA	ATCGCGGGCAGAGGCAGAGA

6.2.2 Micromass culture for initial chondrogenic differentiation

Feeder layer cells were removed using two subtraction steps of 45 minutes on tissue culture plastic separated by a day of culture on 0.1% gelatin (Sigma-Aldrich). Cells were resuspended at a concentration of 2×10^7 cells/ml, and micromasses were established by plating 2×10^5 iPSCs in 10 μl into individual 48 well plates (Corning) or as a set of 30 micromasses in a 10 cm dish (BD). After 2-3 hour incubation, additional iPSC medium with 10% serum without LIF was added. Twenty-four hours after establishing micromasses, the media was switched to serum-free chondrogenic differentiation medium containing DMEM-HG, NEAA, 2-me, ITS+ premix (BD), penicillin-streptomycin (P/S, Gibco), 37.5 μg/ml L-ascorbic acid 2-phosphate (Sigma-Aldrich), and 50 μg/ml L-proline (Sigma-Aldrich). Micromasses were cultured for 15 days, with 50 ng/ml mBMP-4 (R&D Systems) and 100 nM dexamethasone (DEX, Sigma-Aldrich) added to the chondrogenic medium during days 3-5 of culture only.

6.2.3 Cell sorting

Micromasses were digested for 1 hour using 0.4% collagenase type II (Worthington Biochemical), 1320 PKU/ml pronase (Calbiochem), and 10 μg/ml DNAse I (Worthington Biochemical). Cells were centrifuged, incubated with 0.25% tryspin-EDTA (Sigma-Aldrich) for 5 minutes, and resuspended in sort medium containing DMEM-HG, 2% FBS, DNAse I, 10 mM Hepes (Gibco), 2x P/S/F, and 33.3 nM propidium iodide (Biolegend) as a dead cell marker. Cells were sorted based on GFP expression

133

using the 100 μM nozzle of a Cytomation MoFlo® sorter (Beckman Coulter). Sorted

cells were plated onto coverglass chambers (Nunc) for two days before

immunocytochemistry for type II collagen (II-II6B3, Developmental Studies Hybridoma

Bank).

6.2.4 Cell expansion and pellet culture

Cells sorted as GFP- or GFP+ were plated at 1×10^4 cells/cm^2 on gelatin coated

plates in chondrogenic expansion medium consisting of chondrogenic differentiation

medium with the addition of 10% FBS and 4 ng/ml basic fibroblast growth factor (bFGF,

Roche). Cells were passaged upon sub-confluence every 2-3 days using 0.05% trypsin-

EDTA (Sigma-Aldrich). After each passage, some cells were used to form pellets by

centrifuging 2.5×10^5 cells at 200 xg for 5 minutes in 15 ml tubes. Pellets were cultured in

chondrogenic differentiation medium with the addition of 10 ng/ml TGF-β3 (R&D

Systems) and 100 nM DEX for 21 days.

6.2.5 Self-assembled constructs in agarose wells and transwells

To allow for the self-aggregation of cells, iPSCs were cultured at high density in

custom-made agarose wells or on top of transwell inserts. Agarose wells were

constructed by inverting a mold with 5 mm diameter rods into molten agarose, forming

a well with agarose on the sides and bottom. Cells were delivered to the well at high

density (2×10^6 in 90 μl) of serum-free chondrogenic media with DEX and allowed to self-

aggregate for 4 hours before the addition of chondrogenic media containing 10 ng/ml

TGF-β3. For transwell cultures, $2x10^6$ cells in 100 μl of serum-free chondrogenic media were delivered evenly across the top of 6.5 mm transwell inserts with 0.4 μm pores (Costar #3413) in 24 well plates. Transwells located centrally in the plate were centrifuged for 5 minutes at 200 xg and then transferred to new wells on the plate containing chondrogenic media containing 10 ng/ml TGF-β3 and 100 nM DEX. Self-assembled constructs were cultured for 21 days before analysis.

6.2.6 Biochemical analysis

Some pellets were digested using pepsin and elastase over the course of 1 week at 4 °C and analyzed for type I and type II collagen using ELISA kits according to the manufacturer's protocol as recommended (Chondrex). Digested samples were also analyzed for glycosaminoglycans (GAGs) and DNA as described previously (Estes et al., 2010). DNA was converted to cell number using a value of 7.7 pg DNA per cell (Kim et al., 1988).

6.2.7 Cartilage defect repair assay

Cartilage explants of 5 mm diameter were taken from healthy areas of the femoral cartilage of 2-3 year old pigs and kept in chondrogenic differentiation medium containing 10% serum. Explants were then cored using a 3 mm biopsy punch and immobilized on a thin layer of molten 2% agarose (type VII, Sigma-Aldrich) that was allowed to cool to seal the bottom. Sorted cells in chondrogenic differentiation media were mixed 1:1 with 2% agarose for delivery to the defect area, achieving a final

135

concentration of 1×10^6 cells in 10 µl of 1% agarose. Delivering 1% agarose only and

immediately replacing the 3 mm cartilage core served as controls. Samples were

cultured for 21 days with chondrogenic differentiation medium containing 10 ng/ml

TGF-β3 and 100 nM DEX. After 21 days, samples were processed for histology or used

to assess the mechanical strength of the defect repair by measuring the peak shear stress

during a push-out test in a size-adjusted version of a described method (Hennerbichler

et al., 2007). In initial experiments, a 10% PEG-RGD hydrogel (method described in

Chapter 5) solution containing 1×10^6 cells in 10 µl was delivered to the inner area of the

cored explant and was photopolymerized within the defect. A 1 mm defect was used

for a trial experiment using a biopsy punch of self-assembled cartilage to fill the defect.

The self-assembled construct was created using the transwell system and 1 mm biopsy

punch with plunger (Miltex) was taken from the outer region and delivered directly to

the defect.

6.2.8 Statistical analysis

Statistical analysis was carried out using a t-test for comparison of two groups

and analysis of variance (ANOVA) with Fisher's LSD post-hoc analysis for comparison

of multiple groups, using $\alpha = 0.05$. Normality was tested and data log-transformed before

analysis if necessary. For plots showing GFP+ and GFP- cells over passage, significance

was only presented for comparisons between GFP- and GFP+ at each passage and to the

same cell type at passage 1. Data are presented as mean ± standard error of the mean

(SEM).

6.3 Results

6.3.1 Analysis of pluripotency and karyotype

Cells formed rounded colonies on top of the feeder cells and displayed

morphologic similarity to embryonic stem cells (ESCs), including a high nucleus to

cytoplasm ratio (Figure 6-1A). Cells showed positive staining for alkaline phosphatase

activity, Nanog, Oct4/Pou5f1, and SSEA-1 (Figure 6-1A). Additionally, undifferentiated

iPSCs expressed Nanog and endogenous levels of the reprogramming factors at similar

levels to endogenous and exogenous levels combined (Figure 6-1B). Tail fibroblasts and

sorted cells after 2 passages did not express Sox2, Oct4/Pou5f1, or Nanog, but did show

expression of Klf4 and c-Myc . Pluripotency was confirmed by the teratoma formation

assay, in which undifferentiated cells formed tumors containing tissues of all three germ

layers (Figure 6-1C). Tumors formed in both the kidney and testis, and subsequent

histology showed a variety of tissues including gland (endoderm), muscle (mesoderm),

and neuronal rosettes (ectoderm). The karyotype analysis of undifferentiated iPSCs

indicated an interstitial deletion from 2D to 2F3 in chromosome 2 and the loss of the Y

chromosome (Figure 6-2).
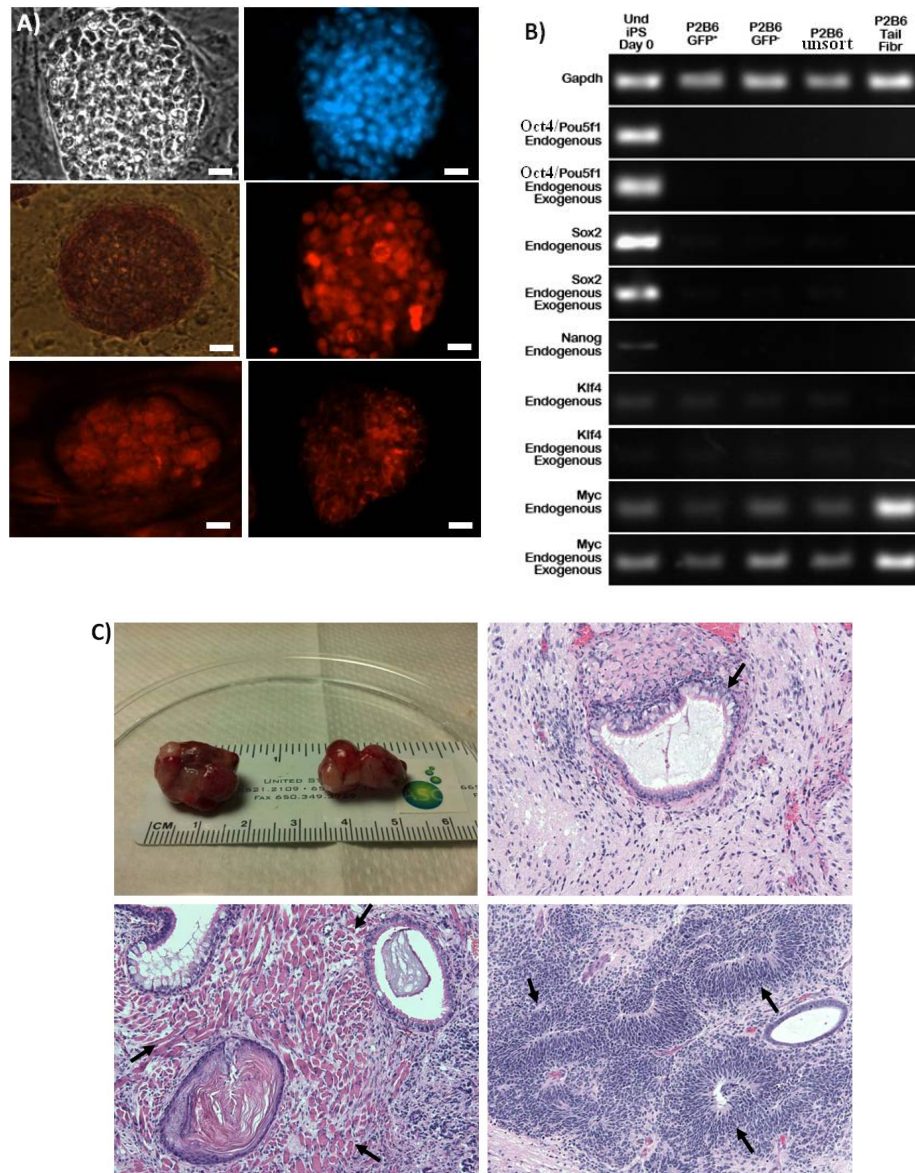
Figure 6-1: Characterization of pluripotency in iPSCs. A) Colonies of iPSCs were analyzed for markers of pluripotency: bright field (top left), DAPI (top right), alkaline phosphatase (middle left), nanog (middle right), Oct4/Pou5f1 (bottom left), and SSEA1 (bottom right), scale = 20 μm. B) RT-PCR for pluripotency markers with primers that are specific to endogenous expression or recognize both endogenous and exogenous gene expression. C) Tumor formation kidney and testis (top left), with histology showing gland formation (endoderm, top right), muscle (mesoderm, bottom left), and neuronal rosettes (ectoderm, bottom right); 200x magnification.

Figure 6-2: Karyotype analysis of undifferentiated iPSCs. The arrow indicates a translocation in chromosome 2. The loss of the Y chromosome was noted.

6.3.2 Cell sorting based on Col2-GFP expression

The addition of BMP-4 and DEX during days 3-5 of micromass culture initiated

chondrogenic differentiation of a subset of the iPSCs. Using gates based on identically

treated iPSCs without the Col2-GFP construct, approximately 10% of cells expressed

GFP under the control of the Col2 promoter/enhancer (Figure 6-3A). Among cells sorted

as GFP+, 86.1% were identified as GFP+ upon immediate reanalysis and 0.3% were

identified as GFP-. Cells sorted as GFP+ displayed a rounded phenotype and showed

expression of type II collagen, while cells sorted as GFP- were fibroblastic and did not

produce type II collagen (Figure 6-3B). Additionally, the chondrogenic gene expression

of GFP+ and GFP- cells immediately after sorting was distinct (Table 6-2). GFP+ cells

139

showed higher expression levels of Col2, Acan, Sox9, and Col10 as compared to GFP-

cells, whereas GFP- cells had higher Col1 expression. Both cell types showed a

downregulation of the pluripotency marker Nanog as compared to day 0

undifferentiated cells.
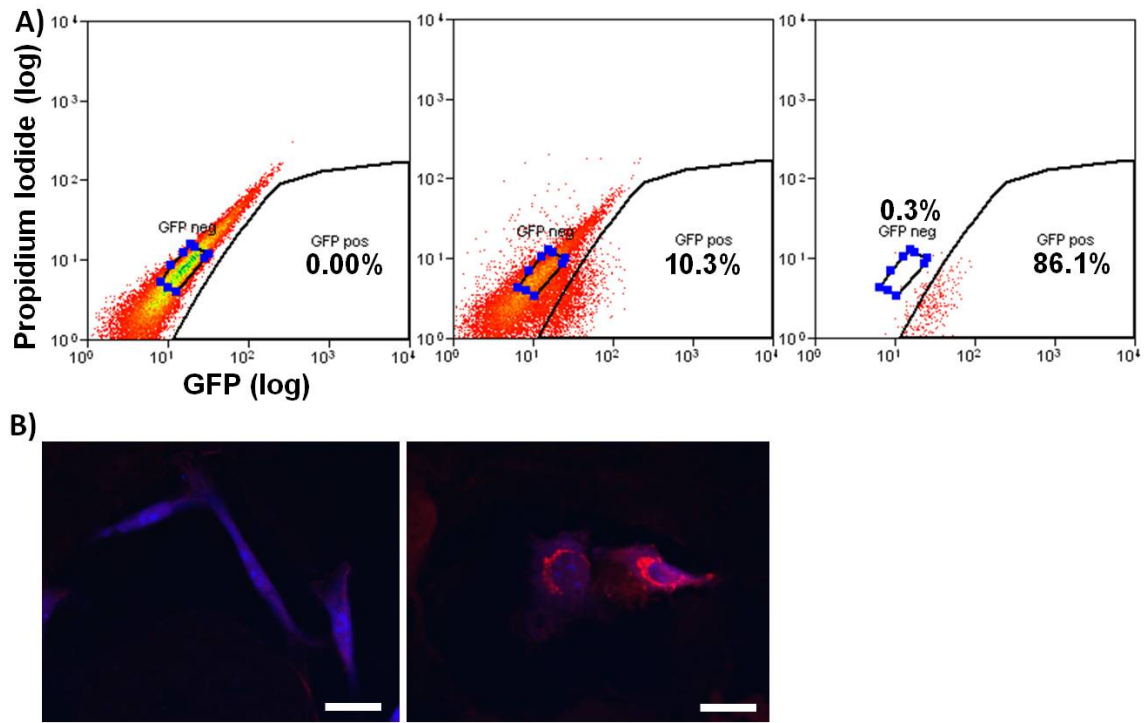
Figure 6-3: Sorting of Col2-GFP cells. A) Sort plots for d15 micromasses from iPSCs without the Col2-GFP construct (left), with the Col2-GFP construct (middle), and a representative analysis of sorted cells (right). B) Immunocytochemistry for type II collagen two days after sorting for GFP- (left) and GFP+ (right), scale bar = 20 μm.

Table 6-2: Gene expression of sorted cells (fold upregulation from day 0 undifferentiated cells, mean ± SEM, n ≥ 4)

	GFP+	GFP-
Col2	13451.0 ± 2611.9	228.1 ± 79.9
Acan	524.2 ± 102.9	17.0 ± 4.3
Sox9	788.8 ± 125.0	425.7 ± 143.3
Col10	34.8 ± 2.7	2.2 ± 0.3
Col1	254.8 ± 41.3	1484.9 ± 499.8
Nanog	-791.6 ± 247.5	-678.6 ± 245.3

6.3.3 Gene expression during monolayer expansion

Sorted cells retained distinctive morphologies in monolayer culture, with GFP-cells being larger and more fibroblastic than GFP+ cells (Figure 6-4A). In the presence of 10% serum and bFGF, both GFP+ and GFP- cells showed extensive proliferation, with a 2366 and 264 cumulative fold expansion over six passages, respectively (Figure 6-4B). The chondrocyte markers Col2 and Acan showed significantly higher expression in GFP+ as compared to GFP- cells after either one or two passages (Figure 6-4C). The expression levels of Col2 and Acan decreased with passaging in both GFP+ and GFP-cells. The expression of the early chondrocyte marker Sox9 was similar in GFP+ and GFP- cells and was generally stable over passaging, with the only significant effect being a decrease in expression of passage 3 GFP+ cells. The hypertrophic chondrocyte marker

Col10 was higher in GFP+ cells as compared to GFP- at the first two passages. Col10 increased with passaging in GFP- cells, but did not significantly increase in GFP+ cells. Expression of Col1 was higher in GFP- cells as compared to GFP+ cells after the first passage. Col1 increased in GFP+ cells after an additional passage, but was stable with passaging in GFP- cells.
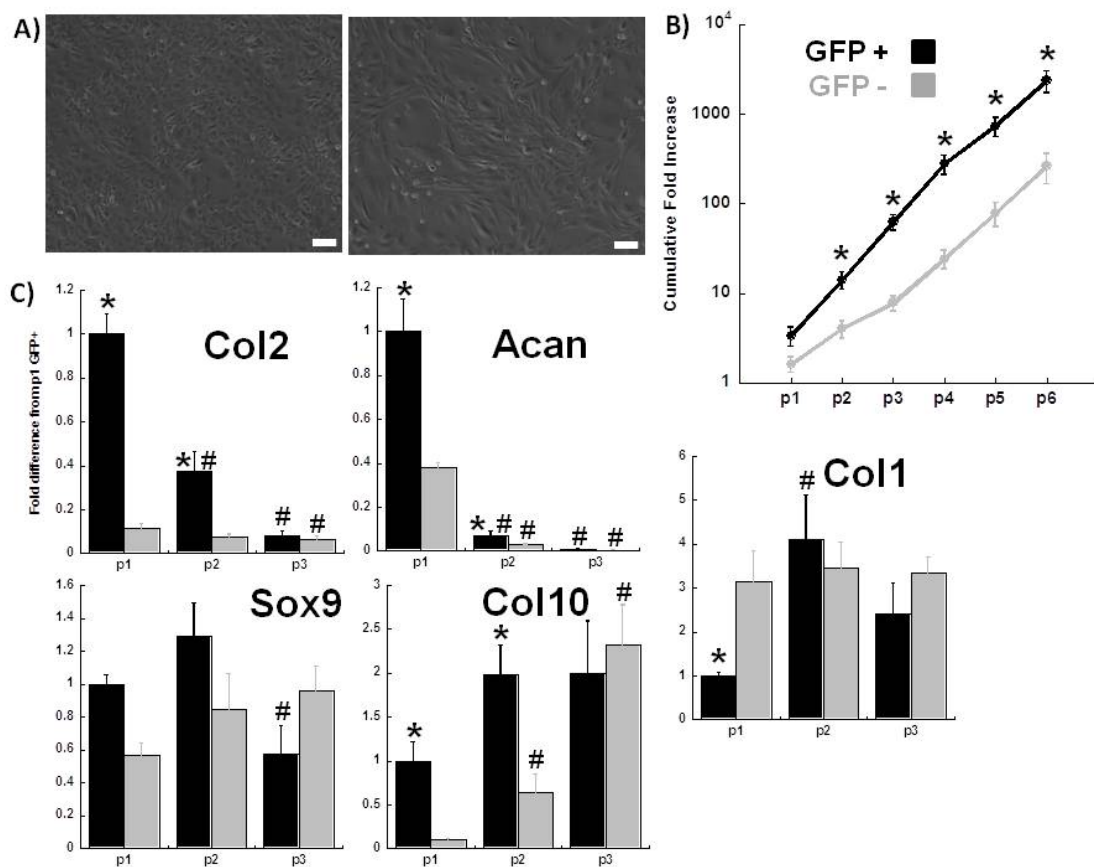
Figure 6-4: Monolayer expansion of sorted cells. A) Passage 2 cells after sorting for GFP+ (left) or GFP- (right), scale bar = 100 μm. B) Cumulative fold increase in cell number over passage, asterisk indicates significance to GFP- of same passage, n≥3 per group. C) RT-PCR for markers related to chondrogenesis. Fold increase normalized to passage 1 GFP+ cells. Asterisk indicates significance to GFP- of same passage, pound indicates significance to passage 1 of own cell type, and significance between other groups not shown; n≥3 per group.

6.3.4 Glycosaminoglycan content of pellets

After monolayer expansion, cells were centrifuged to form pellets and cultured for 21 days with 10 ng/ml TGF-β3 and 100 nM DEX. Pellet cultures from GFP+ cells were larger than those from GFP- cells, and the size of GFP+ pellets decreased with increased passaging. Safranin-O staining of sectioned pellets demonstrated robust production of GAGs in the GFP+ pellets (Figure 6-5A). In both p1 and p3 GFP+ pellets, the central region of the pellet did not show uniform GAG production, but p2 GFP+ pellets had rich GAG throughout the whole pellet. Safranin-O staining was confined to the outer regions of GFP- pellets. Quantification of GAG production supported the histology, as GFP+ pellets had more total GAG production than the corresponding GFP- pellet at each passage (Figure 6-5B). While the total GAG was higher in p1 GFP+ pellets as compared to p2 GFP+ pellets, the GAG per cell was the highest in p2 GFP+ (Figure 6-5C). Passage 2 GFP+ pellets had an average weight of 1.08 ± 0.1 mg, resulting in 51.0 ± 3.3 µg GAG per mg wet weight. When DNA values were converted to approximate cell counts, p2 GFP+ pellets contained an average of 93,050 ± 8158 cells.
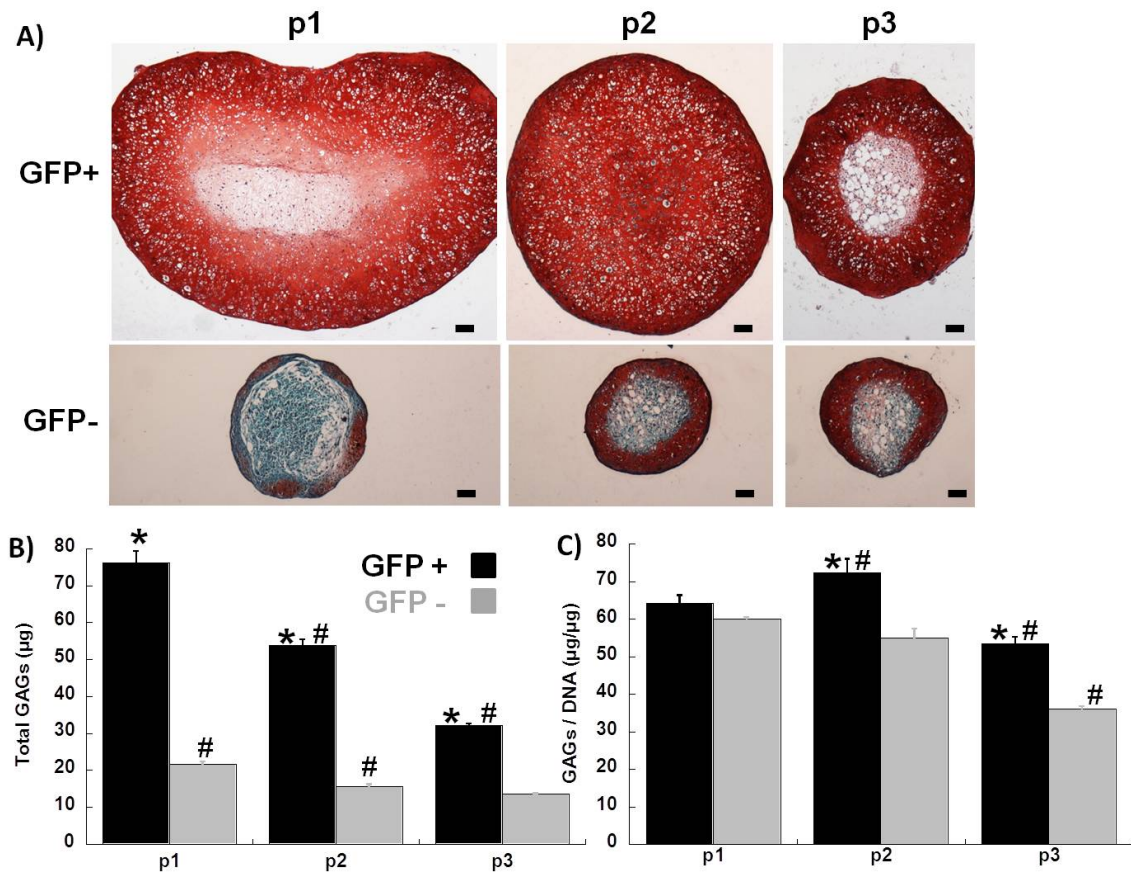
Figure 6-5: GAG content in pellets after cell expansion. A) Safranin-O/Fast Green/Hematoxylin, scale bar = 100 µm. B) Total GAG per pellet. C) GAG normalized to DNA content. Asterisk indicates significance to GFP- of same passage, pound indicates significance to passage 1 of own cell type, and significance between other groups not shown, n≥4 per group

6.3.5 Immunohistochemistry for collagen

To further investigate the extra-cellular matrix produced by pellets, we performed immunohistochemical staining for different types of collagen. Cartilage-specific type II collagen was abundantly produced in the peripheral areas of all pellets (Figure 6-6). Pellets from GFP+ cells had larger areas of type II collagen staining, whereas the central areas of GFP- pellets were largely devoid of staining. Type VI

collagen was present throughout the matrix, including moderate staining in the central

areas of pellets that did not show type II collagen staining. The pellets showed little

presence of type X collagen, with the exception of faint staining in passage 2 GFP+ and

GFP- pellets.
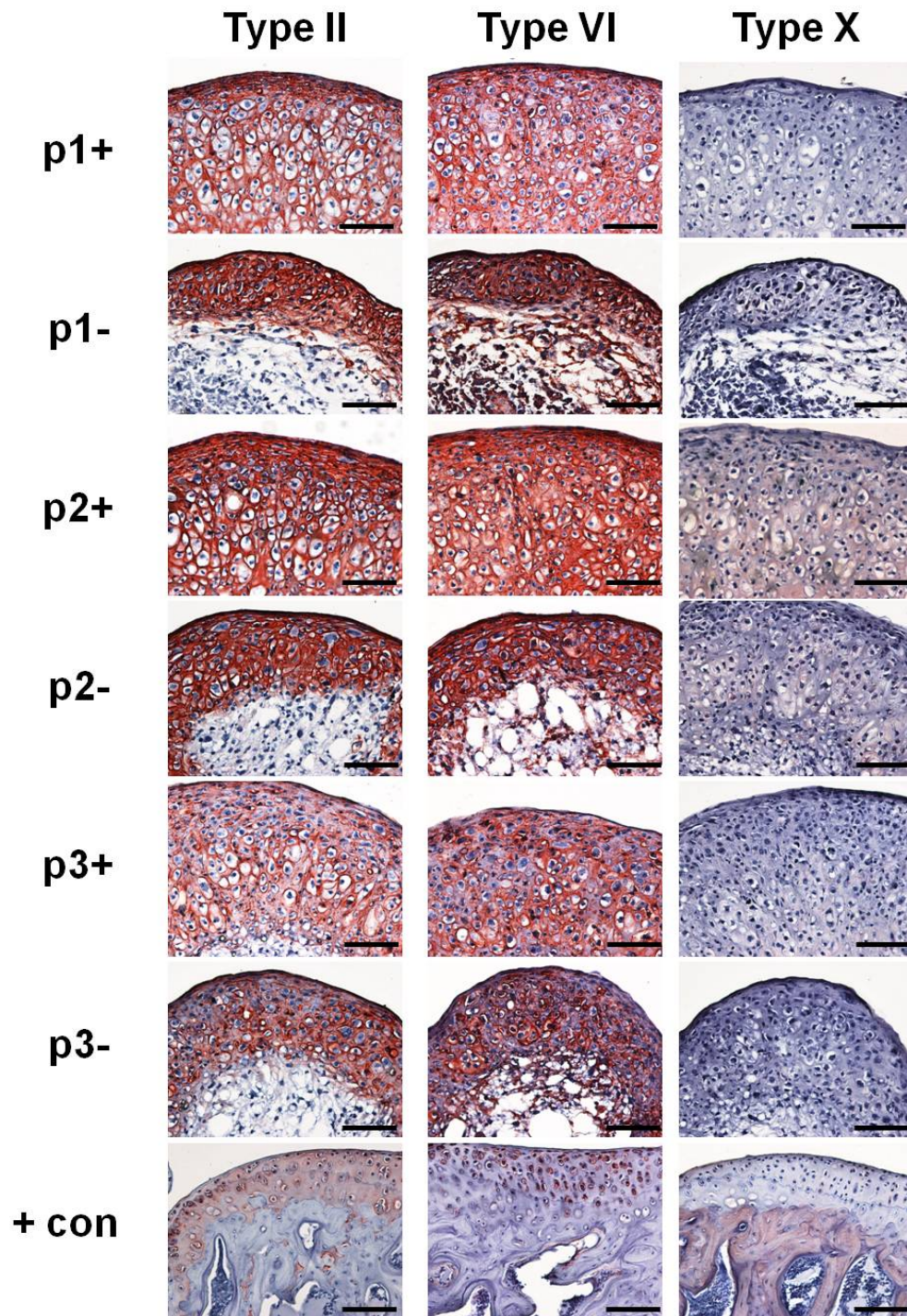
Figure 6-6: Collagen immunohistochemistry of pellets. Pellets cultured for 21 days with TGF-β3 were stained for type II, type VI, or type X collagen. Positive control is mouse osteochondral section. Scale bar = 100 μm.

6.3.6 ELISA for collagen quantification

The amount of type II and type I collagen produced in pellets from GFP+ and GFP- pellets after 1-3 passages was quantified using ELISA. GFP+ pellets showed more type II collagen production than the corresponding GFP- pellets at each passage, and the total type II collagen produced by GFP+ pellets went down with passaging (Figure 6-7A). When normalized to DNA, the maximal production of type II collagen per cell was in the p2 GFP+ pellets. When normalized to wet tissue weight, p2 GFP+ pellets had 1.70 ± 0.14 µg type II collagen per mg wet weight.

For type I collagen, GFP- pellets showed higher levels than GFP+ pellets at p1, but the amount synthesized went up over passage in GFP+ cells and went down over passage in GFP- cells (Figure 6-7B). As a result, there was more type I collagen and more type I collagen per DNA in p3 GFP+ pellets as compared to p3 GFP- pellets. Similarly, the ratio of type II to type I collagen was significantly higher in p1 GFP+ pellets as compare d to p1 GFP-, but significantly higher in p3 GFP- pellets as compared to p3 GFP+ pellets. Passage 2 GFP+ and GFP- cells were also analyzed for collagen content before being put into pellet culture. While the type I collagen levels were not detectable, GFP+ cells had higher levels of total type II collagen as compared to GFP- cells (5.8 ± 0.31 ng vs. 0.31 ± 0.10 ng in 250,000 cells).
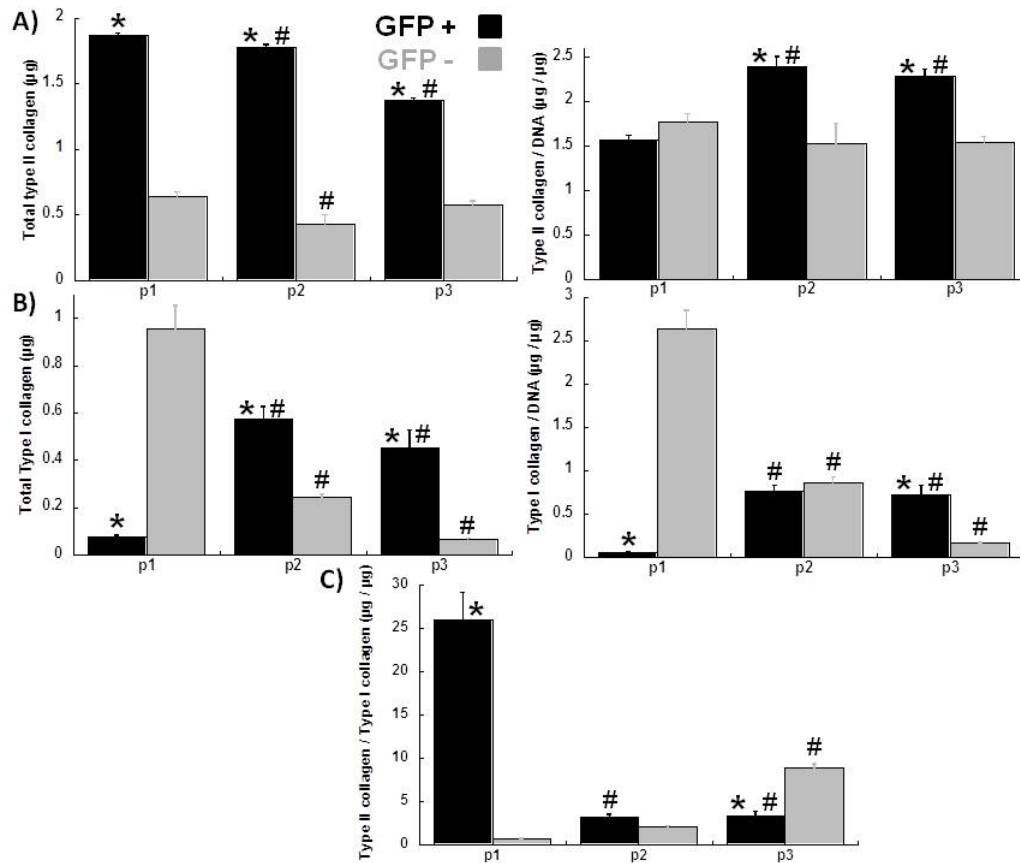
Figure 6-7: Type II and type I collagen content. A) Type II collagen, total and normalized to DNA. B) Type I collagen, total and normalized to DNA. C) Type II to Type I collagen ratio. In all graphs, asterisk indicates p<0.05 to GFP- of same passage and pound indicates p<0.05 to passage 1 of own cell type, n≥4 per group.

6.3.7 Self-assembled construct formation

Self-assembled constructs were established with passage 3 GFP+ cells using either an agarose well method or a transwell culture method. After 21 days of culture with TGF-β3, constructs from the agarose well method were spherical and did not show GAG staining in the central areas of the construct (Figure 6-8). In contrast, constructs formed using the transwell method were disc-shaped and showed GAG staining throughout the construct, although the presence of GAGs was highest in the periphery.

148

When the composition of p2 GFP+ transwell constructs (1×10^6 starting cells) were

compared to p2 GFP+ pellets (2.5×10^5 starting cells), the transwells showed greater total

GAGs (87.6 ± 2.8 vs. 53.9 ± 1.6 µg) and total type II collagen (1.87 ± 0.01 vs. 1.78 ± 0.02 µg)

but lower GAG/DNA (36.6 ± 1.8 vs. 72.3 ± 3.7 µg) and type II collagen/DNA (0.78 ± 0.03

vs. 2.39 ± 0.11 µg).
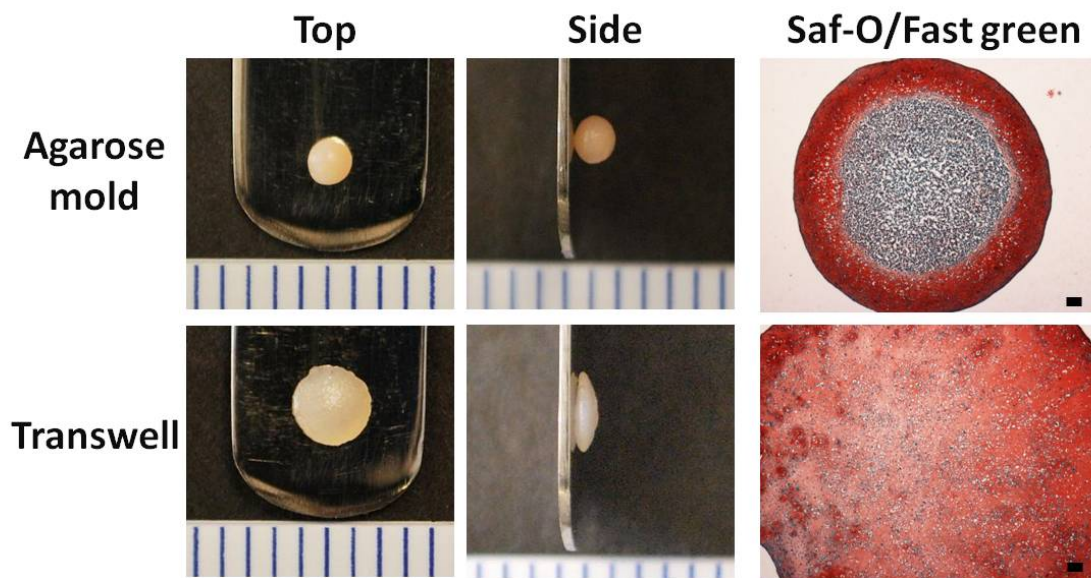
Figure 6-8: Formation of self-assembled constructs. After 21 days of culture with TGF-β3, self-assembled constructs formed with a 5 mm agarose mold or transwell inserts were photographed (scale shown is 1 mm) and stained for Safranin-O/Fast-green/Hematoxylin, scale bar = 100 µm.

6.3.8 Methods for treating in vitro cartilage defects

An in vitro cartilage defect model was established to investigate the ability of

iPSC-derived cells to contribute to defect repair. Various methods were employed to fill

the 3 mm inner core of a cartilage explant over the course of 21 days in culture with

serum-free chondrogenic media containing 10 ng/ml TGF-β3 and 100 nM DEX (Figure

149

6-9). Little to no integration occurred when native cartilage was immediately replaced after coring. A direct injection of 1x10^6 passage 4 GFP+ cells formed a small volume of tissue that stained for GAGs at some areas of the cartilage interface. Both 1% agarose and PEG-RGD hydrogels containing 1x10^6 cells filled most of the defect area. Agarose gels showed integration with the surrounding cartilage but little GAG staining in the interior of the construct, while PEG-RGD hydrogels showed significant GAG staining throughout the interior of the construct but little integration with the cartilage. Finally, a 1 mm defect was filled using a biopsy punch of self-assembled cartilage. The transwell system was used to culture constructs from passage 2 GFP+ cells for 7 days with TGF-β3 before transfer to the defect and an additional 21 days of culture with TGF-β3.
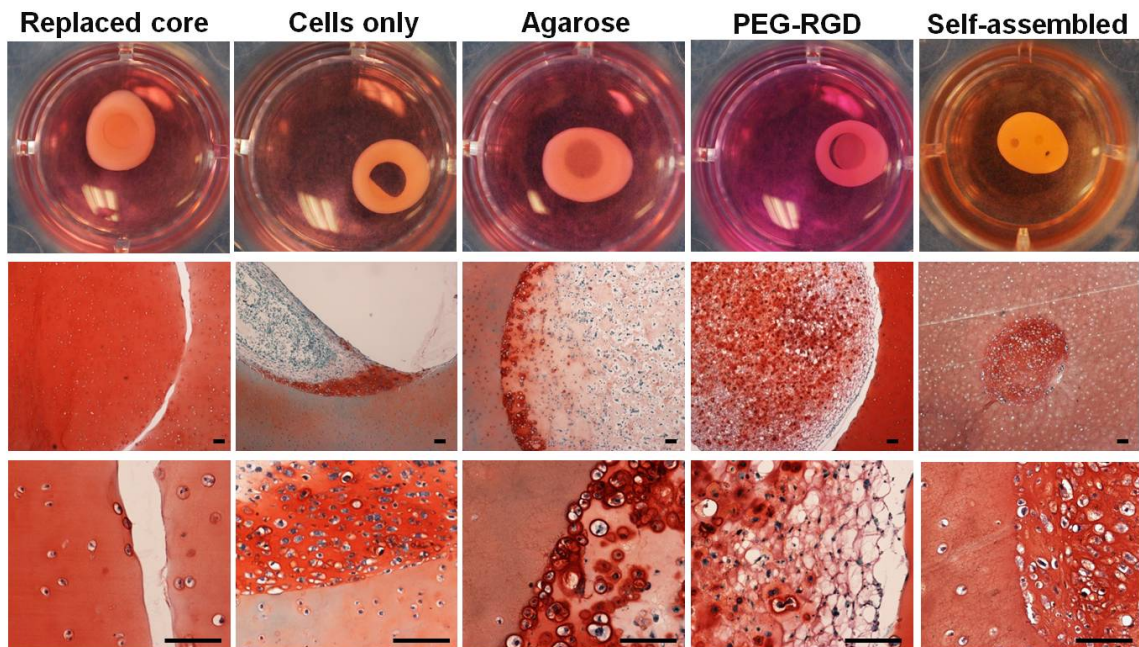
Figure 6-9: Filling of cartilage defect. Inner cores of cartilage were removed and filled immediately with cored cartilage, cells only, agarose, PEG-RGD, or a self-assembled construct. 21 day culture with TGF-β3. Scale bar = 100 μm.

6.3.9 Integrative strength of defect repair

The mechanical integrity of the interface between the filled defect and the surrounding cartilage was assessed by a push-out test. Agarose gels containing 1×10^6 passage 3 GFP+ or GFP- cells were cultured for 21 days with TGF-β3 and showed integration between the gel and surrounding cartilage (Figure 6-10A) . Both cell types significantly enhanced the integrative strength of the filled defect as compared to agarose alone or immediately replacing the cartilage core, with GFP+ cells providing highest peak shear stress before failure (Figure 6-10B). The distribution of cells and GAGs within the construct was altered by the presence of the surrounding cartilage, as the gels within defects showed greater cellularity and staining near the defect edge (Figure 6-10A) while constructs without surrounding cartilage showed uniform distribution (Figure 6-10C).
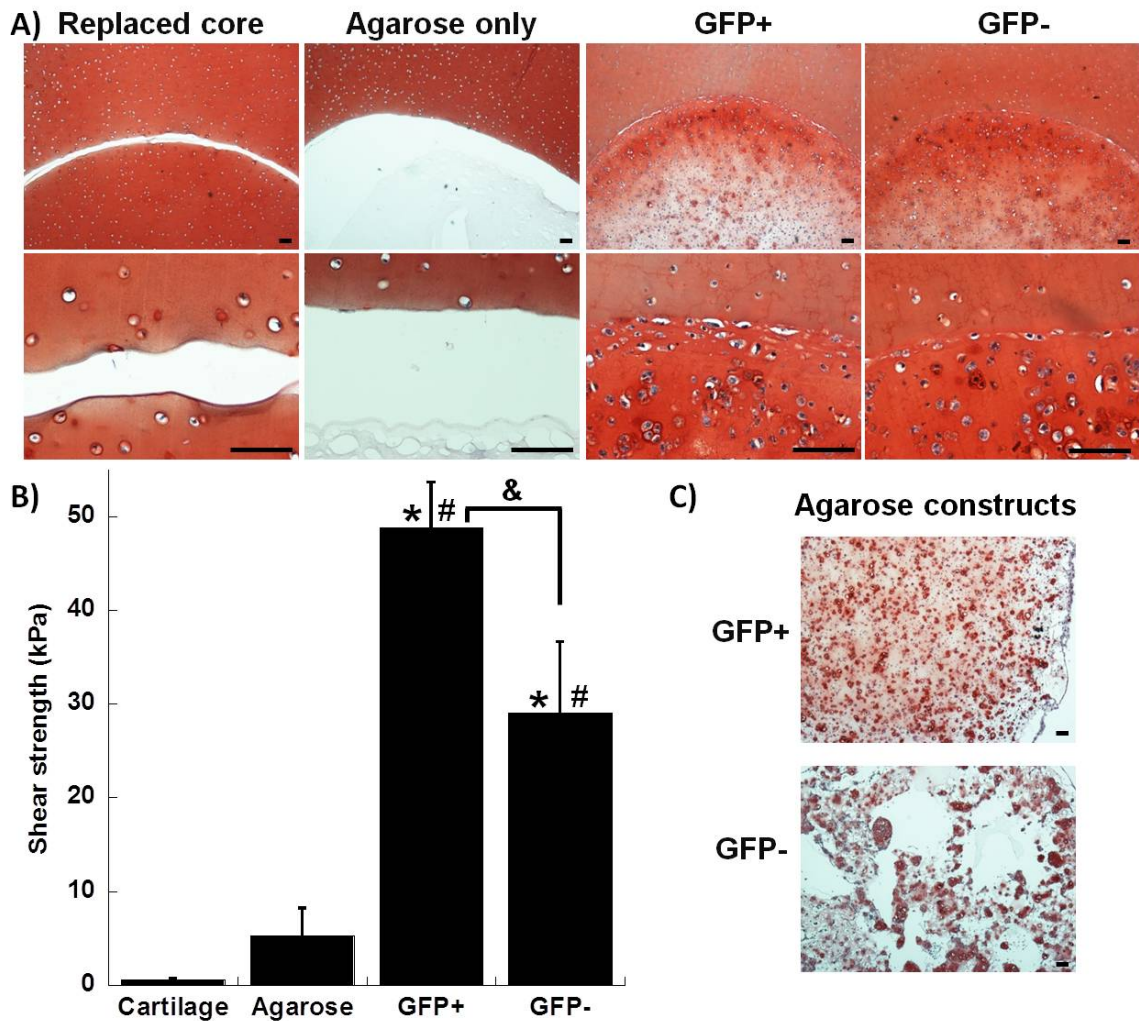
Figure 6-10: Strength of integrative repair. A) Inner cores of cartilage were removed and filled immediately with cored cartilage, agarose only, GFP+ cells in agarose, or GFP- cells in agarose. 21 day culture with TGF-β3. Scale bar = 100 μm. B) Repair strength measured using maximum shear strength during push-out test, n≥5, asterisk indicates p<0.05 to cartilage, pound indicates p<0.05 to agarose, and ampersand indicates p<0.05. C) Cells in agarose constructs were cultured without the presence of surrounding cartilage. Scale bar = 100 μm.

6.4 Discussion

We sought to produce cartilage tissue-engineered constructs from murine iPSCs in order to establish a model system that harnesses the power of mouse genetics for in vitro studies of cartilage injury and osteoarthritis. We accomplished this by using micromass culture with BMP-4 to induce chondrogenesis, sorting for cells expressing Col2, expanding sorted cells for several passages with bFGF, and culturing pellets for 21 days with TGF-β3. The multi-phase approach generated cells that formed constructs with robust GAG and type II collagen production.

There are many advantages to using iPSCs for developing cartilage model systems. First, because iPSCs can proliferate indefinitely in the undifferentiated state, large numbers of tissue constructs can be made for high throughput analysis and drug screening. Second, iPSCs can be obtained from patients regardless of age or disease state, as has been demonstrated using chondrocytes and synovium from OA patients (Kim et al., 2011; Wei et al., 2012). Tissue models from specific patients or mouse strains allow for the possibility of testing personalized treatments and for the study of unique phenotypes (Meng et al., 2010; Robinton and Daley, 2012). In OA research, generating tissue models from knockout mice that are either susceptible to OA or are protected from OA may allow for mechanistic investigations that are challenging to do in animal models. Third, since non-invasive starting cells such fibroblasts or blood cells can be used to generate iPSCs, unnecessary surgery is avoided and there is the possibility of

153

establishing banks to cover a wide range of patient populations (Nakatsuji et al., 2008). Finally, it is important to note that many of the initial successful iPSC models relied on specific genetic mutations related to a particular disease (Park et al., 2008). However, recent work has shown that iPSCs from a complex, polygenic disease such as sporadic Alzheimer's were able to recapitulate the functional deficit of neuronal cells (Israel et al., 2012). This opens up the possibility that patients or mouse strains with subtle OA risk factors such as single nucleotide polymorphisms (Loughlin, 2011), particular biomarkers (Kraus, 2011), or obesity (Griffin and Guilak, 2008) may generate iPSC-derived cartilage models that demonstrate enhanced susceptibility to degradation.

The successful reprogramming of mouse tail fibroblasts was verified by morphology, the presence of pluripotency markers, and teratoma formation involving differentiation to cell types of all three germ layers. The pluripotency markers were lost after the iPSCs were subjected to micromass culture and further monolayer expansion. GFP-, GFP+, and unsorted cells after two passages were negative for pluripotency markers in a RT-PCR panel and immediately sorted cells showed a dramatic reduction in Nanog by quantitative PCR. The karyotype of undifferentiated iPSCs was mostly normal, with the loss of a sex chromosome and small translocations a common finding in cultured pluripotent cells (Ben-David and Benvenisty, 2012; Rebuzzini et al., 2008; Sugawara et al., 2006).

154

We sorted cells at the end of the micromass culture based on the expression of GFP controlled by the Col2a1 promoter/enhancer. This allowed us to demonstrate the importance of cell population homogeneity in creating cartilage tissue models. GFP+ and GFP- cells showed clear differences in morphology, proliferation rate, and gene expression in monolayer culture, indicating that the sorting procedure did generate a distinct and more well-defined starting cell population. Pellets from GFP+ and GFP- cells confirmed these observations, as GFP+ cells produced larger pellets with increased production of cartilage matrix consisting of GAGs and type II collagen. The sorting for GFP+ cells not only enhanced the chondrogenic properties of the tissue-engineered constructs, but also served to eliminate undifferentiated cells that could potentially form teratomas upon transplantation. The benefit of using defined starting cell populations for iPSC-based therapy was demonstrated in a study showing that positive sorting for a cardiovascular progenitor marker not only encouraged robust cardiac repair in vivo, but also eliminated the teratoma formation associated with unpurified differentiated cells (Blin et al., 2010).

Passaging the sorted cells in monolayer culture had an effect on the cell phenotype, with a reduction in Col2 and Acan gene expression along with increased Col1 expression. This was expected, as human and murine chondrocytes are known to rapidly undergo a transition to dedifferentiated chondrocyte phenotype (Darling and Athanasiou, 2005; Gosset et al., 2008). Interestingly, the pellets formed from passage 2

155

GFP+ cells showed a more uniform distribution of GAG staining and higher synthesis of

GAG and type II collagen per cell than passage 1 GFP+ cells. This could be due to a

preferential expansion of more chondrogenic subsets of the GFP+ cells. Sox9, a marker

of chondroprogenitors, actually showed a trend toward increasing with an additional

passage as opposed to the rapid decrease seen with Col2 and Acan. This phenomenon

has been noted in other cell types, as monolayer culture with bFGF and other growth

factors can expand chondrocyte clones with greater differentiation potential (Barbero et

al., 2003), and the presence of bFGF during expansion enhances the proliferation and

chondrogenic capacity of MSCs (Bianchi et al., 2003; Solchaga et al., 2005). This

preferential expansion of a chondrogenic subset may explain the finding that pellets

from GFP- cells showed a reduction in type I collagen with passaging and an increase in

the type II to type I collagen ratio. However, pellets from passage 3 GFP+ cells lost the

ability to form homogeneous cartilaginous pellets and the type II to type I collagen ratio

went down with passaging. These data suggest that competing processes occur during

monolayer expansion that depend on the initial chondrogenic state of the cells, as

expansion of highly chondrogenic subsets may be balanced by the dedifferentiation that

also occurs during monolayer culture.

Identifying the specific collagen composition of pellets using

immunohistochemistry gives an indication of how well the iPSC-derived tissue-

engineered constructs can serve as an in vitro model for cartilage. The pellets from

passage 2 GFP+ cells demonstrated robust production of hyaline cartilage specific type II

collagen, and were generally negative for the hypertrophic chondrocyte marker type X

collagen. The avoidance of a hypertrophic chondrocyte phenotype was of particular

interest because of the observation that this process occurs during chondrogenesis with

adult stem cells (Dickhut et al., 2009; Pelttari et al., 2006). Due to the high cellularity of

the pellets, staining for type VI collagen was widespread, even though this protein is

typically localized to the pericellular matrix in mature cartilage (Poole et al., 1988).

Taken together, the positive staining of types II and VI collagen coupled with the lack of

type X collagen indicate that the iPSC-derived pellets at 21 days have a similar

composition to articular cartilage.   When compared to native cartilage values per

milligram of wet tissue, p2 GFP+ pellets have similar GAG, less type II collagen, and

more cells (Hoemann, 2004).

Autologous chondrocyte implantation (ACI) is the only cell-based treatment that

is FDA-approved for treating focal cartilage defects (Carticel™, Genzyme Biosurgery).

However, an additional surgery is required for chondrocyte harvest, which only yields

approximately 200,000 cells (Minas, 2001). The harvested chondrocytes are therefore

expanded in culture to obtain sufficient cell quantities, but this process results in

dedifferentiation with potential deficiencies in the long-term durability of newly formed

tissue (Dell'Accio et al., 2001; Knutsen et al., 2007; Peterson et al., 2002). To evaluate

iPSCs as a novel cell source for cartilage defect repair, an in vitro model was established

using cored cartilage explants. Similar in vitro defect repair models have been useful for evaluating novel cell sources and the integration of neotissue with surrounding cartilage (de Vries-van Melle et al., 2012; Enders et al., 2010; Obradovic et al., 2001; Vinardell et al., 2009). We used this system to screen several cell delivery methods for the ability to fill the entire defect and integrate with the surrounding cartilage. Delivering cells alone formed a small area of new tissue, but could not fill the entire defect. Utilizing a PEG-RGD hydrogel enhanced the chondrogenesis of the cells throughout the gel, but limited integration was seen with the surrounding cartilage. Agarose gels containing $1x10^6$ cells were able to fill the defect and show good integration with the surrounding cartilage. Additionally, using a transwell method for forming self-assembled cartilage constructs provided a disc-shaped tissue that could integrate with the surrounding cartilage when transferred to the defect with a biopsy punch.

The ability of newly formed tissue to integrate with the surrounding cartilage is a challenging feature of cell-based treatments for cartilage defects (Steinert et al., 2007). Histological sections demonstrated good integration of both GFP- and GFP+ cells in agarose with the cartilage surrounding the defect. To test the mechanical strength of the integration, we performed a push-out test. The shear strength of the repair was highest with GFP+ cells as compared to GFP- cells as well as agarose only and immediately replaced cartilage. These data indicate that iPSCs have potential as a novel cell source for cartilage defect repair.

158

6.5 Summary

This study provided a proof of principle strategy for using iPSCs as a cell source for cartilage tissue engineering. The ability to derive large numbers of cells with chondrogenic potential from a non-invasive starting population is an important advance for the development of cell therapy strategies to treat osteoarthritis. Additionally, techniques to separate a defined cell population from undifferentiated and off-target cell types are essential for maximum therapeutic effectiveness and minimum risk of teratoma formation. This work also established a tool for performing mechanistic in vitro studies using iPSCs from mouse strains with specific phenotypes related to cartilage development, repair, and osteoarthritis.

7. Summary and Conclusions

This work sought to develop new techniques and approaches to extend the manner in which stem cells can be used for the study, prevention, and treatment of cartilage injury and osteoarthritis (OA). Treatment strategies were addressed in cartilage tissue engineering studies to investigate the effect of cell microenvironments and growth factor combinations on the chondrogenesis of human adult stem cells. Prevention of OA was pursued by providing stem cell therapy in the context of post-traumatic arthritis (PTA) after intra-articular fracture in mice. Finally, the study of cartilage injury and OA was engaged by establishing a system for generating a large number of tissue-engineered constructs from mouse strains of interest through the use of induced pluripotent stem cells (iPSCs).

In Chapter 2, we showed data to support the hypothesis that human adipose-derived stem cells (ASCs) and bone marrow-derived mesenchymal stem cells (MSCs) display distinct responses to chondroinductive growth factors and cell microenvironments. In general, MSCs showed higher upregulation of chondrogenic genes and more matrix synthesis as compared to ASCs in the specific conditions studied. ASCs showed greater ACAN1 upregulation in response to bone morphogenetic protein-6 (BMP-6) as compared to transforming growth factor beta-3 (TGF-β3) and more type II collagen production with media containing serum, whereas MSCs showed greater ACAN1 upregulation in response to TGF-β3 as compared to BMP-6 and less type II

collagen production with the presence of serum. MSCs showed a reduction in expression of the hypertrophic chondrocyte marker type X collagen in cartilage-derived matrix (CDM) scaffolds as compared to alginate beads, illustrating the potential influence of cell-matrix interactions during differentiation.

In Chapter 3, we established a method for the rapid expansion of purified murine mesenchymal stem cells by sorting for PDGFRα^+/Sca-1$^+$ cells and culturing them at 2% O_2. This was an important technical advance, as the difficulty in expanding a pure population of MSCs has limited the ability to study how stem cells are related to particular mouse phenotypes. Unexpectedly, the control strain B6 harbored MSCs with greater proliferation and more robust differentiation than the MRL "superhealer" mouse. These data suggested that either enhanced stem cell function is not the cause of the regenerative capabilities of the MRL mouse, or that in vitro characterization is insufficient to observe the mechanism behind the MSC contribution to MRL healing.

In Chapter 4, we supported the hypothesis that delivering MSCs to the knee joint after fracture can prevent the development of PTA. We showed that a single intra-articular injection of 10,000 MSCs eliminated the difference in histological OA grading between control and fractured limbs. MSCs from either B6 or MRL "superhealer" mice were sufficient to prevent PTA, indicating that a different injury model may be required to distinguish the regenerative potential of B6 and MRL MSCs. MSCs altered the timecourse and magnitude of anti-inflammatory cytokines in the serum and synovial

161

fluid, and also encouraged a more robust bone healing response. Future work on the prevention of PTA could take advantage of the proposed mechanisms for stem cell therapy to investigate other strategies that mimic these key functions of the cells, such as anti-inflammatory agents.

In Chapter 5, we provided a detailed analysis of factors influencing the effectiveness of iPSC chondrogenesis as assessed by chondrogenic gene upregulation, the yield of cells positive for green fluorescent protein under the control of the type II collagen promoter/enhancer (GFP+) cells, and the production of cartilaginous matrix. Micromass and pellet culture systems provided a supportive environment for the chondrogenesis of undifferentiated iPSCs, whereas monolayer, embryoid body, agarose, and CDM scaffolds did not. Serum was detrimental to chondrogenesis in all systems tested and even 1% serum during micromass culture abolished the chondrogenic effects of growth factors. BMP-4 provided consistent upregulation of chondrogenic genes, and the yield of GFP+ cells was enhanced by providing the growth factor during only days 3-5 of culture. Expansion of GFP+ cells after sorting was facilitated by basic fibroblast growth factor (bFGF), and subsequent pellet culture with TGF-β3 showed more type II collagen and less type X collagen than pellet culture with BMP-4. Thus, a multi-stage chondrogenic differentiation protocol for iPSCs was developed that involves serum-free micromass culture with BMP-4, sorting for GFP+ cells, expansion with bFGF, and pellet culture with TGF-β3.

162

In Chapter 6, we employed the multi-stage chondrogenic differentiation protocol to generate iPSC-derived cartilage pellets. Pellets showed extensive deposition of glycosaminoglycans (GAGs) and types II and VI collagen without significant production of type X collagen. The importance of sorting successfully differentiated cells was affirmed by the enhanced gene expression and matrix synthesis in GFP+ as compared to GFP- cells. Monolayer expansion decreased the chondrogenic gene expression of GFP+ cells, but passage 2 GFP+ cells produced the most homogenous pellets and synthesized the most GAGs and type II collagen per cell. GFP+ as well as GFP- cells also demonstrated the ability to contribute to the integrative repair of cartilage defects using an in vitro model. These data demonstrate the potential of iPSCs to provide an abundant source of cells for cartilage therapies from a non-invasive starting population. Additionally, the ability to produce cartilaginous pellets from iPSCs establishes a system that can be used to perform in vitro studies on cartilage from specific mouse strains. One application would be to apply catabolic stimuli to pellets from various mouse strains with a high risk for OA in order to assess the interaction of genetic and environmental factors, an important issue in determining risk factors of OA.

A variety of stem cells were used throughout this dissertation in order to gain insight into chondrogenesis, cartilage regeneration, and cartilage injury. The lessons learned regarding the interplay of stem cells and cartilage are valuable for developing regenerative medicine therapies for the prevention and treatment of OA. For example,

163

the observations that cell-matrix interactions in CDM scaffolds can suppress chondrocyte hypertrophy and that ASCs and MSCs respond in distinct fashion to particular growth factors will help guide cartilage tissue engineering strategies. Also, the novel finding that stem cell therapy has the potential to prevent the development of accelerated OA due to joint injury offers a promising avenue for future work in treating patients before extensive degradation of cartilage has occurred.

In an attempt to rigorously answer fundamental questions regarding stem cells and cartilage, techniques were developed that will allow other investigators to pursue related questions. This work demonstrated the value of expanding purified murine MSCs at low oxygen tension and represents the first time that MSCs have been directly delivered to mouse knee joint. Additionally, we developed systems for exploring new paradigms in cartilage and OA research. With iPSC-derived cartilage models, the power of mouse genetics can be converted to an in vitro format for greater control and expanded scale during mechanistic experiments. In principle, the multi-stage approach to pre-differentiate and sort iPSCs can also be used on human iPSCs for generating therapeutic cells or patient-specific cartilage models for personalized drug screening. The diverse applications pursued in this research illustrate the power of stem cells to guide both the understanding of cartilage and the development of therapies aimed at preventing and treating cartilage injury and OA.

References

Abdi, R., Fiorina, P., Adra, C. N., Atkinson, M., Sayegh, M. H., 2008. Immunomodulation by mesenchymal stem cells: a potential therapeutic strategy for type 1 diabetes. *Diabetes*. 57**,** 1759-67.

Abdullah, I., Lepore, J. J., Epstein, J. A., Parmacek, M. S., Gruber, P. J., 2005. MRL mice fail to heal the heart in response to ischemia-reperfusion injury. *Wound Repair Regen*. 13**,** 205-8.

Afizah, H., Yang, Z., Hui, J. H., Ouyang, H. W., Lee, E. H., 2007. A comparison between the chondrogenic potential of human bone marrow stem cells (BMSCs) and adipose-derived stem cells (ADSCs) taken from the same donors. *Tissue Eng*. 13**,** 659-66.

Aggarwal, S., Pittenger, M. F., 2005. Human mesenchymal stem cells modulate allogeneic immune cell responses. *Blood*. 105**,** 1815-22.

Ahrens, P. B., Solursh, M., Reiter, R. S., 1977. Stage-related capacity for limb chondrogenesis in cell culture. *Dev Biol*. 60**,** 69-82.

Akiyama, H., Chaboissier, M. C., Martin, J. F., Schedl, A., de Crombrugghe, B., 2002. The transcription factor Sox9 has essential roles in successive steps of the chondrocyte differentiation pathway and is required for expression of Sox5 and Sox6. *Genes Dev*. 16**,** 2813-28.

Alfaro, M. P., Pagni, M., Vincent, A., Atkinson, J., Hill, M. F., Cates, J., Davidson, J. M., Rottman, J., Lee, E., Young, P. P., 2008. The Wnt modulator sFRP2 enhances mesenchymal stem cell engraftment, granulation tissue formation and myocardial repair. *Proc Natl Acad Sci U S A*. 105**,** 18366-71.

Alsalameh, S., Amin, R., Gemba, T., Lotz, M., 2004. Identification of mesenchymal progenitor cells in normal and osteoarthritic human articular cartilage. *Arthritis Rheum*. 50**,** 1522-32.

Anderson, D. D., Chubinskaya, S., Guilak, F., Martin, J. A., Oegema, T. R., Olson, S. A., Buckwalter, J. A., 2011. Post-traumatic osteoarthritis: Improved understanding and opportunities for early intervention. *J Orthop Res*. 29**,** 802-9.

Anjos-Afonso, F., Bonnet, D., 2008. Isolation, culture, and differentiation potential of mouse marrow stromal cells. *Curr Protoc Stem Cell Biol*. Chapter 2**,** Unit 2B 3.

Arthur, A., Zannettino, A., Gronthos, S., 2009. The therapeutic applications of multipotential mesenchymal/stromal stem cells in skeletal tissue repair. *J Cell Physiol*. 218**,** 237-45.

Ateshian, G. A., 2009. The role of interstitial fluid pressurization in articular cartilage lubrication. *J Biomech*. 42**,** 1163-76.

Aust, L., Devlin, B., Foster, S. J., Halvorsen, Y. D., Hicok, K., du Laney, T., Sen, A., Willingmyre, G. D., Gimble, J. M., 2004. Yield of human adipose-derived adult stem cells from liposuction aspirates. *Cytotherapy*. 6**,** 7-14.

Awad, H. A., Halvorsen, Y. D., Gimble, J. M., Guilak, F., 2003. Effects of transforming growth factor beta1 and dexamethasone on the growth and chondrogenic differentiation of adipose-derived stromal cells. *Tissue Eng*. 9**,** 1301-12.

Awad, H. A., Wickham, M. Q., Leddy, H. A., Gimble, J. M., Guilak, F., 2004. Chondrogenic differentiation of adipose-derived adult stem cells in agarose, alginate, and gelatin scaffolds. *Biomaterials*. 25**,** 3211-22.

Baddoo, M., Hill, K., Wilkinson, R., Gaupp, D., Hughes, C., Kopen, G. C., Phinney, D. G., 2003. Characterization of mesenchymal stem cells isolated from murine bone marrow by negative selection. *J Cell Biochem*. 89**,** 1235-49.

Badylak, S. F., Freytes, D. O., Gilbert, T. W., 2009. Extracellular matrix as a biological scaffold material: Structure and function. *Acta Biomater*. 5**,** 1-13.

Baksh, D., Song, L., Tuan, R. S., 2004. Adult mesenchymal stem cells: characterization, differentiation, and application in cell and gene therapy. *J Cell Mol Med*. 8**,** 301-16.

Ball, S. G., Shuttleworth, C. A., Kielty, C. M., 2007. Platelet-derived growth factor receptor-alpha is a key determinant of smooth muscle alpha-actin filaments in bone marrow-derived mesenchymal stem cells. *Int J Biochem Cell Biol*. 39**,** 379-91.

Ballock, R. T., Reddi, A. H., 1994. Thyroxine is the serum factor that regulates morphogenesis of columnar cartilage from isolated chondrocytes in chemically defined medium. *J Cell Biol*. 126**,** 1311-8.

Barbero, A., Ploegert, S., Heberer, M., Martin, I., 2003. Plasticity of clonal populations of dedifferentiated adult human articular chondrocytes. *Arthritis Rheum*. 48**,** 1315-25.

Basile, P., Dadali, T., Jacobson, J., Hasslund, S., Ulrich-Vinther, M., Soballe, K., Nishio, Y., Drissi, M. H., Langstein, H. N., Mitten, D. J., O'Keefe, R. J., Schwarz, E. M., Awad, H. A., 2008. Freeze-dried tendon allografts as tissue-engineering scaffolds for Gdf5 gene delivery. *Mol Ther*. 16**,** 466-73.

Bedelbaeva, K., Gourevitch, D., Clark, L., Chen, P., Leferovich, J. M., Heber-Katz, E., 2004. The MRL mouse heart healing response shows donor dominance in allogeneic fetal liver chimeric mice. *Cloning Stem Cells*. 6**,** 352-63.

Bedelbaeva, K., Snyder, A., Gourevitch, D., Clark, L., Zhang, X. M., Leferovich, J., Cheverud, J. M., Lieberman, P., Heber-Katz, E., 2010. Lack of p21 expression links cell cycle control and appendage regeneration in mice. *Proc Natl Acad Sci U S A*. 107**,** 5845-50.

Ben-David, U., Benvenisty, N., 2012. High Prevalence of Evolutionarily-conserved and Species-Specific Genomic Aberrations in Mouse Pluripotent Stem Cells. *Stem Cells*.

Bianchi, G., Banfi, A., Mastrogiacomo, M., Notaro, R., Luzzatto, L., Cancedda, R., Quarto, R., 2003. Ex vivo enrichment of mesenchymal cell progenitors by fibroblast growth factor 2. *Exp Cell Res*. 287**,** 98-105.

Bianco, P., Robey, P. G., Saggio, I., Riminucci, M., 2010. "Mesenchymal" stem cells in human bone marrow (skeletal stem cells): a critical discussion of their nature, identity, and significance in incurable skeletal disease. *Hum Gene Ther*. 21**,** 1057-66.

Bilgen, B., Orsini, E., Aaron, R. K., Ciombor, D. M., 2007. FBS suppresses TGF-beta1-induced chondrogenesis in synoviocyte pellet cultures while dexamethasone and dynamic stimuli are beneficial. *J Tissue Eng Regen Med*. 1**,** 436-42.

Blin, G., Nury, D., Stefanovic, S., Neri, T., Guillevic, O., Brinon, B., Bellamy, V., Rucker-Martin, C., Barbry, P., Bel, A., Bruneval, P., Cowan, C., Pouly, J., Mitalipov, S., Gouadon, E., Binder, P., Hagege, A., Desnos, M., Renaud, J. F., Menasche, P., Puceat, M., 2010. A purified population of multipotent cardiovascular

progenitors derived from primate pluripotent stem cells engrafts in postmyocardial infarcted nonhuman primates. *J Clin Invest*. 120**,** 1125-39.

Blom, A. B., van Lent, P. L., Libregts, S., Holthuysen, A. E., van der Kraan, P. M., van Rooijen, N., van den Berg, W. B., 2007. Crucial role of macrophages in matrix metalloproteinase-mediated cartilage destruction during experimental osteoarthritis: involvement of matrix metalloproteinase 3. *Arthritis Rheum*. 56**,** 147-57.

Bondeson, J., Blom, A. B., Wainwright, S., Hughes, C., Caterson, B., van den Berg, W. B., 2010. The role of synovial macrophages and macrophage-produced mediators in driving inflammatory and destructive responses in osteoarthritis. *Arthritis Rheum*. 62**,** 647-57.

Boregowda, S., Krishnappa, V., Chambers, J., Lograsso, P. V., Lai, W. T., Ortiz, L. A., Phinney, D. G., 2012. Atmospheric Oxygen Inhibits Growth and Differentiation of Marrow-Derived Mouse Mesenchymal Stem Cells Via a p53 Dependent Mechanism: Implications for Long-Term Culture Expansion. *Stem Cells*.

Brazelton, T. R., Blau, H. M., 2005. Optimizing techniques for tracking transplanted stem cells in vivo. *Stem Cells*. 23**,** 1251-65.

Brittberg, M., Lindahl, A., Nilsson, A., Ohlsson, C., Isaksson, O., Peterson, L., 1994. Treatment of deep cartilage defects in the knee with autologous chondrocyte transplantation. *N Engl J Med*. 331**,** 889-95.

Brown, T. D., Johnston, R. C., Saltzman, C. L., Marsh, J. L., Buckwalter, J. A., 2006. Posttraumatic osteoarthritis: a first estimate of incidence, prevalence, and burden of disease. *J Orthop Trauma*. 20**,** 739-44.

Bruder, S. P., Kurth, A. A., Shea, M., Hayes, W. C., Jaiswal, N., Kadiyala, S., 1998. Bone regeneration by implantation of purified, culture-expanded human mesenchymal stem cells. *J Orthop Res*. 16**,** 155-62.

Cancedda, R., Descalzi Cancedda, F., Castagnola, P., 1995. Chondrocyte differentiation. *Int Rev Cytol*. 159**,** 265-358.

Caplan, A. I., 1991. Mesenchymal stem cells. *J Orthop Res*. 9**,** 641-50.

Caplan, A. I., 2007. Adult mesenchymal stem cells for tissue engineering versus regenerative medicine. *J Cell Physiol*. 213**,** 341-7.

Caplan, A. I., Dennis, J. E., 2006. Mesenchymal stem cells as trophic mediators. *J Cell Biochem*. 98**,** 1076-84.

Cappellesso-Fleury, S., Puissant-Lubrano, B., Apoil, P. A., Titeux, M., Winterton, P., Casteilla, L., Bourin, P., Blancher, A., 2010. Human fibroblasts share immunosuppressive properties with bone marrow mesenchymal stem cells. *J Clin Immunol*. 30**,** 607-19.

Carey, B. W., Markoulaki, S., Hanna, J., Saha, K., Gao, Q., Mitalipova, M., Jaenisch, R., 2009. Reprogramming of murine and human somatic cells using a single polycistronic vector. *Proc Natl Acad Sci U S A*. 106**,** 157-62.

Caron, J. P., Fernandes, J. C., Martel-Pelletier, J., Tardif, G., Mineau, F., Geng, C., Pelletier, J. P., 1996. Chondroprotective effect of intraarticular injections of interleukin-1 receptor antagonist in experimental osteoarthritis. Suppression of collagenase-1 expression. *Arthritis Rheum*. 39**,** 1535-44.

Chadwick, R. B., Bu, L., Yu, H., Hu, Y., Wergedal, J. E., Mohan, S., Baylink, D. J., 2007. Digit tip regrowth and differential gene expression in MRL/Mpj, DBA/2, and C57BL/6 mice. *Wound Repair Regen*. 15**,** 275-84.

Chang, C. F., Lee, M. W., Kuo, P. Y., Wang, Y. J., Tu, Y. H., Hung, S. C., 2007. Three-dimensional collagen fiber remodeling by mesenchymal stem cells requires the integrin-matrix interaction. *J Biomed Mater Res A*. 80**,** 466-74.

Cheng, N. C., Estes, B. T., Awad, H. A., Guilak, F., 2009. Chondrogenic differentiation of adipose-derived adult stem cells by a porous scaffold derived from native articular cartilage extracellular matrix. *Tissue Eng Part A*. 15**,** 231-41.

Chin, M. H., Mason, M. J., Xie, W., Volinia, S., Singer, M., Peterson, C., Ambartsumyan, G., Aimiuwu, O., Richter, L., Zhang, J., Khvorostov, I., Ott, V., Grunstein, M., Lavon, N., Benvenisty, N., Croce, C. M., Clark, A. T., Baxter, T., Pyle, A. D., Teitell, M. A., Pelegrini, M., Plath, K., Lowry, W. E., 2009. Induced pluripotent stem cells and embryonic stem cells are distinguished by gene expression signatures. *Cell Stem Cell*. 5**,** 111-23.

Chiou, M., Xu, Y., Longaker, M. T., 2006. Mitogenic and chondrogenic effects of fibroblast growth factor-2 in adipose-derived mesenchymal cells. *Biochem Biophys Res Commun*. 343**,** 644-52.

Chun, S. Y., Lim, G. J., Kwon, T. G., Kwak, E. K., Kim, B. W., Atala, A., Yoo, J. J., 2007. Identification and characterization of bioactive factors in bladder submucosa matrix. *Biomaterials*. 28**,** 4251-6.

Clark, L. D., Clark, R. K., Heber-Katz, E., 1998. A new murine model for mammalian wound repair and regeneration. *Clin Immunol Immunopathol*. 88**,** 35-45.

Crisan, M., Yap, S., Casteilla, L., Chen, C. W., Corselli, M., Park, T. S., Andriolo, G., Sun, B., Zheng, B., Zhang, L., Norotte, C., Teng, P. N., Traas, J., Schugar, R., Deasy, B. M., Badylak, S., Buhring, H. J., Giacobino, J. P., Lazzari, L., Huard, J., Peault, B., 2008. A perivascular origin for mesenchymal stem cells in multiple human organs. *Cell Stem Cell*. 3**,** 301-13.

da Silva Meirelles, L., Caplan, A. I., Nardi, N. B., 2008. In search of the in vivo identity of mesenchymal stem cells. *Stem Cells*. 26**,** 2287-99.

Darling, E. M., Athanasiou, K. A., 2005. Rapid phenotypic changes in passaged articular chondrocyte subpopulations. *J Orthop Res*. 23**,** 425-32.

Das, R., Jahr, H., van Osch, G. J., Farrell, E., 2010. The role of hypoxia in bone marrow-derived mesenchymal stem cells: considerations for regenerative medicine approaches. *Tissue Eng Part B Rev*. 16**,** 159-68.

de Almeida, P. E., van Rappard, J. R., Wu, J. C., 2011. In vivo bioluminescence for tracking cell fate and function. *Am J Physiol Heart Circ Physiol*. 301**,** H663-71.

De Bari, C., Dell'Accio, F., Tylzanowski, P., Luyten, F. P., 2001. Multipotent mesenchymal stem cells from adult human synovial membrane. *Arthritis Rheum*. 44**,** 1928-42.

De Ugarte, D. A., Alfonso, Z., Zuk, P. A., Elbarbary, A., Zhu, M., Ashjian, P., Benhaim, P., Hedrick, M. H., Fraser, J. K., 2003a. Differential expression of stem cell mobilization-associated molecules on multi-lineage cells from adipose tissue and bone marrow. *Immunol Lett*. 89**,** 267-70.

De Ugarte, D. A., Morizono, K., Elbarbary, A., Alfonso, Z., Zuk, P. A., Zhu, M., Dragoo, J. L., Ashjian, P., Thomas, B., Benhaim, P., Chen, I., Fraser, J., Hedrick, M. H., 2003b. Comparison of multi-lineage cells from human adipose tissue and bone marrow. *Cells Tissues Organs*. 174**,** 101-9.

de Vries-van Melle, M. L., Mandl, E. W., Kops, N., Koevoet, W. J., Verhaar, J. A., van Osch, G. J., 2012. An osteochondral culture model to study mechanisms involved in articular cartilage repair. *Tissue Eng Part C Methods*. 18**,** 45-53.

Dell'Accio, F., De Bari, C., Luyten, F. P., 2001. Molecular markers predictive of the capacity of expanded human articular chondrocytes to form stable cartilage in vivo. *Arthritis Rheum*. 44**,** 1608-19.

Denoble, A. E., Huffman, K. M., Stabler, T. V., Kelly, S. J., Hershfield, M. S., McDaniel, G. E., Coleman, R. E., Kraus, V. B., 2011. Uric acid is a danger signal of increasing risk for osteoarthritis through inflammasome activation. *Proc Natl Acad Sci U S A*. 108**,** 2088-93.

Dickhut, A., Pelttari, K., Janicki, P., Wagner, W., Eckstein, V., Egermann, M., Richter, W., 2009. Calcification or dedifferentiation: requirement to lock mesenchymal stem cells in a desired differentiation stage. *J Cell Physiol*. 219**,** 219-26.

Diekman, B. O., Rowland, C. R., Lennon, D. P., Caplan, A. I., Guilak, F., 2010. Chondrogenesis of adult stem cells from adipose tissue and bone marrow: induction by growth factors and cartilage-derived matrix. *Tissue Eng Part A*. 16**,** 523-33.

Dominici, M., Le Blanc, K., Mueller, I., Slaper-Cortenbach, I., Marini, F., Krause, D., Deans, R., Keating, A., Prockop, D., Horwitz, E., 2006. Minimal criteria for defining multipotent mesenchymal stromal cells. The International Society for Cellular Therapy position statement. *Cytotherapy*. 8**,** 315-7.

Dowthwaite, G. P., Bishop, J. C., Redman, S. N., Khan, I. M., Rooney, P., Evans, D. J., Haughton, L., Bayram, Z., Boyer, S., Thomson, B., Wolfe, M. S., Archer, C. W., 2004. The surface of articular cartilage contains a progenitor cell population. *J Cell Sci*. 117**,** 889-97.

Ebert, A. D., Yu, J., Rose, F. F., Jr., Mattis, V. B., Lorson, C. L., Thomson, J. A., Svendsen, C. N., 2009. Induced pluripotent stem cells from a spinal muscular atrophy patient. *Nature*. 457**,** 277-80.

Enders, J. T., Otto, T. J., Peters, H. C., Wu, J., Hardouin, S., Moed, B. R., Zhang, Z., 2010. A model for studying human articular cartilage integration in vitro. *J Biomed Mater Res A*. 94**,** 509-14.

Engler, A. J., Sen, S., Sweeney, H. L., Discher, D. E., 2006. Matrix elasticity directs stem cell lineage specification. *Cell*. 126**,** 677-89.

English, K., Barry, F. P., Field-Corbett, C. P., Mahon, B. P., 2007. IFN-gamma and TNF-alpha differentially regulate immunomodulation by murine mesenchymal stem cells. *Immunol Lett*. 110**,** 91-100.

Enobakhare, B. O., Bader, D. L., Lee, D. A., 1996. Quantification of sulfated glycosaminoglycans in chondrocyte/alginate cultures, by use of 1,9-dimethylmethylene blue. *Anal Biochem*. 243**,** 189-91.

Erickson, G. R., Gimble, J. M., Franklin, D. M., Rice, H. E., Awad, H., Guilak, F., 2002. Chondrogenic potential of adipose tissue-derived stromal cells in vitro and in vivo. *Biochem Biophys Res Commun*. 290**,** 763-9.

Estes, B. T., Diekman, B. O., Gimble, J. M., Guilak, F., 2010. Isolation of adipose-derived stem cells and their induction to a chondrogenic phenotype. *Nat Protoc*. 5**,** 1294-311.

Estes, B. T., Diekman, B. O., Guilak, F., 2008. Monolayer cell expansion conditions affect the chondrogenic potential of adipose-derived stem cells. *Biotechnol Bioeng*. 99**,** 986-95.

Estes, B. T., Wu, A. W., Guilak, F., 2006. Potent induction of chondrocytic differentiation of human adipose-derived adult stem cells by bone morphogenetic protein 6. *Arthritis Rheum*. 54**,** 1222-32.

Eyre, D., 2002. Collagen of articular cartilage. *Arthritis Res*. 4**,** 30-5.

Fecek, C., Yao, D., Kacorri, A., Vasquez, A., Iqbal, S., Sheikh, H., Svinarich, D. M., Perez-Cruet, M., Chaudhry, G. R., 2008. Chondrogenic derivatives of embryonic stem cells seeded into 3D polycaprolactone scaffolds generated cartilage tissue in vivo. *Tissue Eng Part A*. 14**,** 1403-13.

Felson, D. T., Lawrence, R. C., Dieppe, P. A., Hirsch, R., Helmick, C. G., Jordan, J. M., Kington, R. S., Lane, N. E., Nevitt, M. C., Zhang, Y., Sowers, M., McAlindon, T., Spector, T. D., Poole, A. R., Yanovski, S. Z., Ateshian, G., Sharma, L., Buckwalter, J. A., Brandt, K. D., Fries, J. F., 2000. Osteoarthritis: new insights. Part 1: the disease and its risk factors. *Ann Intern Med*. 133**,** 635-46.

Fernandes, J. C., Martel-Pelletier, J., Pelletier, J. P., 2002. The role of cytokines in osteoarthritis pathophysiology. *Biorheology*. 39**,** 237-46.

Ferrari, A., Hannouche, D., Oudina, K., Bourguignon, M., Meunier, A., Sedel, L., Petite, H., 2001. In vivo tracking of bone marrow fibroblasts with fluorescent carbocyanine dye. *J Biomed Mater Res*. 56**,** 361-7.

Fiedler, J., Roderer, G., Gunther, K. P., Brenner, R. E., 2002. BMP-2, BMP-4, and PDGF-bb stimulate chemotactic migration of primary human mesenchymal progenitor cells. *J Cell Biochem*. 87**,** 305-12.

Fitzgerald, J., Rich, C., Burkhardt, D., Allen, J., Herzka, A. S., Little, C. B., 2008. Evidence for articular cartilage regeneration in MRL/MpJ mice. *Osteoarthritis Cartilage*. 16**,** 1319-26.

Frisbie, D. D., Oxford, J. T., Southwood, L., Trotter, G. W., Rodkey, W. G., Steadman, J. R., Goodnight, J. L., McIlwraith, C. W., 2003. Early events in cartilage repair after subchondral bone microfracture. *Clin Orthop Relat Res*. 215-27.

Furman, B. D., Huebner, J.L., Seifer, D.R., Kraus, V.B., Guilak, F., Olson, S.A 2009. MRL/MpJ Mouse Shows Reduced Intra-Articular and Systemic Inflammation Following Articular Fracture. *55th Annual Meeting of the Orthopaedic Research Society. Las Vegas, NV*. 1120.

Furman, B. D., Olson, S. A., Guilak, F., 2006. The development of posttraumatic arthritis after articular fracture. *J Orthop Trauma*. 20**,** 719-25.

Furman, B. D., Strand, J., Hembree, W. C., Ward, B. D., Guilak, F., Olson, S. A., 2007. Joint degeneration following closed intraarticular fracture in the mouse knee: a model of posttraumatic arthritis. *J Orthop Res*. 25**,** 578-92.

Gao, J., Dennis, J. E., Muzic, R. F., Lundberg, M., Caplan, A. I., 2001. The dynamic in vivo distribution of bone marrow-derived mesenchymal stem cells after infusion. *Cells Tissues Organs*. 169**,** 12-20.

Ghannam, S., Bouffi, C., Djouad, F., Jorgensen, C., Noel, D., 2010. Immunosuppression by mesenchymal stem cells: mechanisms and clinical applications. *Stem Cell Res Ther*. 1**,** 2.

Gimble, J., Guilak, F., 2003. Adipose-derived adult stem cells: isolation, characterization, and differentiation potential. *Cytotherapy*. 5**,** 362-9.

Gnecchi, M., Zhang, Z., Ni, A., Dzau, V. J., 2008. Paracrine mechanisms in adult stem cell signaling and therapy. *Circ Res*. 103**,** 1204-19.

Goldring, M. B., Otero, M., 2011. Inflammation in osteoarthritis. *Curr Opin Rheumatol*.

Gong, G., Ferrari, D., Dealy, C. N., Kosher, R. A., 2010. Direct and progressive differentiation of human embryonic stem cells into the chondrogenic lineage. *J Cell Physiol*. 224**,** 664-71.

Gosset, M., Berenbaum, F., Thirion, S., Jacques, C., 2008. Primary culture and phenotyping of murine chondrocytes. *Nat Protoc*. 3**,** 1253-60.

Gourevitch, D., Clark, L., Chen, P., Seitz, A., Samulewicz, S. J., Heber-Katz, E., 2003. Matrix metalloproteinase activity correlates with blastema formation in the regenerating MRL mouse ear hole model. *Dev Dyn*. 226**,** 377-87.

Granero-Molto, F., Weis, J. A., Miga, M. I., Landis, B., Myers, T. J., O'Rear, L., Longobardi, L., Jansen, E. D., Mortlock, D. P., Spagnoli, A., 2009. Regenerative effects of transplanted mesenchymal stem cells in fracture healing. *Stem Cells*. 27**,** 1887-98.

Grant, T. D., Cho, J., Ariail, K. S., Weksler, N. B., Smith, R. W., Horton, W. A., 2000. Col2-GFP reporter marks chondrocyte lineage and chondrogenesis during mouse skeletal development. *Dev Dyn*. 218**,** 394-400.

Grayson, W. L., Zhao, F., Bunnell, B., Ma, T., 2007. Hypoxia enhances proliferation and tissue formation of human mesenchymal stem cells. *Biochem Biophys Res Commun*. 358**,** 948-53.

Gregory, C. A., Gunn, W. G., Peister, A., Prockop, D. J., 2004. An Alizarin red-based assay of mineralization by adherent cells in culture: comparison with cetylpyridinium chloride extraction. *Anal Biochem*. 329**,** 77-84.

Griffin, T. M., Guilak, F., 2008. Why is obesity associated with osteoarthritis? Insights from mouse models of obesity. *Biorheology*. 45**,** 387-98.

Gronthos, S., Zannettino, A. C., Hay, S. J., Shi, S., Graves, S. E., Kortesidis, A., Simmons, P. J., 2003. Molecular and cellular characterisation of highly purified stromal stem cells derived from human bone marrow. *J Cell Sci*. 116**,** 1827-35.

Guerne, P. A., Zuraw, B. L., Vaughan, J. H., Carson, D. A., Lotz, M., 1989. Synovium as a source of interleukin 6 in vitro. Contribution to local and systemic manifestations of arthritis. *J Clin Invest*. 83**,** 585-92.

Guilak, F., Butler, D. L., Goldstein, S. A., 2001. Functional tissue engineering: the role of biomechanics in articular cartilage repair. *Clin Orthop Relat Res*. S295-305.

Guilak, F., Estes, B. T., Diekman, B. O., Moutos, F. T., Gimble, J. M., 2010. 2010 Nicolas Andry Award: Multipotent adult stem cells from adipose tissue for musculoskeletal tissue engineering. *Clin Orthop Relat Res*. 468**,** 2530-40.

Guilak, F., Fermor, B., Keefe, F. J., Kraus, V. B., Olson, S. A., Pisetsky, D. S., Setton, L. A., Weinberg, J. B., 2004. The role of biomechanics and inflammation in cartilage injury and repair. *Clin Orthop Relat Res*. 17-26.

Guilak, F., Lott, K. E., Awad, H. A., Cao, Q., Hicok, K. C., Fermor, B., Gimble, J. M., 2006. Clonal analysis of the differentiation potential of human adipose-derived adult stem cells. *J Cell Physiol*. 206**,** 229-37.

Guo, Z., Li, H., Li, X., Yu, X., Wang, H., Tang, P., Mao, N., 2006. In vitro characteristics and in vivo immunosuppressive activity of compact bone-derived murine mesenchymal progenitor cells. *Stem Cells*. 24**,** 992-1000.

Hall, B. K., Miyake, T., 2000. All for one and one for all: condensations and the initiation of skeletal development. *Bioessays*. 22**,** 138-47.

Haniffa, M. A., Wang, X. N., Holtick, U., Rae, M., Isaacs, J. D., Dickinson, A. M., Hilkens, C. M., Collin, M. P., 2007. Adult human fibroblasts are potent immunoregulatory cells and functionally equivalent to mesenchymal stem cells. *J Immunol*. 179**,** 1595-604.

Harty, M., Neff, A. W., King, M. W., Mescher, A. L., 2003. Regeneration or scarring: an immunologic perspective. *Dev Dyn*. 226, 268-79.

Hatakeyama, Y., Tuan, R. S., Shum, L., 2004. Distinct functions of BMP4 and GDF5 in the regulation of chondrogenesis. *J Cell Biochem*. 91, 1204-17.

Heber-Katz, E., 1999. The regenerating mouse ear. *Semin Cell Dev Biol*. 10, 415-9.

Hellingman, C. A., Davidson, E. N., Koevoet, W., Vitters, E. L., van den Berg, W. B., van Osch, G. J., van der Kraan, P. M., 2011. Smad signaling determines chondrogenic differentiation of bone-marrow-derived mesenchymal stem cells: inhibition of Smad1/5/8P prevents terminal differentiation and calcification. *Tissue Eng Part A*. 17, 1157-67.

Heng, B. C., Cao, T., Lee, E. H., 2004. Directing stem cell differentiation into the chondrogenic lineage in vitro. *Stem Cells*. 22, 1152-67.

Hennerbichler, A., Moutos, F. T., Hennerbichler, D., Weinberg, J. B., Guilak, F., 2007. Repair response of the inner and outer regions of the porcine meniscus in vitro. *Am J Sports Med*. 35, 754-62.

Hennig, T., Lorenz, H., Thiel, A., Goetzke, K., Dickhut, A., Geiger, F., Richter, W., 2007. Reduced chondrogenic potential of adipose tissue derived stromal cells correlates with an altered TGFbeta receptor and BMP profile and is overcome by BMP-6. *J Cell Physiol*. 211, 682-91.

Hjelle, K., Solheim, E., Strand, T., Muri, R., Brittberg, M., 2002. Articular cartilage defects in 1,000 knee arthroscopies. *Arthroscopy*. 18, 730-4.

Hoemann, C. D., 2004. Molecular and biochemical assays of cartilage components. *Methods Mol Med*. 101, 127-56.

Horie, M., Sekiya, I., Muneta, T., Ichinose, S., Matsumoto, K., Saito, H., Murakami, T., Kobayashi, E., 2009. Intra-articular Injected synovial stem cells differentiate into meniscal cells directly and promote meniscal regeneration without mobilization to distant organs in rat massive meniscal defect. *Stem Cells*. 27, 878-87.

Horwitz, E. M., Le Blanc, K., Dominici, M., Mueller, I., Slaper-Cortenbach, I., Marini, F. C., Deans, R. J., Krause, D. S., Keating, A., 2005. Clarification of the nomenclature

for MSC: The International Society for Cellular Therapy position statement. *Cytotherapy*. 7**,** 393-5.

Hu, J. C., Athanasiou, K. A., 2006. A self-assembling process in articular cartilage tissue engineering. *Tissue Eng*. 12**,** 969-79.

Huang, H. I., Chen, S. K., Ling, Q. D., Chien, C. C., Liu, H. T., Chan, S. H., 2010. Multilineage differentiation potential of fibroblast-like stromal cells derived from human skin. *Tissue Eng Part A*. 16**,** 1491-501.

Huang, J. I., Kazmi, N., Durbhakula, M. M., Hering, T. M., Yoo, J. U., Johnstone, B., 2005. Chondrogenic potential of progenitor cells derived from human bone marrow and adipose tissue: a patient-matched comparison. *J Orthop Res*. 23**,** 1383-9.

Hunt, D., Campbell, P. H., Zambon, A. C., Vranizan, K., Evans, S. M., Kuo, H. C., Yamaguchi, K. D., Omens, J. H., McCulloch, A. D., 2011. Early post-myocardial infarction survival in MRL mice is mediated by attenuated apoptosis and inflammation but depends on genetic background. *Exp Physiol*.

Hunziker, E. B., 2002. Articular cartilage repair: basic science and clinical progress. A review of the current status and prospects. *Osteoarthritis Cartilage*. 10**,** 432-63.

Hwang, N. S., Kim, M. S., Sampattavanich, S., Baek, J. H., Zhang, Z., Elisseeff, J., 2006a. Effects of three-dimensional culture and growth factors on the chondrogenic differentiation of murine embryonic stem cells. *Stem Cells*. 24**,** 284-91.

Hwang, N. S., Varghese, S., Zhang, Z., Elisseeff, J., 2006b. Chondrogenic differentiation of human embryonic stem cell-derived cells in arginine-glycine-aspartate-modified hydrogels. *Tissue Eng*. 12**,** 2695-706.

Im, G. I., Shin, Y. W., Lee, K. B., 2005. Do adipose tissue-derived mesenchymal stem cells have the same osteogenic and chondrogenic potential as bone marrow-derived cells? *Osteoarthritis Cartilage*. 13**,** 845-53.

Ip, J. E., Wu, Y., Huang, J., Zhang, L., Pratt, R. E., Dzau, V. J., 2007. Mesenchymal stem cells use integrin beta1 not CXC chemokine receptor 4 for myocardial migration and engraftment. *Mol Biol Cell*. 18**,** 2873-82.

Irie, K., Uchiyama, E., Iwaso, H., 2003. Intraarticular inflammatory cytokines in acute anterior cruciate ligament injured knee. *Knee*. 10**,** 93-6.

177

Israel, M. A., Yuan, S. H., Bardy, C., Reyna, S. M., Mu, Y., Herrera, C., Hefferan, M. P., Van Gorp, S., Nazor, K. L., Boscolo, F. S., Carson, C. T., Laurent, L. C., Marsala, M., Gage, F. H., Remes, A. M., Koo, E. H., Goldstein, L. S., 2012. Probing sporadic and familial Alzheimer's disease using induced pluripotent stem cells. *Nature*. 482**,** 216-20.

Ivanovic, Z., 2009. Hypoxia or in situ normoxia: The stem cell paradigm. *J Cell Physiol*. 219**,** 271-5.

Iyer, S. S., Rojas, M., 2008. Anti-inflammatory effects of mesenchymal stem cells: novel concept for future therapies. *Expert Opin Biol Ther*. 8**,** 569-81.

Izadpanah, R., Trygg, C., Patel, B., Kriedt, C., Dufour, J., Gimble, J. M., Bunnell, B. A., 2006. Biologic properties of mesenchymal stem cells derived from bone marrow and adipose tissue. *J Cell Biochem*. 99**,** 1285-97.

Johnstone, B., Hering, T. M., Caplan, A. I., Goldberg, V. M., Yoo, J. U., 1998. In vitro chondrogenesis of bone marrow-derived mesenchymal progenitor cells. *Exp Cell Res*. 238**,** 265-72.

Kench, J. A., Russell, D. M., Fadok, V. A., Young, S. K., Worthen, G. S., Jones-Carson, J., Henson, J. E., Henson, P. M., Nemazee, D., 1999. Aberrant wound healing and TGF-beta production in the autoimmune-prone MRL/+ mouse. *Clin Immunol*. 92**,** 300-10.

Kern, S., Eichler, H., Stoeve, J., Kluter, H., Bieback, K., 2006. Comparative analysis of mesenchymal stem cells from bone marrow, umbilical cord blood, or adipose tissue. *Stem Cells*. 24**,** 1294-301.

Kim, H. J., Im, G. I., 2008. Chondrogenic differentiation of adipose tissue-derived mesenchymal stem cells: Greater doses of growth factor are necessary. *J Orthop Res*.

Kim, M. J., Son, M. J., Son, M. Y., Seol, B., Kim, J., Park, J., Kim, J. H., Kim, Y. H., Park, S. A., Lee, C. H., Lee, K. S., Han, Y. M., Chang, J. S., Cho, Y. S., 2011. Generation of human induced pluripotent stem cells from osteoarthritis patient-derived synovial cells. *Arthritis Rheum*. 63**,** 3010-21.

Kim, Y. J., Kim, H. J., Im, G. I., 2008. PTHrP promotes chondrogenesis and suppresses hypertrophy from both bone marrow-derived and adipose tissue-derived MSCs. *Biochem Biophys Res Commun*. 373**,** 104-8.

Kim, Y. J., Sah, R. L., Doong, J. Y., Grodzinsky, A. J., 1988. Fluorometric assay of DNA in cartilage explants using Hoechst 33258. *Anal Biochem*. 174**,** 168-76.

Knutsen, G., Drogset, J. O., Engebretsen, L., Grontvedt, T., Isaksen, V., Ludvigsen, T. C., Roberts, S., Solheim, E., Strand, T., Johansen, O., 2007. A randomized trial comparing autologous chondrocyte implantation with microfracture. Findings at five years. *J Bone Joint Surg Am*. 89**,** 2105-12.

Koay, E. J., Hoben, G. M., Athanasiou, K. A., 2007. Tissue engineering with chondrogenically differentiated human embryonic stem cells. *Stem Cells*. 25**,** 2183-90.

Kolf, C. M., Cho, E., Tuan, R. S., 2007. Mesenchymal stromal cells. Biology of adult mesenchymal stem cells: regulation of niche, self-renewal and differentiation. *Arthritis Res Ther*. 9**,** 204.

Kostyk, S. K., Popovich, P. G., Stokes, B. T., Wei, P., Jakeman, L. B., 2008. Robust axonal growth and a blunted macrophage response are associated with impaired functional recovery after spinal cord injury in the MRL/MpJ mouse. *Neuroscience*. 156**,** 498-514.

Kramer, J., Bohrnsen, F., Lindner, U., Behrens, P., Schlenke, P., Rohwedel, J., 2006. In vivo matrix-guided human mesenchymal stem cells. *Cell Mol Life Sci*. 63**,** 616-26.

Kramer, J., Hegert, C., Guan, K., Wobus, A. M., Muller, P. K., Rohwedel, J., 2000. Embryonic stem cell-derived chondrogenic differentiation in vitro: activation by BMP-2 and BMP-4. *Mech Dev*. 92**,** 193-205.

Kraus, V. B., 2011. Osteoarthritis year 2010 in review: biochemical markers. *Osteoarthritis Cartilage*. 19**,** 346-53.

Kreuz, P. C., Steinwachs, M. R., Erggelet, C., Krause, S. J., Konrad, G., Uhl, M., Sudkamp, N., 2006. Results after microfracture of full-thickness chondral defects in different compartments in the knee. *Osteoarthritis Cartilage*. 14**,** 1119-25.

Kruyt, M. C., De Bruijn, J., Veenhof, M., Oner, F. C., Van Blitterswijk, C. A., Verbout, A. J., Dhert, W. J., 2003. Application and limitations of chloromethyl-benzamidodialkylcarbocyanine for tracing cells used in bone Tissue engineering. *Tissue Eng*. 9**,** 105-15.

Kumar, S., Ponnazhagan, S., 2007. Bone homing of mesenchymal stem cells by ectopic alpha 4 integrin expression. *FASEB J*. 21**,** 3917-27.

Kurth, T., Hedbom, E., Shintani, N., Sugimoto, M., Chen, F. H., Haspl, M., Martinovic, S., Hunziker, E. B., 2007. Chondrogenic potential of human synovial mesenchymal stem cells in alginate. *Osteoarthritis Cartilage*. 15**,** 1178-89.

Kurth, T. B., Dell'accio, F., Crouch, V., Augello, A., Sharpe, P. T., De Bari, C., 2011. Functional mesenchymal stem cell niches in adult mouse knee joint synovium in vivo. *Arthritis Rheum*. 63**,** 1289-300.

Kurtz, S. M., Lau, E., Ong, K., Zhao, K., Kelly, M., Bozic, K. J., 2009. Future young patient demand for primary and revision joint replacement: national projections from 2010 to 2030. *Clin Orthop Relat Res*. 467**,** 2606-12.

Lawrence, J. T., Birmingham, J., Toth, A. P., 2011. Emerging ideas: prevention of posttraumatic arthritis through interleukin-1 and tumor necrosis factor-alpha inhibition. *Clin Orthop Relat Res*. 469**,** 3522-6.

Lawrence, R. C., Felson, D. T., Helmick, C. G., Arnold, L. M., Choi, H., Deyo, R. A., Gabriel, S., Hirsch, R., Hochberg, M. C., Hunder, G. G., Jordan, J. M., Katz, J. N., Kremers, H. M., Wolfe, F., 2008. Estimates of the prevalence of arthritis and other rheumatic conditions in the United States. Part II. *Arthritis Rheum*. 58**,** 26-35.

Le Blanc, K., Rasmusson, I., Sundberg, B., Gotherstrom, C., Hassan, M., Uzunel, M., Ringden, O., 2004. Treatment of severe acute graft-versus-host disease with third party haploidentical mesenchymal stem cells. *Lancet*. 363**,** 1439-41.

Le Blanc, K., Tammik, C., Rosendahl, K., Zetterberg, E., Ringden, O., 2003. HLA expression and immunologic properties of differentiated and undifferentiated mesenchymal stem cells. *Exp Hematol*. 31**,** 890-6.

Lee, C. R., Grodzinsky, A. J., Hsu, H. P., Martin, S. D., Spector, M., 2000. Effects of harvest and selected cartilage repair procedures on the physical and biochemical properties of articular cartilage in the canine knee. *J Orthop Res*. 18**,** 790-9.

Lee, K. B., Hui, J. H., Song, I. C., Ardany, L., Lee, E. H., 2007. Injectable mesenchymal stem cell therapy for large cartilage defects--a porcine model. *Stem Cells*. 25**,** 2964-71.

Lee, R. H., Kim, B., Choi, I., Kim, H., Choi, H. S., Suh, K., Bae, Y. C., Jung, J. S., 2004. Characterization and expression analysis of mesenchymal stem cells from human bone marrow and adipose tissue. *Cell Physiol Biochem*. 14**,** 311-24.

Lee, R. H., Pulin, A. A., Seo, M. J., Kota, D. J., Ylostalo, J., Larson, B. L., Semprun-Prieto, L., Delafontaine, P., Prockop, D. J., 2009. Intravenous hMSCs improve myocardial infarction in mice because cells embolized in lung are activated to secrete the anti-inflammatory protein TSG-6. *Cell Stem Cell*. 5**,** 54-63.

Lee, S. Y., Miwa, M., Sakai, Y., Kuroda, R., Oe, K., Niikura, T., Matsumoto, T., Fujioka, H., Doita, M., Kurosaka, M., 2008. Isolation and characterization of connective tissue progenitor cells derived from human fracture-induced hemarthrosis in vitro. *J Orthop Res*. 26**,** 190-9.

Leferovich, J. M., Bedelbaeva, K., Samulewicz, S., Zhang, X. M., Zwas, D., Lankford, E. B., Heber-Katz, E., 2001. Heart regeneration in adult MRL mice. *Proc Natl Acad Sci U S A*. 98**,** 9830-5.

Lennon, D. P., Caplan, A. I., 2006a. Isolation of human marrow-derived mesenchymal stem cells. *Exp Hematol*. 34**,** 1604-5.

Lennon, D. P., Caplan, A. I., 2006b. Isolation of rat marrow-derived mesenchymal stem cells. *Exp Hematol*. 34**,** 1606-7.

Lewis, J. S., Furman, B.D., Guilak, F, Olson. S.A., 2010. Reduced macrophage infiltration and synovitis in the MRL/MpJ mouse after articular fracture. *56th Annual Meeting of the Orthopaedic Research Society; New Orleans, LA*. 0368.

Lewis, J. S., Hembree, W. C., Furman, B. D., Tippets, L., Cattel, D., Huebner, J. L., Little, D., Defrate, L. E., Kraus, V. B., Guilak, F., Olson, S. A., 2011. Acute joint pathology and synovial inflammation is associated with increased intra-articular fracture severity in the mouse knee. *Osteoarthritis Cartilage*.

Li, X., Makarov, S. S., 2006. An essential role of NF-kappaB in the "tumor-like" phenotype of arthritic synoviocytes. *Proc Natl Acad Sci U S A*. 103**,** 17432-7.

Li, X., Mohan, S., Gu, W., Baylink, D. J., 2001. Analysis of gene expression in the wound repair/regeneration process. *Mamm Genome*. 12**,** 52-9.

Liu, T. M., Martina, M., Hutmacher, D. W., Hui, J. H., Lee, E. H., Lim, B., 2007. Identification of common pathways mediating differentiation of bone marrow- and adipose tissue-derived human mesenchymal stem cells into three mesenchymal lineages. *Stem Cells*. 25**,** 750-60.

Livak, K. J., Schmittgen, T. D., 2001. Analysis of relative gene expression data using real-time quantitative PCR and the 2 (-Delta Delta C (T)) Method. *Methods*. 25**,** 402-8.

Loughlin, J., 2011. Genetic indicators and susceptibility to osteoarthritis. *Br J Sports Med*. 45**,** 278-82.

Lutolf, M. P., Hubbell, J. A., 2005. Synthetic biomaterials as instructive extracellular microenvironments for morphogenesis in tissue engineering. *Nat Biotechnol*. 23**,** 47-55.

Macchiarini, P., Jungebluth, P., Go, T., Asnaghi, M. A., Rees, L. E., Cogan, T. A., Dodson, A., Martorell, J., Bellini, S., Parnigotto, P. P., Dickinson, S. C., Hollander, A. P., Mantero, S., Conconi, M. T., Birchall, M. A., 2008. Clinical transplantation of a tissue-engineered airway. *Lancet*. 372**,** 2023-30.

Mackay, A. M., Beck, S. C., Murphy, J. M., Barry, F. P., Chichester, C. O., Pittenger, M. F., 1998. Chondrogenic differentiation of cultured human mesenchymal stem cells from marrow. *Tissue Eng*. 4**,** 415-28.

Marion, R. M., Strati, K., Li, H., Tejera, A., Schoeftner, S., Ortega, S., Serrano, M., Blasco, M. A., 2009. Telomeres acquire embryonic stem cell characteristics in induced pluripotent stem cells. *Cell Stem Cell*. 4**,** 141-54.

Marsell, R., Einhorn, T. A., 2011. The biology of fracture healing. *Injury*.

Matsumoto, T., Okabe, T., Ikawa, T., Iida, T., Yasuda, H., Nakamura, H., Wakitani, S., 2010. Articular cartilage repair with autologous bone marrow mesenchymal cells. *J Cell Physiol*. 225**,** 291-5.

Maumus, M., Guerit, D., Toupet, K., Jorgensen, C., Noel, D., 2011. Mesenchymal stem cell-based therapies in regenerative medicine: applications in rheumatology. *Stem Cell Res Ther*. 2**,** 14.

McBeath, R., Pirone, D. M., Nelson, C. M., Bhadriraju, K., Chen, C. S., 2004. Cell shape, cytoskeletal tension, and RhoA regulate stem cell lineage commitment. *Dev Cell*. 6**,** 483-95.

Medvedev, S. P., Grigor'eva, E. V., Shevchenko, A. I., Malakhova, A. A., Dementyeva, E. V., Shilov, A. A., Pokushalov, E. A., Zaidman, A. M., Aleksandrova, M. A., Plotnikov, E. Y., Sukhikh, G. T., Zakian, S. M., 2011. Human induced pluripotent stem cells derived from fetal neural stem cells successfully undergo directed differentiation into cartilage. *Stem Cells Dev*. 20**,** 1099-112.

Mehlhorn, A. T., Niemeyer, P., Kaiser, S., Finkenzeller, G., Stark, G. B., Sudkamp, N. P., Schmal, H., 2006. Differential expression pattern of extracellular matrix molecules during chondrogenesis of mesenchymal stem cells from bone marrow and adipose tissue. *Tissue Eng*. 12**,** 2853-62.

Meirelles Lda, S., Nardi, N. B., 2003. Murine marrow-derived mesenchymal stem cell: isolation, in vitro expansion, and characterization. *Br J Haematol*. 123**,** 702-11.

Meng, X. L., Shen, J. S., Kawagoe, S., Ohashi, T., Brady, R. O., Eto, Y., 2010. Induced pluripotent stem cells derived from mouse models of lysosomal storage disorders. *Proc Natl Acad Sci U S A*. 107**,** 7886-91.

Minas, T., 2001. Autologous chondrocyte implantation for focal chondral defects of the knee. *Clin Orthop Relat Res*. S349-61.

Mishima, Y., Lotz, M., 2008. Chemotaxis of human articular chondrocytes and mesenchymal stem cells. *J Orthop Res*. 26**,** 1407-12.

Morikawa, S., Mabuchi, Y., Kubota, Y., Nagai, Y., Niibe, K., Hiratsu, E., Suzuki, S., Miyauchi-Hara, C., Nagoshi, N., Sunabori, T., Shimmura, S., Miyawaki, A., Nakagawa, T., Suda, T., Okano, H., Matsuzaki, Y., 2009. Prospective identification, isolation, and systemic transplantation of multipotent mesenchymal stem cells in murine bone marrow. *J Exp Med*. 206**,** 2483-96.

Moutos, F. T., Freed, L. E., Guilak, F., 2007. A biomimetic three-dimensional woven composite scaffold for functional tissue engineering of cartilage. *Nat Mater*. 6**,** 162-7.

Mow, V. C., Kuei, S. C., Lai, W. M., Armstrong, C. G., 1980. Biphasic creep and stress relaxation of articular cartilage in compression? Theory and experiments. *J Biomech Eng*. 102**,** 73-84.

Mow, V. C., Ratcliffe, A., Poole, A. R., 1992. Cartilage and diarthrodial joints as paradigms for hierarchical materials and structures. *Biomaterials*. 13**,** 67-97.

Mueller, M. B., Tuan, R. S., 2008. Functional characterization of hypertrophy in chondrogenesis of human mesenchymal stem cells. *Arthritis Rheum*. 58**,** 1377-88.

Muir, H., 1995. The chondrocyte, architect of cartilage. Biomechanics, structure, function and molecular biology of cartilage matrix macromolecules. *Bioessays*. 17**,** 1039-48.

Murphy, J. M., Dixon, K., Beck, S., Fabian, D., Feldman, A., Barry, F., 2002. Reduced chondrogenic and adipogenic activity of mesenchymal stem cells from patients with advanced osteoarthritis. *Arthritis Rheum*. 46**,** 704-13.

Murphy, J. M., Fink, D. J., Hunziker, E. B., Barry, F. P., 2003. Stem cell therapy in a caprine model of osteoarthritis. *Arthritis Rheum*. 48**,** 3464-74.

Muschler, G. F., Nitto, H., Boehm, C. A., Easley, K. A., 2001. Age- and gender-related changes in the cellularity of human bone marrow and the prevalence of osteoblastic progenitors. *J Orthop Res*. 19**,** 117-25.

Nagata, S., Suda, T., 1995. Fas and Fas ligand: lpr and gld mutations. *Immunol Today*. 16**,** 39-43.

Nakagawa, T., Lee, S. Y., Reddi, A. H., 2009. Induction of chondrogenesis from human embryonic stem cells without embryoid body formation by bone morphogenetic protein 7 and transforming growth factor beta1. *Arthritis Rheum*. 60**,** 3686-92.

Nakatsuji, N., Nakajima, F., Tokunaga, K., 2008. HLA-haplotype banking and iPS cells. *Nat Biotechnol*. 26**,** 739-40.

Nakayama, N., Duryea, D., Manoukian, R., Chow, G., Han, C. Y., 2003. Macroscopic cartilage formation with embryonic stem-cell-derived mesodermal progenitor cells. *J Cell Sci*. 116**,** 2015-28.

Nemeth, K., Leelahavanichkul, A., Yuen, P. S., Mayer, B., Parmelee, A., Doi, K., Robey, P. G., Leelahavanichkul, K., Koller, B. H., Brown, J. M., Hu, X., Jelinek, I., Star, R. A., Mezey, E., 2009. Bone marrow stromal cells attenuate sepsis via prostaglandin E (2)-dependent reprogramming of host macrophages to increase their interleukin-10 production. *Nat Med*. 15**,** 42-9.

Noel, D., Caton, D., Roche, S., Bony, C., Lehmann, S., Casteilla, L., Jorgensen, C., Cousin, B., 2008. Cell specific differences between human adipose-derived and mesenchymal-stromal cells despite similar differentiation potentials. *Exp Cell Res*. 314**,** 1575-84.

Noth, U., Osyczka, A. M., Tuli, R., Hickok, N. J., Danielson, K. G., Tuan, R. S., 2002. Multilineage mesenchymal differentiation potential of human trabecular bone-derived cells. *J Orthop Res*. 20**,** 1060-9.

Noth, U., Steinert, A. F., Tuan, R. S., 2008. Technology insight: adult mesenchymal stem cells for osteoarthritis therapy. *Nat Clin Pract Rheumatol*. 4**,** 371-80.

Obradovic, B., Martin, I., Padera, R. F., Treppo, S., Freed, L. E., Vunjak-Novakovic, G., 2001. Integration of engineered cartilage. *J Orthop Res*. 19**,** 1089-97.

Oldershaw, R. A., Baxter, M. A., Lowe, E. T., Bates, N., Grady, L. M., Soncin, F., Brison, D. R., Hardingham, T. E., Kimber, S. J., 2010. Directed differentiation of human embryonic stem cells toward chondrocytes. *Nat Biotechnol*. 28**,** 1187-94.

Ortiz, L. A., Dutreil, M., Fattman, C., Pandey, A. C., Torres, G., Go, K., Phinney, D. G., 2007. Interleukin 1 receptor antagonist mediates the antiinflammatory and antifibrotic effect of mesenchymal stem cells during lung injury. *Proc Natl Acad Sci U S A*. 104**,** 11002-7.

Ott, H. C., Matthiesen, T. S., Goh, S. K., Black, L. D., Kren, S. M., Netoff, T. I., Taylor, D. A., 2008. Perfusion-decellularized matrix: using nature's platform to engineer a bioartificial heart. *Nat Med*. 14**,** 213-21.

Ozaki, Y., Nishimura, M., Sekiya, K., Suehiro, F., Kanawa, M., Nikawa, H., Hamada, T., Kato, Y., 2007. Comprehensive analysis of chemotactic factors for bone marrow mesenchymal stem cells. *Stem Cells Dev*. 16**,** 119-29.

Park, I. H., Arora, N., Huo, H., Maherali, N., Ahfeldt, T., Shimamura, A., Lensch, M. W., Cowan, C., Hochedlinger, K., Daley, G. Q., 2008. Disease-specific induced pluripotent stem cells. *Cell*. 134**,** 877-86.

Peister, A., Mellad, J. A., Larson, B. L., Hall, B. M., Gibson, L. F., Prockop, D. J., 2004. Adult stem cells from bone marrow (MSCs) isolated from different strains of inbred mice vary in surface epitopes, rates of proliferation, and differentiation potential. *Blood*. 103**,** 1662-8.

Pelttari, K., Winter, A., Steck, E., Goetzke, K., Hennig, T., Ochs, B. G., Aigner, T., Richter, W., 2006. Premature induction of hypertrophy during in vitro chondrogenesis of human mesenchymal stem cells correlates with calcification and vascular invasion after ectopic transplantation in SCID mice. *Arthritis Rheum*. 54**,** 3254-66.

Peters, L. L., Robledo, R. F., Bult, C. J., Churchill, G. A., Paigen, B. J., Svenson, K. L., 2007. The mouse as a model for human biology: a resource guide for complex trait analysis. *Nat Rev Genet*. 8**,** 58-69.

Peterson, L., Brittberg, M., Kiviranta, I., Akerlund, E. L., Lindahl, A., 2002. Autologous chondrocyte transplantation. Biomechanics and long-term durability. *Am J Sports Med*. 30**,** 2-12.

Phinney, D. G., 2008. Isolation of mesenchymal stem cells from murine bone marrow by immunodepletion. *Methods Mol Biol*. 449**,** 171-86.

Phinney, D. G., Hill, K., Michelson, C., DuTreil, M., Hughes, C., Humphries, S., Wilkinson, R., Baddoo, M., Bayly, E., 2006. Biological activities encoded by the murine mesenchymal stem cell transcriptome provide a basis for their developmental potential and broad therapeutic efficacy. *Stem Cells*. 24**,** 186-98.

Phinney, D. G., Kopen, G., Isaacson, R. L., Prockop, D. J., 1999. Plastic adherent stromal cells from the bone marrow of commonly used strains of inbred mice: variations in yield, growth, and differentiation. *J Cell Biochem*. 72**,** 570-85.

Phinney, D. G., Prockop, D. J., 2007. Concise review: mesenchymal stem/multipotent
stromal cells: the state of transdifferentiation and modes of tissue repair--current
views. *Stem Cells*. 25**,** 2896-902.

Pickvance, E. A., Oegema, T. R., Jr., Thompson, R. C., Jr., 1993. Immunolocalization of
selected cytokines and proteases in canine articular cartilage after transarticular
loading. *J Orthop Res*. 11**,** 313-23.

Pittenger, M. F., Mackay, A. M., Beck, S. C., Jaiswal, R. K., Douglas, R., Mosca, J. D.,
Moorman, M. A., Simonetti, D. W., Craig, S., Marshak, D. R., 1999. Multilineage
potential of adult human mesenchymal stem cells. *Science*. 284**,** 143-7.

Poole, C. A., Ayad, S., Schofield, J. R., 1988. Chondrons from articular cartilage: I.
Immunolocalization of type VI collagen in the pericellular capsule of isolated
canine tibial chondrons. *J Cell Sci*. 90 (Pt 4)**,** 635-43.

Porcheray, F., Viaud, S., Rimaniol, A. C., Leone, C., Samah, B., Dereuddre-Bosquet, N.,
Dormont, D., Gras, G., 2005. Macrophage activation switching: an asset for the
resolution of inflammation. *Clin Exp Immunol*. 142**,** 481-9.

Prockop, D. J., 1997. Marrow stromal cells as stem cells for nonhematopoietic tissues.
Science. 276**,** 71-4.

Prockop, D. J., 2007. "Stemness" does not explain the repair of many tissues by
mesenchymal stem/multipotent stromal cells (MSCs). *Clin Pharmacol Ther*. 82**,**
241-3.

Prockop, D. J., Youn Oh, J., 2011. Mesenchymal Stem/Stromal Cells (MSCs): Role as
Guardians of Inflammation. *Mol Ther*.

Quarto, N., Leonard, B., Li, S., Marchand, M., Anderson, E., Behr, B., Francke, U., Reijo-
Pera, R., Chiao, E., Longaker, M. T., 2012. Skeletogenic phenotype of human
Marfan embryonic stem cells faithfully phenocopied by patient-specific induced-
pluripotent stem cells. *Proc Natl Acad Sci U S A*. 109**,** 215-20.

Quintana, L., zur Nieden, N. I., Semino, C. E., 2009. Morphogenetic and regulatory
mechanisms during developmental chondrogenesis: new paradigms for cartilage
tissue engineering. *Tissue Eng Part B Rev*. 15**,** 29-41.

Rebelatto, C. K., Aguiar, A. M., Moretao, M. P., Senegaglia, A. C., Hansen, P., Barchiki, F., Oliveira, J., Martins, J., Kuligovski, C., Mansur, F., Christofis, A., Amaral, V. F., Brofman, P. S., Goldenberg, S., Nakao, L. S., Correa, A., 2008. Dissimilar differentiation of mesenchymal stem cells from bone marrow, umbilical cord blood, and adipose tissue. *Exp Biol Med (Maywood)*. 233**,** 901-13.

Rebuzzini, P., Neri, T., Mazzini, G., Zuccotti, M., Redi, C. A., Garagna, S., 2008. Karyotype analysis of the euploid cell population of a mouse embryonic stem cell line revealed a high incidence of chromosome abnormalities that varied during culture. *Cytogenet Genome Res*. 121**,** 18-24.

Ren, G., Zhang, L., Zhao, X., Xu, G., Zhang, Y., Roberts, A. I., Zhao, R. C., Shi, Y., 2008. Mesenchymal stem cell-mediated immunosuppression occurs via concerted action of chemokines and nitric oxide. *Cell Stem Cell*. 2**,** 141-50.

Retting, K. N., Song, B., Yoon, B. S., Lyons, K. M., 2009. BMP canonical Smad signaling through Smad1 and Smad5 is required for endochondral bone formation. *Development*. 136**,** 1093-104.

Richter, W., 2009. Mesenchymal stem cells and cartilage in situ regeneration. *J Intern Med*. 266**,** 390-405.

Rider, D. A., Dombrowski, C., Sawyer, A. A., Ng, G. H., Leong, D., Hutmacher, D. W., Nurcombe, V., Cool, S. M., 2008. Autocrine fibroblast growth factor 2 increases the multipotentiality of human adipose-derived mesenchymal stem cells. *Stem Cells*. 26**,** 1598-608.

Ringe, J., Strassburg, S., Neumann, K., Endres, M., Notter, M., Burmester, G. R., Kaps, C., Sittinger, M., 2007. Towards in situ tissue repair: human mesenchymal stem cells express chemokine receptors CXCR1, CXCR2 and CCR2, and migrate upon stimulation with CXCL8 but not CCL2. *J Cell Biochem*. 101**,** 135-46.

Roark, E. F., Greer, K., 1994. Transforming growth factor-beta and bone morphogenetic protein-2 act by distinct mechanisms to promote chick limb cartilage differentiation in vitro. *Dev Dyn*. 200**,** 103-16.

Robinton, D. A., Daley, G. Q., 2012. The promise of induced pluripotent stem cells in research and therapy. *Nature*. 481**,** 295-305.

Rombouts, W. J., Ploemacher, R. E., 2003. Primary murine MSC show highly efficient homing to the bone marrow but lose homing ability following culture. *Leukemia*. 17**,** 160-70.

Sacchetti, B., Funari, A., Michienzi, S., Di Cesare, S., Piersanti, S., Saggio, I., Tagliafico, E., Ferrari, S., Robey, P. G., Riminucci, M., Bianco, P., 2007. Self-renewing osteoprogenitors in bone marrow sinusoids can organize a hematopoietic microenvironment. *Cell*. 131**,** 324-36.

Saha, K., Jaenisch, R., 2009. Technical challenges in using human induced pluripotent stem cells to model disease. *Cell Stem Cell*. 5**,** 584-95.

Sakaguchi, Y., Sekiya, I., Yagishita, K., Muneta, T., 2005. Comparison of human stem cells derived from various mesenchymal tissues: superiority of synovium as a cell source. *Arthritis Rheum*. 52**,** 2521-9.

Scanzello, C. R., McKeon, B., Swaim, B. H., DiCarlo, E., Asomugha, E. U., Kanda, V., Nair, A., Lee, D. M., Richmond, J. C., Katz, J. N., Crow, M. K., Goldring, S. R., 2011. Synovial inflammation in patients undergoing arthroscopic meniscectomy: molecular characterization and relationship to symptoms. *Arthritis Rheum*. 63**,** 391-400.

Schulze-Tanzil, G., Zreiqat, H., Sabat, R., Kohl, B., Halder, A., Muller, R. D., John, T., 2009. Interleukin-10 and articular cartilage: experimental therapeutical approaches in cartilage disorders. *Curr Gene Ther*. 9**,** 306-15.

Seda Tigli, R., Ghosh, S., Laha, M. M., Shevde, N. K., Daheron, L., Gimble, J., Gumusderelioglu, M., Kaplan, D. L., 2009. Comparative chondrogenesis of human cell sources in 3D scaffolds. *J Tissue Eng Regen Med*. 3**,** 348-60.

Segawa, Y., Muneta, T., Makino, H., Nimura, A., Mochizuki, T., Ju, Y. J., Ezura, Y., Umezawa, A., Sekiya, I., 2008. Mesenchymal stem cells derived from synovium, meniscus, anterior cruciate ligament, and articular chondrocytes share similar gene expression profiles. *J Orthop Res*.

Seifer, D. R., Furman, B. D., Guilak, F., Olson, S. A., Brooks, S. C., 3rd, Kraus, V. B., 2008. Novel synovial fluid recovery method allows for quantification of a marker of arthritis in mice. *Osteoarthritis Cartilage*. 16**,** 1532-8.

Sekiya, I., Colter, D. C., Prockop, D. J., 2001. BMP-6 enhances chondrogenesis in a subpopulation of human marrow stromal cells. *Biochem Biophys Res Commun*. 284, 411-8.

Serhan, C. N., Savill, J., 2005. Resolution of inflammation: the beginning programs the end. *Nat Immunol*. 6, 1191-7.

Shakibaei, M., 1998. Inhibition of chondrogenesis by integrin antibody in vitro. *Exp Cell Res*. 240, 95-106.

Short, B. J., Brouard, N., Simmons, P. J., 2009. Prospective isolation of mesenchymal stem cells from mouse compact bone. *Methods Mol Biol*. 482, 259-68.

Solchaga, L. A., Goldberg, V. M., Caplan, A. I., 2001. Cartilage regeneration using principles of tissue engineering. *Clin Orthop Relat Res*. S161-70.

Solchaga, L. A., Penick, K., Porter, J. D., Goldberg, V. M., Caplan, A. I., Welter, J. F., 2005. FGF-2 enhances the mitotic and chondrogenic potentials of human adult bone marrow-derived mesenchymal stem cells. *J Cell Physiol*. 203, 398-409.

Soleimani, M., Nadri, S., 2009. A protocol for isolation and culture of mesenchymal stem cells from mouse bone marrow. *Nat Protoc*. 4, 102-6.

Song, L., Baksh, D., Tuan, R. S., 2004. Mesenchymal stem cell-based cartilage tissue engineering: cells, scaffold and biology. *Cytotherapy*. 6, 596-601.

Sotiropoulou, P. A., Papamichail, M., 2007. Immune properties of mesenchymal stem cells. *Methods Mol Biol*. 407, 225-43.

Steinert, A. F., Ghivizzani, S. C., Rethwilm, A., Tuan, R. S., Evans, C. H., Noth, U., 2007. Major biological obstacles for persistent cell-based regeneration of articular cartilage. *Arthritis Res Ther*. 9, 213.

Sugawara, A., Goto, K., Sotomaru, Y., Sofuni, T., Ito, T., 2006. Current status of chromosomal abnormalities in mouse embryonic stem cell lines used in Japan. *Comp Med*. 56, 31-4.

Sun, N., Longaker, M. T., Wu, J. C., 2010. Human iPS cell-based therapy: considerations before clinical applications. *Cell Cycle*. 9, 880-5.

Sun, S., Guo, Z., Xiao, X., Liu, B., Liu, X., Tang, P. H., Mao, N., 2003. Isolation of mouse marrow mesenchymal progenitors by a novel and reliable method. *Stem Cells*. 21**,** 527-35.

Sung, J. H., Yang, H. M., Park, J. B., Choi, G. S., Joh, J. W., Kwon, C. H., Chun, J. M., Lee, S. K., Kim, S. J., 2008. Isolation and characterization of mouse mesenchymal stem cells. *Transplant Proc*. 40**,** 2649-54.

Svoboda, K. K., 1998. Chondrocyte-matrix attachment complexes mediate survival and differentiation. *Microsc Res Tech*. 43**,** 111-22.

Taichman, R. S., Wang, Z., Shiozawa, Y., Jung, Y., Song, J., Balduino, A., Wang, J., Patel, L. R., Havens, A. M., Kucia, M., Ratajczak, M. Z., Krebsbach, P. H., 2010. Prospective Identification and Skeletal Localization of Cells Capable of Multilineage Differentiation In Vivo. *Stem Cells Dev*.

Taipaleenmaki, H., Suomi, S., Hentunen, T., Laitala-Leinonen, T., Saamanen, A. M., 2008. Impact of stromal cell composition on BMP-induced chondrogenic differentiation of mouse bone marrow derived mesenchymal cells. *Exp Cell Res*. 314**,** 2400-10.

Takahashi, K., Tanabe, K., Ohnuki, M., Narita, M., Ichisaka, T., Tomoda, K., Yamanaka, S., 2007. Induction of pluripotent stem cells from adult human fibroblasts by defined factors. *Cell*. 131**,** 861-72.

Takahashi, K., Yamanaka, S., 2006. Induction of pluripotent stem cells from mouse embryonic and adult fibroblast cultures by defined factors. *Cell*. 126**,** 663-76.

Taylor, J. R., 1982. An introduction to error analysis. University Science Books, Mill Valley, Calif.

Teramura, T., Onodera, Y., Mihara, T., Hosoi, Y., Hamanishi, C., Fukuda, K., 2010. Induction of mesenchymal progenitor cells with chondrogenic property from mouse-induced pluripotent stem cells. *Cell Reprogram*. 12**,** 249-61.

Thomson, J. A., Itskovitz-Eldor, J., Shapiro, S. S., Waknitz, M. A., Swiergiel, J. J., Marshall, V. S., Jones, J. M., 1998. Embryonic stem cell lines derived from human blastocysts. *Science*. 282**,** 1145-7.

Toghraie, F. S., Chenari, N., Gholipour, M. A., Faghih, Z., Torabinejad, S., Dehghani, S., Ghaderi, A., 2011. Treatment of osteoarthritis with infrapatellar fat pad derived mesenchymal stem cells in Rabbit. *Knee*. 18**,** 71-5.

Toh, W. S., Yang, Z., Liu, H., Heng, B. C., Lee, E. H., Cao, T., 2007. Effects of culture conditions and bone morphogenetic protein 2 on extent of chondrogenesis from human embryonic stem cells. *Stem Cells*. 25**,** 950-60.

Tropel, P., Noel, D., Platet, N., Legrand, P., Benabid, A. L., Berger, F., 2004. Isolation and characterisation of mesenchymal stem cells from adult mouse bone marrow. *Exp Cell Res*. 295**,** 395-406.

Uccelli, A., Moretta, L., Pistoia, V., 2008. Mesenchymal stem cells in health and disease. *Nat Rev Immunol*. 8**,** 726-36.

Ueno, M., Lyons, B. L., Burzenski, L. M., Gott, B., Shaffer, D. J., Roopenian, D. C., Shultz, L. D., 2005. Accelerated wound healing of alkali-burned corneas in MRL mice is associated with a reduced inflammatory signature. *Invest Ophthalmol Vis Sci*. 46**,** 4097-106.

Uezumi, A., Fukada, S., Yamamoto, N., Takeda, S., Tsuchida, K., 2010. Mesenchymal progenitors distinct from satellite cells contribute to ectopic fat cell formation in skeletal muscle. *Nat Cell Biol*. 12**,** 143-52.

Usas, A., Huard, J., 2007. Muscle-derived stem cells for tissue engineering and regenerative therapy. *Biomaterials*. 28**,** 5401-6.

Valtieri, M., Sorrentino, A., 2008. The mesenchymal stromal cell contribution to homeostasis. *J Cell Physiol*. 217**,** 296-300.

van der Kraan, P. M., Vitters, E. L., van Beuningen, H. M., van de Putte, L. B., van den Berg, W. B., 1990. Degenerative knee joint lesions in mice after a single intra-articular collagenase injection. A new model of osteoarthritis. *J Exp Pathol (Oxford)*. 71**,** 19-31.

Van Meurs, J. B., Van Lent, P. L., Joosten, L. A., Van der Kraan, P. M., Van den Berg, W. B., 1997. Quantification of mRNA levels in joint capsule and articular cartilage of the murine knee joint by RT-PCR: kinetics of stromelysin and IL-1 mRNA levels during arthritis. *Rheumatol Int*. 16**,** 197-205.

Varma, M. J., Breuls, R. G., Schouten, T. E., Jurgens, W. J., Bontkes, H. J., Schuurhuis, G. J., van Ham, S. M., van Milligen, F. J., 2007. Phenotypical and functional characterization of freshly isolated adipose tissue-derived stem cells. *Stem Cells Dev*. 16**,** 91-104.

Vinardell, T., Thorpe, S. D., Buckley, C. T., Kelly, D. J., 2009. Chondrogenesis and integration of mesenchymal stem cells within an in vitro cartilage defect repair model. *Ann Biomed Eng*. 37**,** 2556-65.

Waese, E. Y., Stanford, W. L., 2011. One-step generation of murine embryonic stem cell-derived mesoderm progenitors and chondrocytes in a serum-free monolayer differentiation system. *Stem Cell Res*. 6**,** 34-49.

Wagner, W., Wein, F., Seckinger, A., Frankhauser, M., Wirkner, U., Krause, U., Blake, J., Schwager, C., Eckstein, V., Ansorge, W., Ho, A. D., 2005. Comparative characteristics of mesenchymal stem cells from human bone marrow, adipose tissue, and umbilical cord blood. *Exp Hematol*. 33**,** 1402-16.

Wakitani, S., Goto, T., Pineda, S. J., Young, R. G., Mansour, J. M., Caplan, A. I., Goldberg, V. M., 1994. Mesenchymal cell-based repair of large, full-thickness defects of articular cartilage. *J Bone Joint Surg Am*. 76**,** 579-92.

Wakitani, S., Imoto, K., Yamamoto, T., Saito, M., Murata, N., Yoneda, M., 2002. Human autologous culture expanded bone marrow mesenchymal cell transplantation for repair of cartilage defects in osteoarthritic knees. *Osteoarthritis Cartilage*. 10**,** 199-206.

Wan, D. C., Shi, Y. Y., Nacamuli, R. P., Quarto, N., Lyons, K. M., Longaker, M. T., 2006. Osteogenic differentiation of mouse adipose-derived adult stromal cells requires retinoic acid and bone morphogenetic protein receptor type IB signaling. *Proc Natl Acad Sci U S A*. 103**,** 12335-40.

Ward, B. D., Furman, B. D., Huebner, J. L., Kraus, V. B., Guilak, F., Olson, S. A., 2008. Absence of posttraumatic arthritis following intraarticular fracture in the MRL/MpJ mouse. *Arthritis Rheum*. 58**,** 744-53.

Wei, Y., Zeng, W., Wan, R., Wang, J., Zhou, Q., Qiu, S., Singh, S. R., 2012. Chondrogenic differentiation of induced pluripotent stem cells from osteoarthritic chondrocytes in alginate matrix. *Eur Cell Mater*. 23**,** 1-12.

Wickham, M. Q., Erickson, G. R., Gimble, J. M., Vail, T. P., Guilak, F., 2003. Multipotent stromal cells derived from the infrapatellar fat pad of the knee. *Clin Orthop Relat Res*. 196-212.

Wieland, H. A., Michaelis, M., Kirschbaum, B. J., Rudolphi, K. A., 2005. Osteoarthritis - an untreatable disease? *Nat Rev Drug Discov*. 4**,** 331-44.

Winter, A., Breit, S., Parsch, D., Benz, K., Steck, E., Hauner, H., Weber, R. M., Ewerbeck, V., Richter, W., 2003. Cartilage-like gene expression in differentiated human stem cell spheroids: a comparison of bone marrow-derived and adipose tissue-derived stromal cells. *Arthritis Rheum*. 48**,** 418-29.

Yamashita, A., Nishikawa, S., Rancourt, D. E., 2010. Identification of five developmental processes during chondrogenic differentiation of embryonic stem cells. *PLoS One*. 5**,** e10998.

Yang, Q., Peng, J., Guo, Q., Huang, J., Zhang, L., Yao, J., Yang, F., Wang, S., Xu, W., Wang, A., Lu, S., 2008. A cartilage ECM-derived 3-D porous acellular matrix scaffold for in vivo cartilage tissue engineering with PKH26-labeled chondrogenic bone marrow-derived mesenchymal stem cells. *Biomaterials*. 29**,** 2378-87.

Yang, X., Chen, L., Xu, X., Li, C., Huang, C., Deng, C. X., 2001. TGF-beta/Smad3 signals repress chondrocyte hypertrophic differentiation and are required for maintaining articular cartilage. *J Cell Biol*. 153**,** 35-46.

Yeung, C. W., Cheah, K., Chan, D., Chan, B. P., 2009. Effects of reconstituted collagen matrix on fates of mouse embryonic stem cells before and after induction for chondrogenic differentiation. *Tissue Eng Part A*. 15**,** 3071-85.

Yin, S., Cen, L., Wang, C., Zhao, G., Sun, J., Liu, W., Cao, Y., Cui, L., 2010. Chondrogenic transdifferentiation of human dermal fibroblasts stimulated with cartilage-derived morphogenetic protein 1. *Tissue Eng Part A*. 16**,** 1633-43.

Yoo, J. U., Barthel, T. S., Nishimura, K., Solchaga, L., Caplan, A. I., Goldberg, V. M., Johnstone, B., 1998. The chondrogenic potential of human bone-marrow-derived mesenchymal progenitor cells. *J Bone Joint Surg Am*. 80**,** 1745-57.

Yoshida, Y., Yamanaka, S., 2010. Recent stem cell advances: induced pluripotent stem cells for disease modeling and stem cell-based regeneration. *Circulation*. 122**,** 80-7.

Yu, H., Mohan, S., Masinde, G. L., Baylink, D. J., 2005. Mapping the dominant wound healing and soft tissue regeneration QTL in MRL x CAST. *Mamm Genome*. 16**,** 918-24.

Yu, J., Vodyanik, M. A., Smuga-Otto, K., Antosiewicz-Bourget, J., Frane, J. L., Tian, S., Nie, J., Jonsdottir, G. A., Ruotti, V., Stewart, R., Slukvin, II, Thomson, J. A., 2007. Induced pluripotent stem cell lines derived from human somatic cells. *Science*. 318**,** 1917-20.

Zachos, T., Diggs, A., Weisbrode, S., Bartlett, J., Bertone, A., 2007a. Mesenchymal stem cell-mediated gene delivery of bone morphogenetic protein-2 in an articular fracture model. *Mol Ther*. 15**,** 1543-50.

Zachos, T. A., Bertone, A. L., Wassenaar, P. A., Weisbrode, S. E., 2007b. Rodent models for the study of articular fracture healing. *J Invest Surg*. 20**,** 87-95.

Zannettino, A. C., Paton, S., Arthur, A., Khor, F., Itescu, S., Gimble, J. M., Gronthos, S., 2008. Multipotential human adipose-derived stromal stem cells exhibit a perivascular phenotype in vitro and in vivo. *J Cell Physiol*. 214**,** 413-21.

Zhang, P., Li, J., Tan, Z., Wang, C., Liu, T., Chen, L., Yong, J., Jiang, W., Sun, X., Du, L., Ding, M., Deng, H., 2008. Short-term BMP-4 treatment initiates mesoderm induction in human embryonic stem cells. *Blood*. 111**,** 1933-41.

Zhu, H., Guo, Z. K., Jiang, X. X., Li, H., Wang, X. Y., Yao, H. Y., Zhang, Y., Mao, N., 2010. A protocol for isolation and culture of mesenchymal stem cells from mouse compact bone. *Nat Protoc*. 5**,** 550-60.

Zins, S. R., Amare, M. F., Anam, K., Elster, E. A., Davis, T. A., 2010. Wound trauma mediated inflammatory signaling attenuates a tissue regenerative response in MRL/MpJ mice. *J Inflamm (Lond)*. 7**,** 25.

Zscharnack, M., Hepp, P., Richter, R., Aigner, T., Schulz, R., Somerson, J., Josten, C., Bader, A., Marquass, B., Repair of Chronic Osteochondral Defects Using Predifferentiated Mesenchymal Stem Cells in an Ovine Model. *Am J Sports Med*.

Zuk, P. A., Zhu, M., Mizuno, H., Huang, J., Futrell, J. W., Katz, A. J., Benhaim, P., Lorenz, H. P., Hedrick, M. H., 2001. Multilineage cells from human adipose tissue: implications for cell-based therapies. *Tissue Eng*. 7**,** 211-28.

Biography

Brian O. Diekman was born in West Lafayette, IN on February 25, 1983. He

earned a Bachelor of Science in Biomedical Engineering *cum laude* from Duke University

in 2005, receiving the Biomedical Engineering Society Rita Schaffer Award for

Undergraduate Research. In 2006, Brian received a Fulbright student grant to perform

stem cell research at the Regenerative Medicine Institute in Galway, Ireland under the

direction of Dr. Frank Barry and Dr. Mary Murphy. Brian was a National Science

Foundation Graduate Research Fellow from 2008-2010 and received the 2011 Wake

Forest Institute for Regenerative Medicine Young Investigator Award at the Tissue

Engineering and Regenerative Medicine International Society annual meeting.

Journal Articles:

Diekman BO, Rowland CR, Caplan AI, Lennon D, Guilak F. Chondrogenesis of adult stem cells from adipose tissue and bone marrow: Induction by growth factors and cartilage derived matrix. Tissue Eng Part A. 2010 Feb;16 (2):523-33.

Diekman BO*, Estes BT*, Guilak F. The effects of BMP6 overexpression on adipose stem cell chondrogenesis: Interactions with dexamethasone and exogenous growth factors. J Biomed Mater Res A. 2010 Jun 1;93 (3):994-1003.
*co-first authors

Estes BT, **Diekman BO**, Guilak F. Monolayer cell expansion conditions affect the chondrogenic potential of adipose-derived stem cells. Biotechnol Bioeng. 2008 Mar 1;99 (4):986-95.

Valonen PK, Moutos FT, Kusanagi A, Moretti MG, **Diekman BO**, Welter JF, Caplan AI, Guilak F, Freed LE. In vitro generation of mechanically functional cartilage grafts based on adult human stem cells and 3D-woven poly (epsilon-caprolactone) scaffolds. Biomaterials. 2010 Mar; 31 (8):2193-200.

Estes BT, **Diekman BO**, Gimble JM, Guilak F. Isolation of adipose-derived stem cells and their induction to a chondrogenic phenotype. Nat Protoc. 2010 Jul;5 (7):1294-311. Epub 2010 Jun 17.

Guilak F, Estes BT, **Diekman BO**, Moutos FT, Gimble JM. 2010 Nicolas Andry award: multipotent adult stem cells from adipose tissue for musculoskeletal tissue engineering. Monolayer cell expansion conditions affect the chondrogenic potential of adipose-derived stem cells. Clin Orthop Relat Res. 2010 Sep;468 (9):2530-40.

Fermor B, Gurumurthy A, **Diekman BO**. Hypoxia, RONS and energy metabolism in articular cartilage. Osteoarthritis Cartilage. 2010 Sep;18 (9):1167-73.

Conference Presentations:

Podium Presentation, 2012 Orthopaedic Research Society meeting, San Francisco, CA. **Diekman BO**, Christoforou N, Sun A, Leong K, Guilak F. Chondrogenesis of induced pluripotent stem cells: Purification of differentiated cells for tissue engineering.

Podium Presentation, 2011 Tissue Engineering and Regenerative Medicine International Society NA meeting. Houston, Texas. **Diekman BO**, Wu CL, Louer CR, Furman BD, Olson SA, Guilak F. Prevention of post-traumatic arthritis by mesenchymal stem cell therapy.
- *Associated with Wake Forest Institute for Regenerative Medicine Young Investigator Award*

Podium Presentation, 2011 North Carolina Tissue Engineering and Regenerative Medicine Society. **Diekman BO**, Wu CL, Louer CR, Furman BD, Olson SA, Guilak F. Prevention of post-traumatic arthritis by mesenchymal stem cell therapy.

Podium Presentation, 2010 Tissue Engineering and Regenerative Medicine International Society EU meeting. Galway, Ireland. **Diekman BO**, Wu CL, Guilak F. Characterization of stem cells derived from C57BL/6 and MRL/MpJ "Superhealer" Mice.
- *Received "50 Best Abstracts Award"*

Podium Presentation, 2009 Hilton Head Regenerative Medicine Workshop. Hilton Head, SC. **Diekman BO**, Rowland CR, Lennon D, Caplan AI, Guilak F. Chondrogenesis of adult stem cells from adipose tissue and bone marrow: Induction by growth factors and cartilage derived matrix.

Poster, 2012 Orthopaedic Research Society meeting, San Francisco, CA. **Diekman BO**, Wu CL, Louer CR, Furman BD, Olson SA, Guilak F. Prevention of post-traumatic arthritis by mesenchymal stem cell therapy.

Poster, 2012 Orthopaedic Research Society meeting, San Francisco, CA. Wu CL, **Diekman BO**, Guilak F. Obesity alters the multilineage potential of bone marrow-derived mesenchymal stem cells and infrapatellar fat pad-derived stem cells.

Poster, 2011 Tissue Engineering and Regenerative Medicine International Society NA meeting. Houston, Texas. **Diekman BO**, Christoforou N, Sun A, Leong K, Guilak F. Chondrogenesis of induced pluripotent stem cells: Purification of differentiated cells for tissue engineering.

- *Received first place in student and young investigator poster competition*

Poster, 2008 Orthopaedic Research Society meeting. **Diekman BO**, Estes BT, Guilak F. San Francisco, CA. Dexamethasone enhances BMP-6-induced chondrogenesis of adipose-derived stem cells.

Invited Lectures:

Purdue University Stem Cell Biology Course (Fall 2011). Part 1: Stem cells for tissue engineering. Part 2: Induced pluripotent stem cells for cartilage tissue engineering.